DESIGN, FABRICATION AND TESTING OF A PARABOLIC TROUGH SOLAR COLLECTOR AIR HEATER FOR A GREENHOUSE SOLAR DRYER

BY

ERIC KING'ORI NJERI

A DISSERTATION SUBMITTED TO THE UNIVERSITY OF ZAMBIA IN PARTIAL FULFILMENT OF THE REQUIREMENTS FOR THE AWARD OF THE DEGREE OF MASTER OF ENGINEERING IN RENEWABLE ENERGY

THE UNIVERSITY OF ZAMBIA

2022

DECLARATION

I, **ERIC KING'ORI NJERI** do hereby declare that the contents in this dissertation are my original work and have not been previously submitted to any university for the award of a degree or any other qualification.

Signature……..Date……..

CERTIFICATE OF APPROVAL

This dissertation submitted by **ERIC KING'ORI NJERI** is approved as fulfilling the requirements for the award of the degree of Master of Engineering in Renewable Energy Engineering at the University of Zambia.

Supervisor…….Sign…..….....….Date…….

Chairperson (Board of Examiners)
Name…….....Sign……..….Date……..……..

Examiner 1……Sign……Date……..……

Examiner 2……Sign……Date……..……

Examiner 3……Sign……Date……..……

ABSTRACT

In an effort to mitigate post-harvest losses (PHL) of agricultural products from farmers and the markets, greenhouse solar dryers (GSD) have been extensively employed by various stakeholders. The operation of these conventional GSD is though allowing cool or cold ambient air to enter them during drying. Consequently, temperature and relative humidity of the air inside the GSD is lowered and increased respectively thereby increasing the drying time which is undesirable, and reducing the overall efficiency of the GSD. The research study aimed at designing, fabricating a parabolic trough solar collector (PTSC) air heater for a GSD and testing its performance. Additionally, the performance of the modified GSD with and without the PTSC was investigated. Quantitative research design was employed in carrying out of this research study. The specific methodological approaches of the research study included, design of the PTSC air heater, fabrication of the PTSC air heater, testing of the PTSC air heater, experimentation for data collection, data analysis using Microsoft Excel and reporting. Key geometrical parameters for the designed PTSC air heater were rim angle of 98^{o}, focal length of 0.2608 m, height of 0.3451 m, aperture width of 1.2 m and PTSC length of 2m giving a collector area of 2.4m^{2}. The PTSC air heater was tested and attached to the GSD that acted as the drying chamber with a total volume of 35.625 m^{3}. With a PTSC air heater thermal efficiency of 5.3 percent, the results showed that the maximum temperature at the absorber tube was 86.7 ^{o}C and temperature of the heated air was 80.1 ^{o}C. The maximum temperature recorded inside the GSD with and without the PTSC connected was 62 ^{o}C and 44 ^{o}C respectively. The new modification of the GSD with a PTSC increased the temperature of the GSD to the optimum and stable levels of 45 ^{o}C to 60 ^{o}C required for drying tomatoes. Performance analysis of the GSD that were done included initial and final moisture content determination of tomatoes, found and reported to be 94 percent on average and 14 respectively. Drying rates of the GSD with and without the PTSC was found to be 1.738 kg/hr and 1.227 kg/hr respectively. Percentage saved time of drying 15kg equal amounts of tomatoes was found to be 27.3 percent when the PTSC air heater was connected to the GSD compared to unmodified GSD respectively. Specific energy consumption of the GSD with and without the PTSC air heater was found to be 5.54 kWh/kg and 7.627 kWh/kg respectively, specific moisture extraction rate was found to be 0.1778 kg/kWh and 0.1311 kg/kWh for the GSD with and without the PTSC air heater respectively. The thermal efficiency of the GSD was found to be 11.3 percent at 15 kg loading capacity, comparable to other hitherto similar work done by various researchers. These findings showed the significance of modifying the GSD with a PTSC air heater in improving the drying technologies of agro-based products in mitigating PHL.

Key words: Parabolic Trough Solar Collector (PTSC), Greenhouse Solar Dryer (GSD)

DEDICATION

This research work is dedicated to my family members, particularly my mum for their prayers, and unconditional support in all spheres of life during the study period. May the good Lord bless them always.

ACKNOWLEDGEMENTS

First and foremost, I would like to thank the Almighty God for the gift of life and good health throughout the study period of my Masters of Engineering program at the University of Zambia.

I will forever be indebted to the European Union (EU) and African Union (AU) through the Mobility for Innovative Renewable Energy Technologies (MIRET) program for funding my studies at the University of Zambia.

The dedication and commitment of my supervisor Dr. Isaac N. Simate to see me through the research study despite my busy schedule at campus was above and beyond my expectations. I sincerely thank him for his understanding, guidance, unwavering support and invaluable intellectual discourse we had together about my research work. God bless him always.

I would like also to acknowledge the support, assistances and contributions made by all the members of staff at the School of Engineering, particularly Mr. Chewe for his immense experience. They provided me with access to all the laboratory equipment, data and information that I needed for this research project, for this I am eternally grateful.

Finally, I would like to thank all my fellow students at the University of Zambia for their constructive critics, aid and support throughout the research study period.

TABLE OF CONTENTS

LIST OF TABLES

LIST OF FIGURES, MAPS AND ILLUSTRATIONS

LIST OF ABBREVIATIONS AND ACRONYMS

ABBREVIATIONS		SUBSCRIPTS	
PHLs	Post-Harvest Losses	o/i	initial
CSP	Concentrated Solar Power	f	final
kWe	Kilowatt energy	d/dm	Dry matter
PTSC	Parabolic Trough Solar Collector	wb	Wet bulb
OSD	Open Sun Drying	db	Dry bulb
GSD	Greenhouse Solar Dryer	p	product
PV/T	Photovoltaic/Thermal	w	water
DC	Direct Current	r	rate
SHS	Sensible Heat Storage	a	air
HUF	Heat Utilization Factor		
COP	Coefficient of Performance		
LPG	Liquefied Petroleum Gas		
M	Moisture Content		
W	Weight		
m	Mass		
t	Temperature		
h	Enthalpy		
I	Solar Radiation		
CR	Concentration Ratio		
GI	Galvanized Iron		
PVC	Polyvinyl Chloride		
AC	Alternating Current		
HTF	Heat Transfer Fluid		
RH	Relative Humidity		
SEC	Specific Energy Consumption		
SMER	Specific Moisture Extraction rate		

CHAPTER 1: INTRODUCTION

This chapter briefly introduces the research study in terms of the background, problem statement, aim of the study, study objectives, research questions, significance of the research study, and the scope of the research study.

1.1 Background

1.1.1 Post-Harvest Losses

Post harvest losses refer to the measurable qualitative and quantitative food loss along the supply chain from harvest to the final consumer (Hodges, et al., 2011). In many countries, a large number of fruits and vegetables are discarded at the postharvest stage. This occurs because many fruits and vegetables spoil before being delivered to consumers. This challenge is considered to be particularly serious in developing countries mainly due to a lack of capital and technology for food storage, processing (i.e. threshing, drying and packaging) and distribution. Improvements in storage and processing technologies can delay spoilage.

Postharvest loss is divided into food loss and food waste. 'Food loss is the decrease in the quantity or quality of food resulting from decisions and actions by food suppliers in the chain, excluding retailers, food service providers and consumers' (FAO, 2022). 'Food waste refers to the decrease in the quantity or quality of food resulting from decisions and actions by retailers, food service providers and consumers' (FAO, 2022).

One study argues that solutions for reducing postharvest losses require relatively modest investment and can result in higher returns than increasing crop production to meet food demand (Kumar & Kalita, 2017).

1.1.2 Technologies to mitigate PHLs

Different technologies have been employed to reduce PHLs of agricultural products especially fruits and vegetables. These include, (1) drying, (2) refrigeration, (3) use of cold rooms, (4) hermetic or modified atmosphere, and use of chemical treatment. Research work hereafter mainly covers the drying technology in mitigating PHLs.

1.1.2.1 Drying technology

Drying is one of the means of preservation of foods such as fruits and vegetables to last for a long time with good quality. The drying process is one of the most energy inefficient operations in the food industry (Feng, et al., 2012). Agricultural products, especially fruits and vegetables require hot air in the temperature range of 45–60˚C for safe drying. When any agricultural

product is drying under controlled conditions at specific humidity as well as temperature it gives rapid superior quality of dry product (Gutti, et al., 2012).

Drying involves the application of heat to vaporize moisture and some means of removing water vapour after its separation from the food products. It is, thus a combined heat and mass transfer operation for which energy must be supplied. The removal of moisture prevents the growth and reproduction of microorganisms like bacteria, yeasts and moulds that cause decay, and minimizes many of the moisture-mediated deteriorative reactions. It is observed that drying enables a reduction in weight and volume, minimizing packing, storage, and transportation costs and enables storability of the product under ambient temperatures (Zhang, et al., 2011).

Drying process can be achieved through open sun drying and use of dryers. The purpose of a dryer is to supply more heat to the product than that available naturally under ambient conditions, thus increasing sufficiently the vapour pressure of the crop moisture. Therefore, moisture migration from the crop is improved. The dryer also significantly decreases the relative humidity of the drying air, and by doing so, its moisture-carrying capability increases, thus ensuring sufficiently low equilibrium moisture content.

Dryers can be designed to use electricity, biomass, gas and solar energy. This research work is mainly concerned with solar dryers and in particular greenhouse solar dryers as they have the potential of being used in most rural environments. Solar dryers can be classified as direct dryers, indirect dryers, mixed mode dryers and hybrid dryers.

1.1.2.2 Air preheaters of solar dryers

These are devices which are intentionally used to improve the performance and efficiency of the solar dryers. Air preheaters heat cool ambient air before it enters the solar dryers to temperatures suitable for drying the different products. They can be devices that use solar energy to preheat the air and they are referred as solar collectors. These solar collectors are classified as flat plate solar collectors and concentrating/focusing solar collectors. Other devices that preheat air utilize electricity or fossil fuels. Out of these air preheaters, concentrating/focusing solar collectors are studied in this research work.

1.2 Problem Statement

Traditional greenhouse solar dryers heat the air inside them using the greenhouse effect. They are designed to have air inlets for allowing ambient air to enter and outlets where warm and moist air escapes from after carrying moisture from the products being dried. Ambient air usually have low temperatures. The traditional greenhouse solar dryers take in cooler ambient air into the dryer during drying, thereby lowering the temperature inside the dryer. Consequently, longer time and

higher energy is required for drying agricultural products to the desired safe moisture content level. It is therefore envisaged that preheating ambient air will significantly reduce on drying time.

1.3 Aim/purpose of the study

The research study aimed at investigating the effectiveness of a parabolic trough solar collector for preheating air used for drying in a greenhouse solar tunnel dryer.

1.4 Study objectives

1.4.1 General objective

- To design, fabricate and test the performance of a parabolic trough solar collector air heater for a greenhouse solar dryer.

1.4.2 Specific objectives

i. To design the parabolic trough solar collector for preheating drying air.
ii. To fabricate the parabolic trough solar collector.
iii. To determine the thermal performance of the fabricated parabolic trough solar collector.
iv. To compare the performance of the greenhouse solar dryer with and without the attached parabolic trough solar collector.

1.5 Research questions

i. How should the proposed parabolic trough concentrator for preheating air be designed?
ii. How should the proposed parabolic trough concentrator be fabricated and attached to an existing greenhouse dryer?
iii. What will be the thermal performance of the modified solar tunnel greenhouse dryer?
iv. Will the performance of the greenhouse solar dryer with the fabricated parabolic trough solar collector improve compared to that without the fabricated parabolic trough solar collector?

1.6 Significance of the study

New knowledge that focused on improving the performance of greenhouse solar dryers was developed which ultimately benefit the food processing industry in mitigating post-harvest losses of agricultural products.

1.7 Scope of the study

The research study was limited to solar dryers specifically greenhouse solar tunnel dryer with a parabolic trough solar concentrator air preheater as the solar thermal collector.

1.8 Ethical considerations

In line with the Natural and Applied Sciences Research Ethics Committee (NASREC) of the University of Zambia, an approved ethical clearance certificate was obtained before the research study was conducted.

1.9 Chapter Summary

This introductory chapter most importantly outlined the objectives that gave a clear direction of the research study. It was therefore imperative to constantly assess the progress of the research work at any stage against the outlined objectives. The next chapter two considers the review of the relevant literature.

CHAPTER TWO: LITERATURE REVIEW

This chapter presents various relevant literature in relation to solar energy conversion processes, solar thermal systems, parabolic trough solar collector systems and their applications, drying technology, types of dryers, greenhouse solar dryers, solar thermal collectors, modifications of greenhouse solar dryers using various methods and factors affecting solar drying.

2.0 Introduction

Solar energy is one of the most promising renewable energy sources in the world for the drying agricultural and industrial products. Solar energy is increasingly being applied in drying because of the gradual reduction in price of solar collectors coupled with the increasing concern about atmospheric pollution caused by conventional fossil fuels used for drying crops.

2.1 Solar Energy Conversion Processes

There are three energy conversion processes that are associated with the sun. These energy conversion processes are outlined and explained as follows (Weisman & Eckart, 1985):

i. Heliochemical, which is principally the photosysnthesis process,
ii. Helioelectrical, which is commonly exploited in solar cells called photovoltaics; the conversion of light directly into electricity through semiconductor materials and,
iii. Heliothermal, which is conversion of sunlight into thermal heat as employed within in solar thermal systems like concentrating solar power (CSP) plants.

The research work particularly and specifically considered solar thermal systems and their innovative applications to drying technology of agricultural products.

2.2 Solar Thermal Systems

Solar thermal (Heliothermal) systems convert solar energy to thermal (heat) energy. They can be used directly for heating purposes like hot water, domestic and industrial processing, and hot air for drying purposes. Solar thermal technologies can be classified in terms of the temperature reached by the working fluid, as exhibited in figure 2.1.

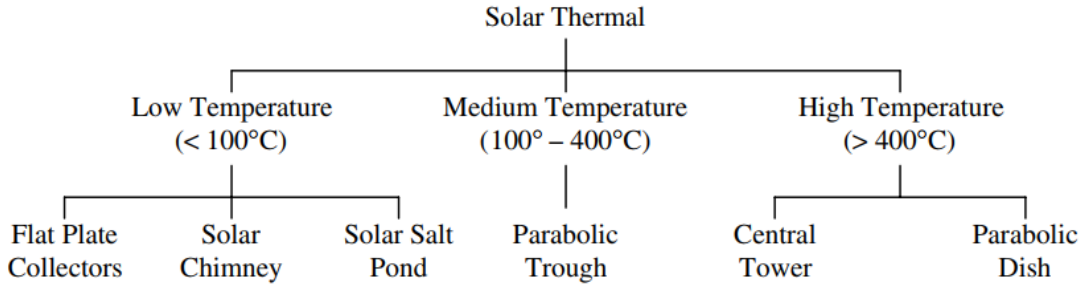

Figure 2. 1 Categorization of solar thermal technologies according to temperature *(Zobaa & Bansal, 2011)*

The CSP systems may be categorized as:

a. *Large point focus*: These CSP systems employ heliostats to concentrate light at a central receiver (power tower systems), with plants sizes of 100 kWe to 100 MWe;
b. *Small point focus*: These CSP systems use parabolic hemispherical dishes to reflect light to a focal point for each individual dish, (5–25 kWe); and
c. *Line focus systems*: These CSP systems utilize parabolic shaped troughs or linear Fresnel reflectors but having lower efficiency than the above, with plant output ranging from a few to hundreds of MWe.

In each of these three systems, a concentrator redirects (reflects) sunlight to a receiver (absorber). As can be noted in table 2.1, the working fluid temperatures for concentrating collectors are noticeably above ambient; hence, receivers may utilize vacuum barriers to prevent absorber heat loss due to convection to the surroundings.

Table 2. 1 Representative solar thermal collector operating parameters(Crabtree et al., 2008, (Zobaa & Bansal, 2011))

Thermal collector type	Concentration ratio	Working fluid temperature
Flat plate and solar pond	1	40^{o}C-100^{o}C
Line focus (parabolic trough)	10-50	150^{o}C-350^{o}C
Point focus (parabolic dish and central receiver)	100-1500	250^{o}C-1500^{o}C

2.3 Parabolic Trough Solar Collector (PTSC) System

2.3.1 Conventional PTSC

The conventional PTSC consists of a linear parabolic shape concentrator, a linear tubular receiver and a metallic support structure. The PTSC tracks the sun usually with a single axis mechanism in order for the solar rays to be delivered properly in the collector aperture. Usually, the PTSC is

placed with their axis in the North-South direction and they track the sun in the East-West direction (Duffie & Beckman, 2013).

2.3.2 Position of the absorber tube

Incident solar radiation from the parabolic trough collector to the absorber tube depends on the rim angle. In the working of PTSC, incident solar radiation will hit the reflector Aluminium foil, which reflects most of the radiation to the absorber tube placed on the focal line of the parabolic trough reflector. The following is a discussion of three different case scenarios relating to the position of the absorber tube.

2.3.2.1 Case I: Rim angle (φ_r) = 90^o

Figure 2.2 below shows how the radiation is reflected on to the absorber at the focal line. It is evident that 50% of the absorber is not exposed to concentrated radiation and thus is disadvantageous due to heat loss through conduction. However, a rim angle of 90° is found to be a more suitable option in the application of PTSC because it minimizes reflected beam spread, tracking, and slope error (Motwani, et al., 2020). Additionally, it will make the focal length to be equal to the height or depth of the PTSC.

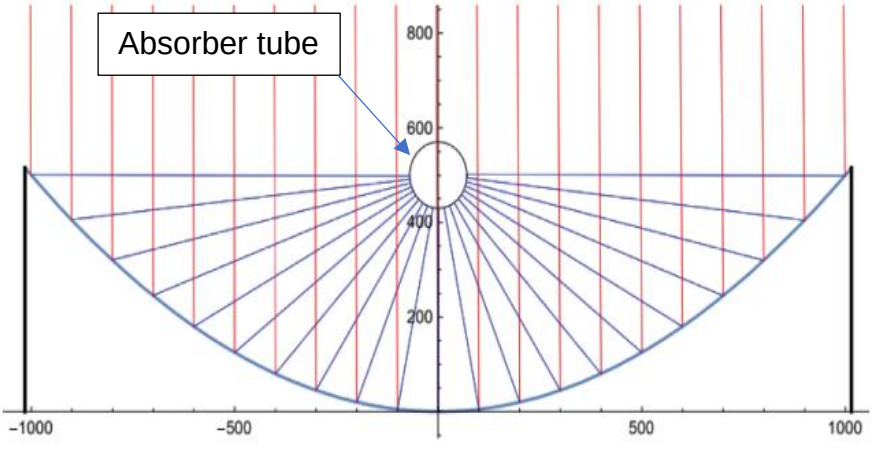

Figure 2. 2 Effect of solar radiation over absorber tube with rim angle (φ_r) = 90^o (Motwani, et al., 2020)

2.3.2.2 Case II: Rim angle (φ_r) < 90^o

It can also be observed from the figure 2.3 below that when the rim angle is ≤ 90°, then all the sun rays would cause an incident from the middle half to the lower part of the absorber tube. Therefore, the area above the upper half (50%) of the absorber tube does not receive any concentrated radiation, and due to the high conductivity of the absorber tube, it plays an essential

part in heat losses which is undesirable. A small rim angle of less than 90° causes a reduction in the collector surface area, which directly affects the performance of PTSC.

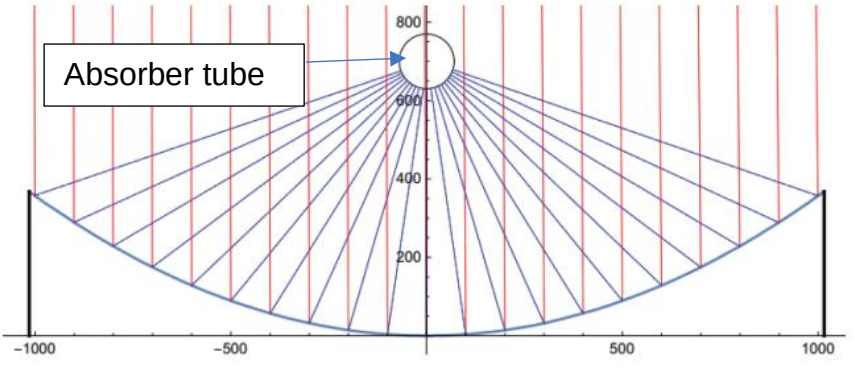

Figure 2. 3 Effect of solar radiation over absorber tube with rim angle (φ_r) < 90^o (Motwani, et al., 2020)

2.3.2.3 Case III: Rim angle (φ_r) > 90^o

The rim angle greater than 90° causes few radiations to strike on the upper half of the absorber, which adds an advantage of reducing heat loss through conduction. However, a rim angle higher than 90° increases the cost of the collector as a result of an increase in the surface area. Figure 2.4 below shows the effect of solar radiation on the absorber tube when rim angle (φ_r) > 90^o.

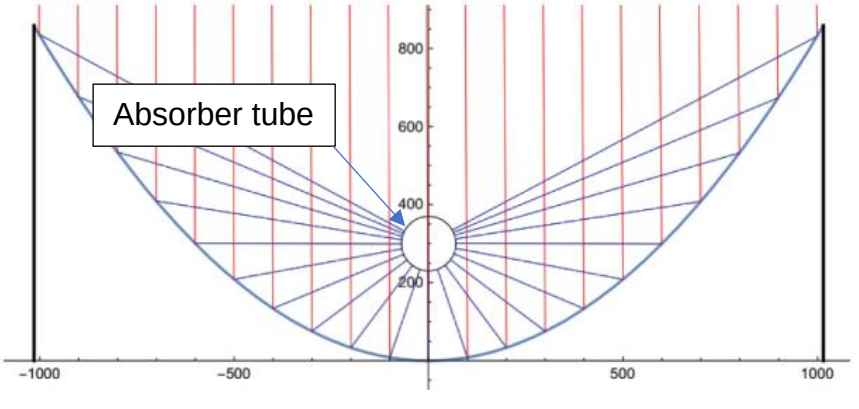

Figure 2. 4 Effect of solar radiations over absorber tube with rim angle (φ_r) > 90^o (Motwani, et al., 2020)

2.3.3 Applications of PTSC

There are numerous applications regarding the PTSCs for a specific geographic location, as for example power generation, heat pump, cooking, desalination, water pasteurization, low enthalpy processes, and solar air heating systems to industrial processes(Abdulhamed et al., 2018). The solar air heating system has no negative impact on the environment because it is sourced from green energy. The solar air heating systems is used to heat buildings and for drying applications

in the marine foodstuff, agriculture, and textiles industries. This research study specifically looks into how PTSCs can be applied in drying applications for agricultural products.

2.4 Drying

Drying is a post-harvest process carried out for preserving agricultural products like vegetables, fruits and spices. Most of the agricultural products possess a certain amount of moisture content. The reduction of moisture contents present in the agricultural products results in reducing the growth of microorganisms, which cause decaying and deterioration of the product. Another advantage of reducing the moisture content of the product is reduction in the weight to volume ratio, which in turn leads to a reduction in storage space, packaging, and transportation of dried crops (Okos, et al., 2006).

Drying is carried out mainly to increase the storage life of the harvested agro-based products and to preserve their nutrition values. Drying process can be accomplished by the use of traditional open sun drying (OSD) method, solar dryers and electrical dryers. This research work is more inclined to solar dryers and OSD methods as both utilize the renewable solar energy resource.

2.4.1 Principle of Drying

The drying of any material involves the migration of water from the interior of the material to its surface and the removal of the water from the surface. The rate of movement differs from one substance to another. The rate of drying is dependent on the volume, temperature and moisture content of the air passing over the material (Karim & Hawlader, 2004).

Simultaneous heat and mass transfer processes occur during the drying process. The water in the product is heated, and evaporated as vapour from the product surface during the drying process. The movement of water vapour within the product is governed by different mechanisms like, capillary flow, pressure gradient, diffusion, and gravity (Mujumdar, 2014).

The usual practice is to heat ambient air which lowers its relative humidity and increases its capacity to absorb water. This warm dry air is then passed over the material to be dried. The warm air absorbs the moisture and dries the produce and then the moisture laden air is exhausted. The energy requirement for drying different products can be determined from the initial and final moisture content of each product (Zobaa & Bansal, 2011).

Agro-based products have different drying rates and maximum allowable temperatures. For this research study, tomatoes were used as the product for drying. To achieve the highest quality of tomatoes, many studies, including Andritso, et al., (2003), recommend drying tomatoes at mild temperatures between 45 ^{o}C and 60 °C. Temperatures lower than this lead to longer drying times,

increasing the risk of microbial activity. Higher temperatures can result in shell hardening, and can cause color and aroma quality losses (Andritso, et al., 2003).

2.4.2 Open Sun Drying

Open sun drying is one of the traditional drying methods used by farmers across the globe for preserving the agricultural products. Traditionally, the drying of agricultural products is carried out under the open sun. Open sun drying method removes the moisture content present in the product by evaporation using the heat received from the sun's incident solar radiation (Belessiotis & Delyannis, 2011). Open sun drying has several drawbacks, including long drying time, wastage of products due to rain, dust, bird droppings and growth of fungi, reabsorption of moisture due to interrupted drying, and deterioration of the colour (Srinivasan & Muthukumar, 2021). This leads to losses due to uncontrolled drying, besides causing contamination of the product.

2.4.3 Solar Drying

A solar dryer is a device which uses solar energy for drying of agricultural products. There are several processes by which heat can be transferred to a substance like conduction, convention and radiation. Solar heated air is suitably used for the moisture removal without damaging the products. Solar dryers can be grouped according to two main aspects (i) the movement of air inside the dryer, and (ii) products exposure to solar radiation as well as hybrid that is shown in figure 2.5.

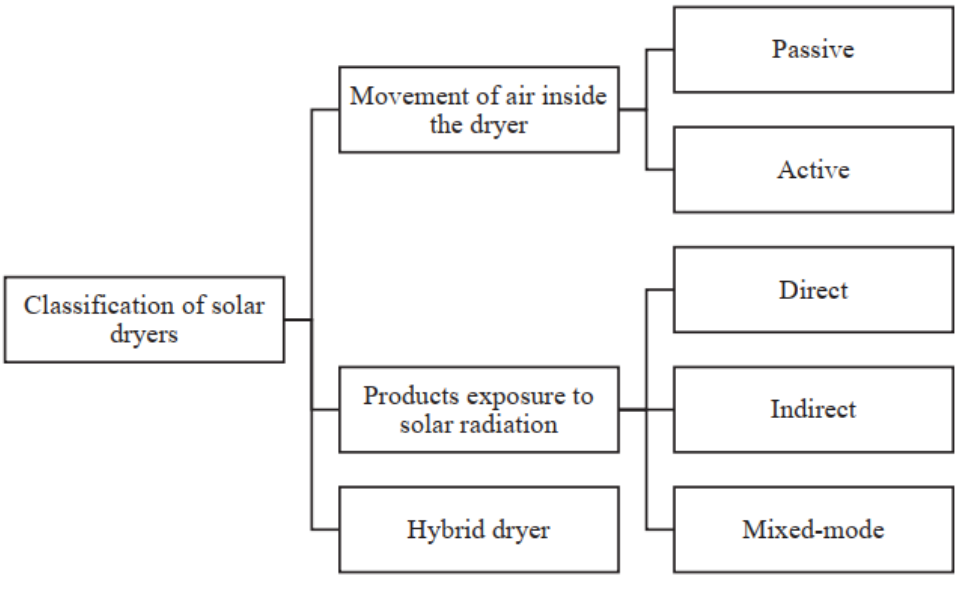

Figure 2. 5 Classification of solar dryers (Kamarulzaman et al., 2021a)

2.4.3.1 Solar dryer technologies based on the movement of air

According to the air motion within the solar dryer, solar dryers are mainly divided as passive and active solar dryers. A brief description of each of them is as follows:

a. Passive solar dryers

They are also called natural circulation solar dryers. These types of solar dryers are made of simple construction whereby the air moves naturally inside the dryer due to buoyancy effect. There are several designs that have been developed by various researchers. Figure 2.6 shows a box solar dryer type of passive mode.

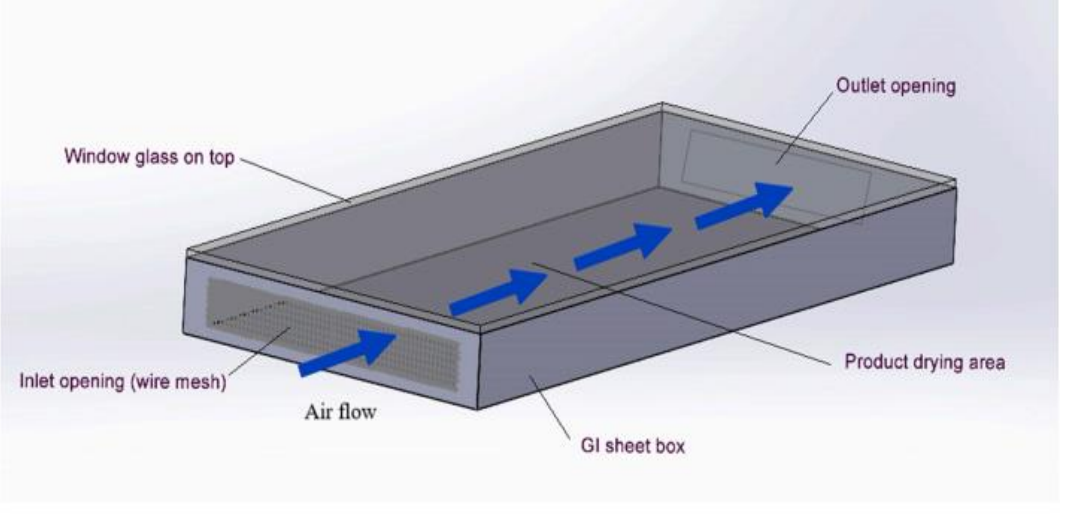

Figure 2. 6 Box type passive solar dryer (Mohsin et al., 2011)

b. Active solar dryers

Active solar dryers are also called forced circulation solar dryers. In the active solar drying system, hot air is generated outside the drying chamber. In these types of solar dryers, a fan or blower is used to facilitate the flow of air within the dryer and drying chamber, enhancing heat transfer to the product. In addition, the fan also maintains the required air flow rate in the dryer and hence moisture evaporation from the product is more consistent. Figure 2.7 shows a schematic diagram of an active solar dryer.

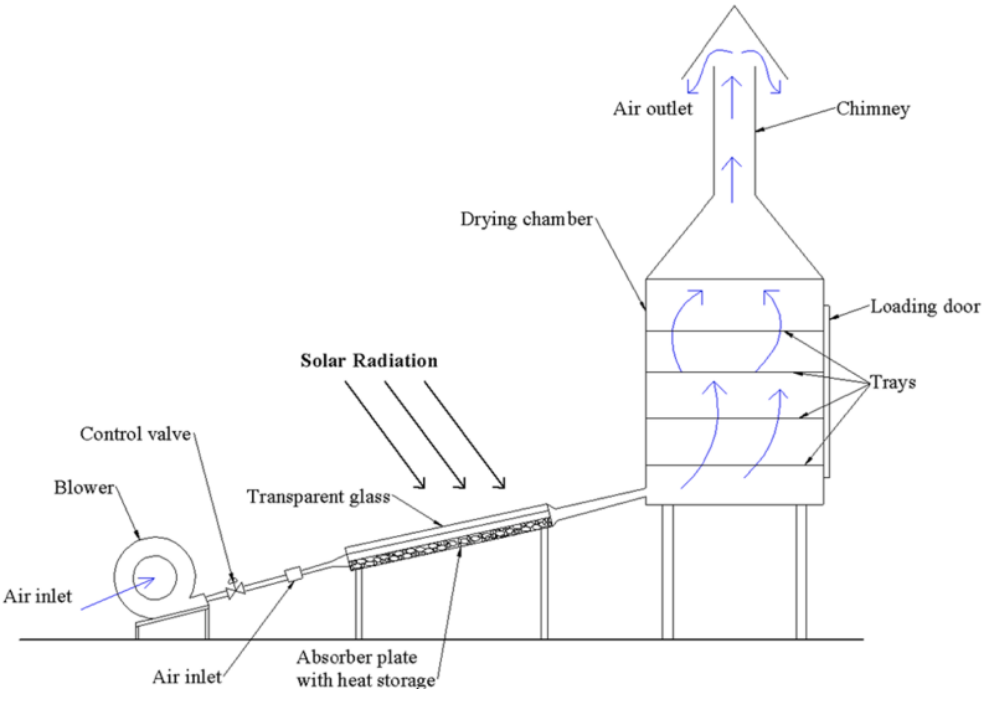

Figure 2. 7 Schematic diagram of an active solar dryer (Vijayan et al., 2020)

2.4.3.2 Solar dryer technologies based on product exposure to the solar radiation

According to the product exposure to the solar radiation, the solar dryers can be divided mainly into direct, indirect and mixed-mode solar dryer. Their description is covered in the following sections:

a. *Direct solar dryers*

In these types of solar dryers, the products to be dried are placed inside a drying chamber and directly exposed to the solar radiation. Figure 2.8 below shows a direct solar dryer.

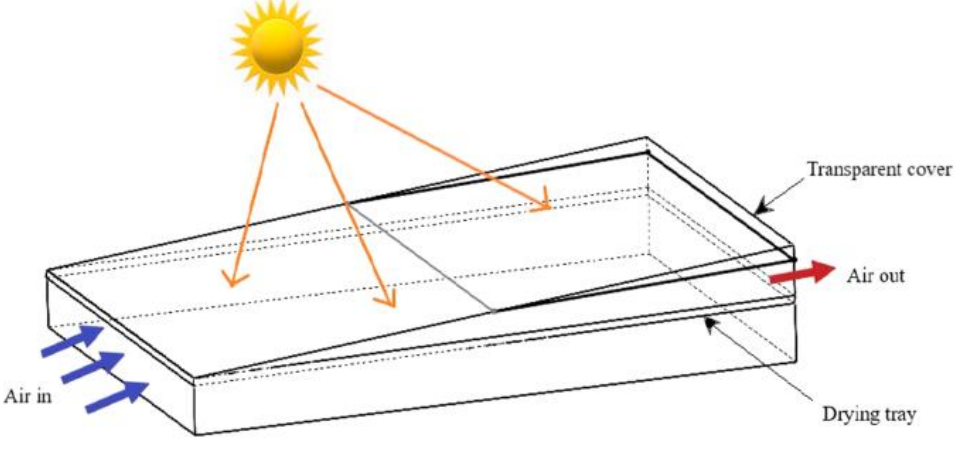

Figure 2. 8 Direct solar dryer (Kumar et al., 2016)

b. Indirect solar dryers

In these types of solar dryers, the solar radiation is incident on a separate solar collector which subsequently heats the air inside it. The heated air thereafter travels to the drying chamber to remove moisture from the products. The drying chamber is made of an opaque or solid material which prevents direct sunlight exposure of the products as shown in figure 2.9 below.

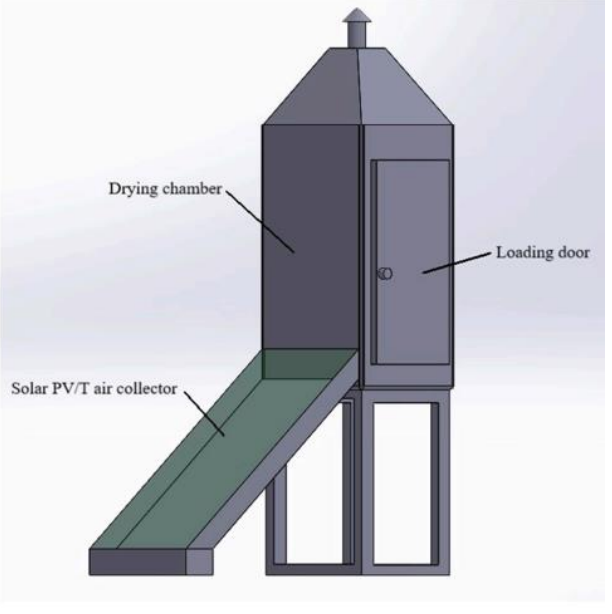

Figure 2. 9 Indirect solar dryer (Slimani et al., 2016)

c. Mixed-mode solar dryers

The combination of direct and indirect types is the one described as a mixed-mode solar dryer. In mixed-mode solar dryers, the products are directly and indirectly exposed to the solar radiation as shown in figure 2.10 below.

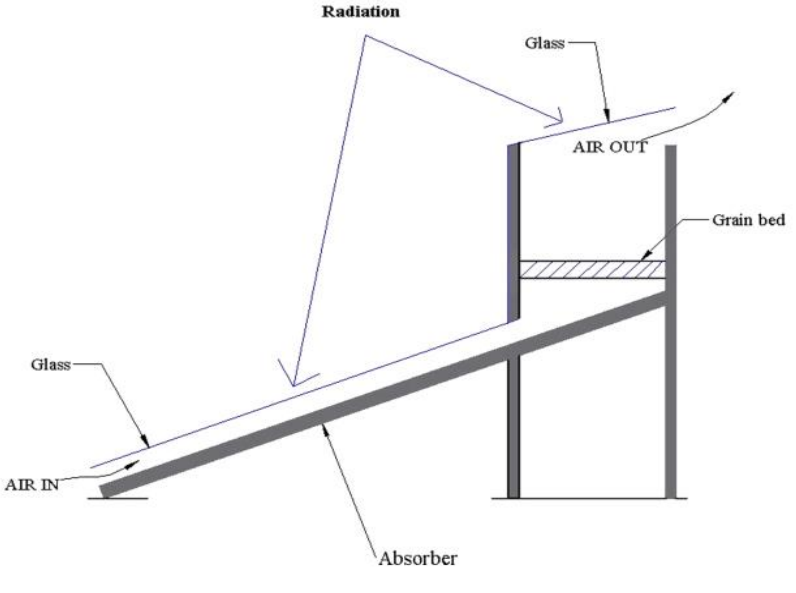

Figure 2. 10 Mixed-mode type solar dryer (Simate, 2001)

2.4.4 Greenhouse Solar Drying (GSD)

The GSD is essentially a poly house made of different shaped frames, over which a glass, polycarbonate or poly-urathane sheet is wrapped, where temperature, air flow rate and relative humidity required for drying the products can be maintained by placing the axis of tunnel in such a way that maximum sunlight can be trapped during the day (Zobaa & Bansal, 2011).

Greenhouse solar drying has two drying modes. The first mode is called passive drying. The passive greenhouse dryer has no forced convection equipment such as fans. During the drying process, according to the principle of thermosiphon effect, the hot and humid air after heat exchange with the drying material is ventilated through the ventilation device on the roof or through the chimney of the dryer. This kind of drying device is suitable for drying some materials with low moisture content and small quantity.

The second mode is called active drying. The active greenhouse dryer realizes forced circulation by adding a fan in the dryer. Compared with the passive type, the added fan and other equipment could speed up the flow of wind in the greenhouse, and could take more moisture from the surface of agricultural products. Therefore, the active greenhouse drying is suitable for drying large amounts of agricultural products with high moisture content like tomatoes.

2.5 Solar Thermal Collectors

The heart of any solar thermal device is the solar collector. Solar radiation is absorbed in a solar collector and the absorbed solar energy is converted into heat to raise the temperature of the working fluid. There are two types of collectors namely: flat-plate collector and focusing collector. Following is their description in details.

2.5.1.1 Flat plate collector

Flat-plate collectors are the more commonly used types of collectors in drying operations. They are also used for domestic household hot-water heating and for space heating, where the demand temperature is low. The schematic view of flat plate collector is shown in figure 2.11.

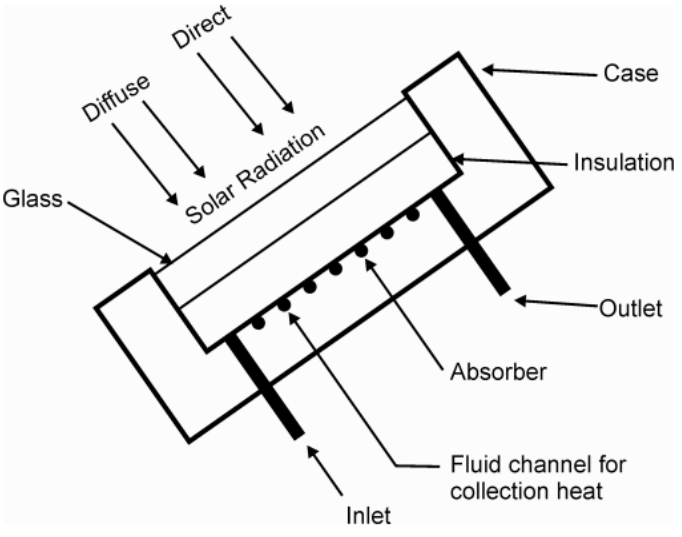

Figure 2. 11 Schematic view of a flat plate collector (Zobaa & Bansal, 2011)

The basic parts noted are an absorber, transparent cover and an insulated box. The absorber is usually a sheet of high thermal conductivity metal with tubes or ducts either integral or attached. Its surface is painted or coated to maximize radiant energy absorption. The transparent cover called glazing, lets sunlight pass through to the absorber but insulate the space above the absorber to prevent cool air from flowing into this space. The insulated box provides structure and sealing and reduces heat loss from the back and sides of the collector.

2.5.1.2 Concentrating (focusing) solar collector

Concentrating solar collectors employ an optical device to focus the incoming solar radiation to a smaller collection area, thus more concentrated heat and higher temperature are attainable. Significant advantages of concentrating solar collectors include higher temperature, higher thermodynamic efficiency, and greater thermal efficiency, less material required for reflecting surface and economically viable(Kamarulzaman et al., 2021b). The schematic diagram of a focusing solar collector is shown in figure 2.12.

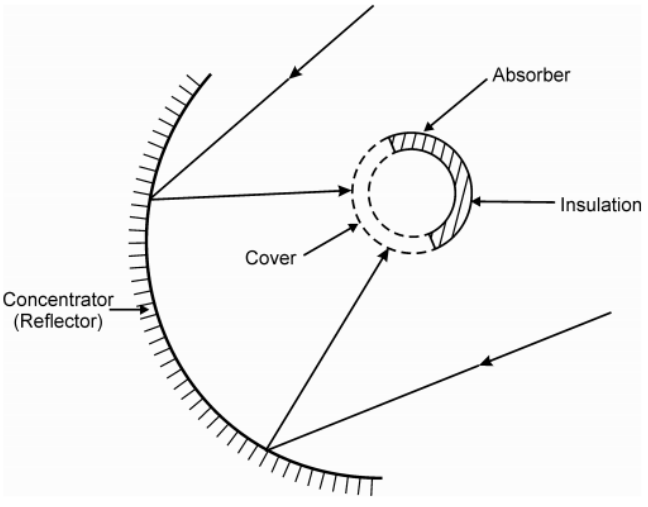

Figure 2. 12 Schematic diagram of a focusing collector (Zobaa & Bansal, 2011)

The next section, covers some applications of the solar thermal collectors in modifying and improving the greenhouse solar dryers.

2.6 GSD Modifications

In the last two decades, many types of solar tunnel dryers have been developed in various countries. Many studies on natural convection solar drying of agricultural products have been reported. However, the success achieved by natural convection solar dryers has been limited due to low buoyancy induced air flow. This has prompted researchers to develop forced convection solar dryer.

Prakash & Kumar, (2013) have done a comprehensive review on recent trends in solar dryers and reported that forced convection of solar dryers are effective and more controllable than natural circulation. The authors also pointed out that solar energy can be effectively used for low temperature drying and there is a huge demand for efficient solar dryers incorporated with thermal energy storage medium.

Greenhouse dryers operating in active or passive mode have been reported to give better results in terms of quality, color, drying time, etc. as compared to drying under the open sun. Various research works have been done to improve the efficiency of greenhouse solar dryers.

Some GSD have been modified to hybrid ones to give higher drying efficiencies by researchers. The result of a hybrid GSD is a step forward towards the utilization of solar energy in a more effective manner. Hybrid greenhouse solar dryers are those which utilize two sources of energy or utilize single source (solar energy) in different ways.

The methods by which the GSD are converted into a hybrid GSD are shown in the figure 2.13 below.

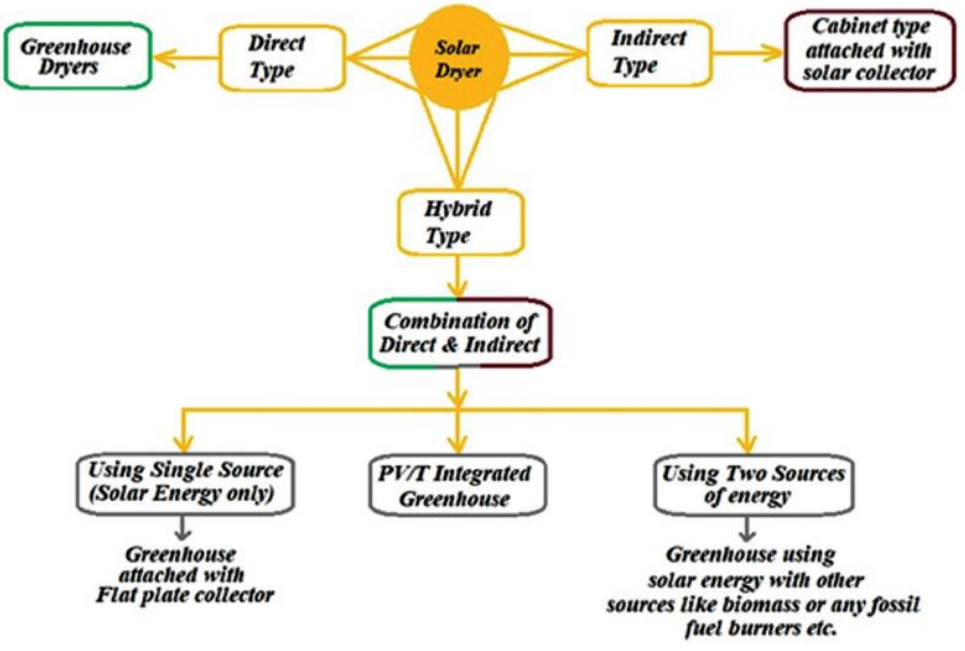

Figure 2. 13 Methods used for making a GSD hybrid (Singh & Gaur, 2022).

Figure 2.13 shows that GSD can be converted into hybrid ones by three methods namely:

i. Photovoltaic/Thermal (PV/T) integrated greenhouse solar dryers
ii. Greenhouse attached to solar collectors (flat plate or focusing/concentrating)
iii. Greenhouse attached with other air heating devices like biomass or any other fossil fuel burners.

A more elaborate discussion follows with examples of each of the above methods above.

2.6.1.1 PVT integrated with GSD

The GSD are usually modified by attaching the PV/T modules for generating electric energy to operate the fans and other auxiliary devices. PV/T panels are those which not only produce electricity from solar energy but also heat for heating the air inside the dryer.

Barnwal & Tiwari, (2008) developed a GSD integrated with a PV/T collector shown in figure 2.14. The GSD was evenly spanned roof type, having 6.5 m^2 floor area and enclosed with polyethylene sheet. DC fans operated by PV modules were used to circulate air inside the dryer. Matured (GR-II) and pre-matured (GR-I) grapes were dried in the GSD and compared. The heat transfer coefficient for the GR-II type was found to be greater than GR-I type.

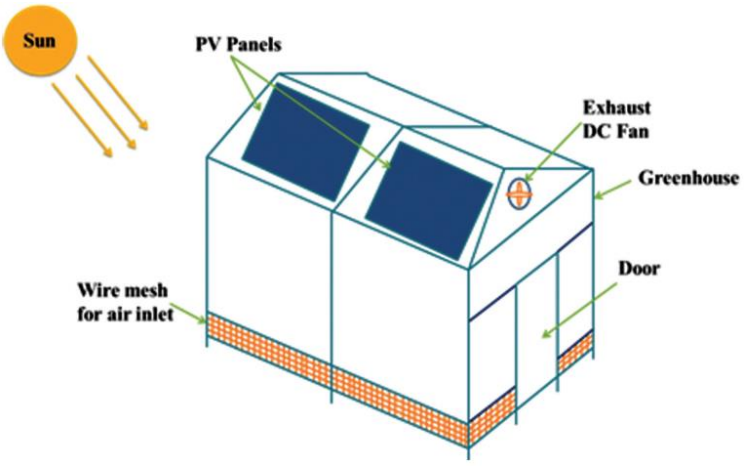

Figure 2. 14 PV/T integrated with the GSD (Barnwal & Tiwari, 2008)

Tiwari et al., (2016) developed a PV/T integrated mixed-mode hybrid dryer having a ground area of 1.066 m^2 and was enclosed with 3mm glass. Two DC fans operated by PV panels were provided for forced circulation of air. MATLAB 2013 was used for numerical computation of thermal models developed to consider parameters like the temperature of the crop and of the greenhouse, and PV module, among others. Figure 2.15 shows how the GSD was modified with the PV module.

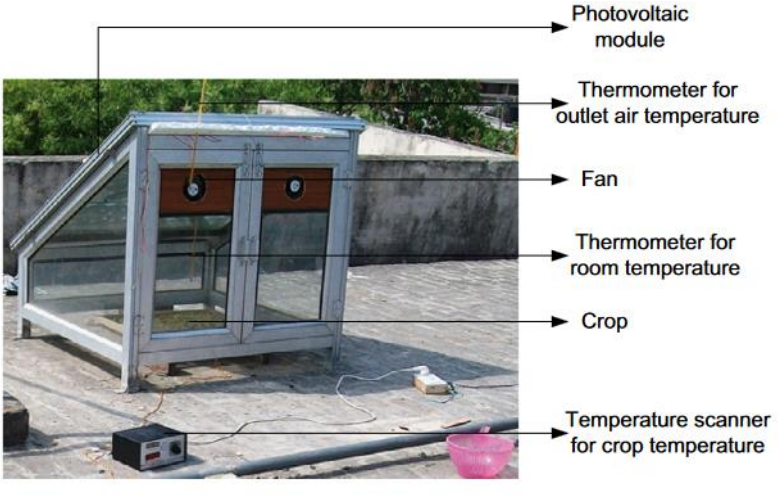

Figure 2. 15 Photograph of PV integrated GSD (Tiwari et al., 2016)

Benedict, et al., (2019), developed a cost-effective PV ventilated greenhouse dryer for commercial preservation of tomatoes in a rural setting. The researchers designed a forced convection solar dryer ventilated by fans operated by a photo-voltaic system. This drying unit was integrated into a solar collector with a cost-friendly thermal energy storage system to store solar energy during the day for use after sunset for better performance. Sensible heat storage (SHS) systems are relatively simple and relatively of lower cost compared to chemical or latent thermal energy storage systems. The study concluded that forced convection type of dryers dried products faster than natural convection ones.

2.6.1.2 GSD attached with solar collectors

Solar collectors, both flat and concentrating have also been used by different researchers to preheat the air externally in the collectors and then supplying it to the greenhouse drying chamber. A schematic representation of the GSD attached to a solar collector is shown in figure 2.16.

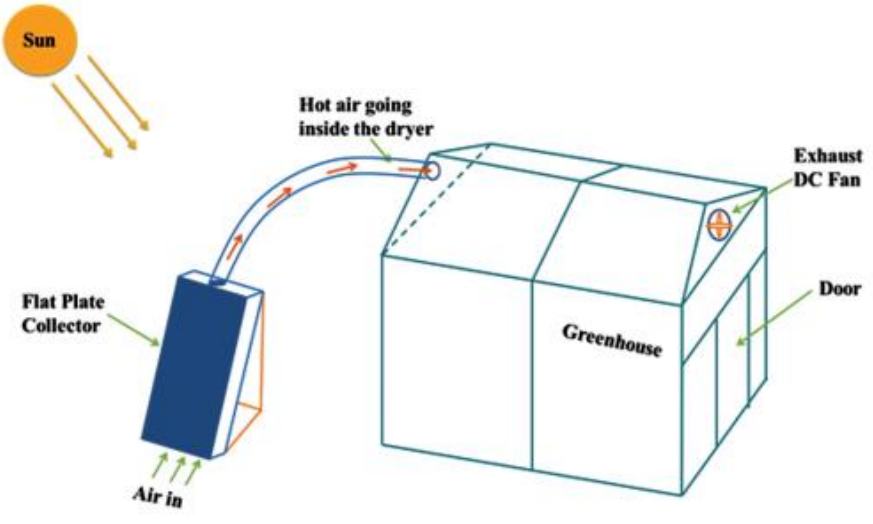

Figure 2. 16 GSD integrated with a flat plate collector (Singh & Gaur, 2022)

Simate & Simukonda, (2022) developed a GSD modified with a vertical flat collector for drying. They reported that the incorporation of a vertical solar collector inside the drying chamber aided in storing heat in its mass. In addition, the vertical thermal collector preheated and stabilized the drying chamber air temperature which was on average 14.7 ^{o}C above ambient and made the forced convection dryer more compact. The figure 2.17 below shows the fabricated GSD incorporated with a vertical solar thermal collector.

Figure 2. 17 GSD modified with a vertical solar thermal collector (Simate & Simukonda, 2022)

Eltawil et al., (2018) developed a tunnel type dryer coupled with flat-plate collector and PV panels. Peppermint was dried inside the dryer in one, two, and three layers for evaluating dryer performance. The maximum drying time was 360 minutes inside the dryer while 420 minutes was under the open sun. The use of a thermal curtain gave better quality mint as compared to drying under the open sun. The dryer was reported to have an efficiency of 30.71%. Figure 2.18 below shows the GSD modified with a flat-plate solar thermal collector and PV module.

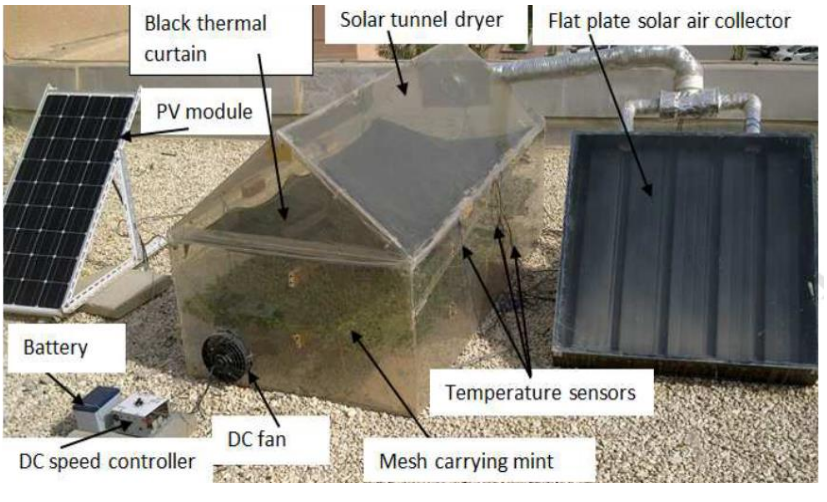

Figure 2. 18 GSD modified with a flat plate solar thermal collector and PV module (Eltawil et al., 2018)

ELkhadraoui et al., (2015) carried out an economic analysis and performance evaluation of the GSD modified with a flat plate solar thermal collector shown in figure 2.19 below. The GSD operated in forced convection mode and was used for drying red peppers and grapes. The GSD payback duration was reported to be 1.6 years. The result showed that the drying time for grapes

and red pepper was 50 hours and 17 hours respectively inside the dryer while it was 67 hours and 24 hours respectively under the open sun.

Figure 2. 19 GSD modified with a flat plate solar thermal collector (ELkhadraoui et al., 2015)

A semi-cylindrical greenhouse dryer with a flat-plate solar collector was constructed by Mehta et al., (2018). Fish was dried inside the dryer to test its performance. To predict the collector temperature at its outlet, a mathematical model was established and then solved by the SageMath programming language. The drying time of fish was 18 hours inside the dryer while it took 38 hours in the open sun. Figure 2.20 below shows the modified GSD.

Figure 2. 20 GSD modified with flat plate collectors (Mehta et al., 2018)

Chauhan & Kumar, (2016)constructed the north wall insulated GSD shown in the figure 2.21. The GSD was tested with and without a solar collector. The dryer was operated in passive mode and tested in a no-load condition. The dryer performance in terms of heat utilization factor (HUF), coefficient of performance (COP), heat loss factor, among other parameters were

calculated. The result showed that the GSD with a collector had better HUF and COP than the dryer without a collector.

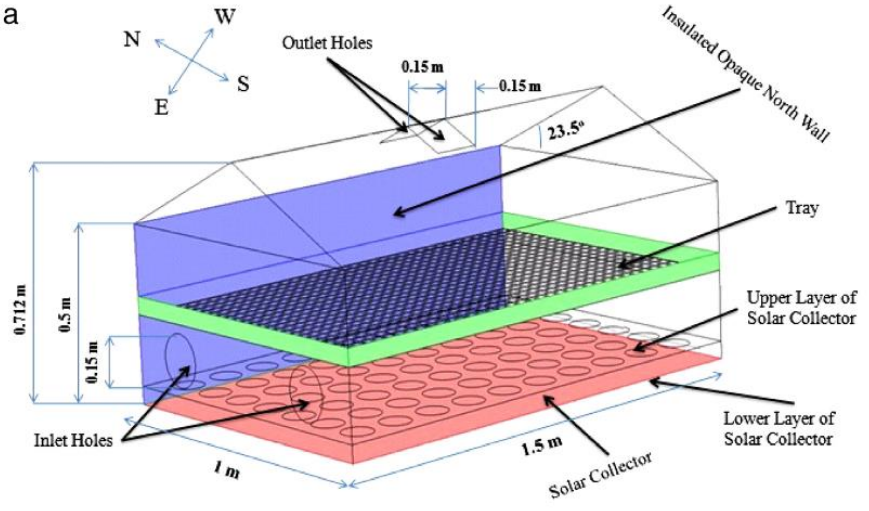

Figure 2. 21 GSD with a solar collector (Chauhan & Kumar, 2016)

Sookramoon, (2016a) developed a tunnel GSD combined with a parabolic trough for paddy drying as shown in figure 2.22 below. A 2.27 m² parabolic trough stainless steel collector made with a single-axis solar tracking system produced hot water and delivered to the crossflow heat exchanger equipped with a tunnel GSD with the size of flat plate collector of 2.112 m^2. The system received solar radiation and reflected sunlight to the receiver at the focal point of a parabolic trough. At this point, a copper heat pipe with the inside diameter of 25.4 mm for water heating was placed. The average drying temperature was 57.73 °C. The paddy moisture content was reduced from 49.96% to 15.61% dry bulb in 6 hours.

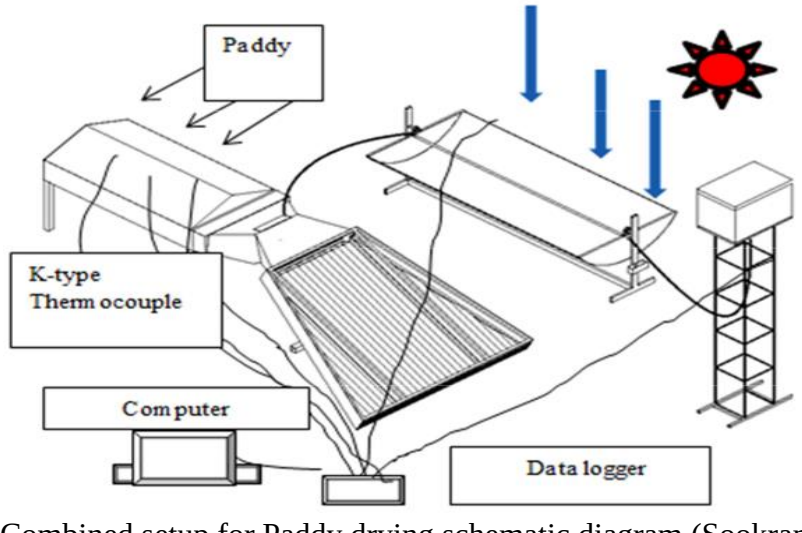

Figure 2. 22 Combined setup for Paddy drying schematic diagram (Sookramoon, 2016a)

2.6.1.3 Other air heating devices attached to the GSD

The other method applied in modifying the GSD is the attachment of auxiliary air heating devices like biomass or LPG burner. In addition, these devices supply the hot air during the off sunshine period. This increases the operating time of dryer so its drying time also gets reduced.

Hamdani et al., (2018) developed the tunnel type greenhouse dryer shown in the figure 2.23 below attached with biomass burner. The drying area was 2.08m^2 and the dryer was enclosed with a transparent plastic sheet. Queenfish was dried for evaluating the dryer performance. Wood was used as fuel for supplying hot air during off-sunshine hours. The result shows that in 15 hours, the fish was dried to 12% moisture level.

Figure 2. 23 GSD modified with a biomass burner (Hamdani et al., 2018)

Deeto et al., (2018) developed a greenhouse attached with a solar collector and heat storage unit. The floor area of the dryer was 0.3 m^2 and was mounted on a black PVC sheet. A water storage tank of 180-liter capacity and insulated with polyurethane foam was attached to the dryer for storing hot water. Coffee beans were dehumidified from 55% to 12% wet bulb in 12 hours. The model suitable for coffee drying was also determined. Figure 2.24 below is the schematic setup for the model.

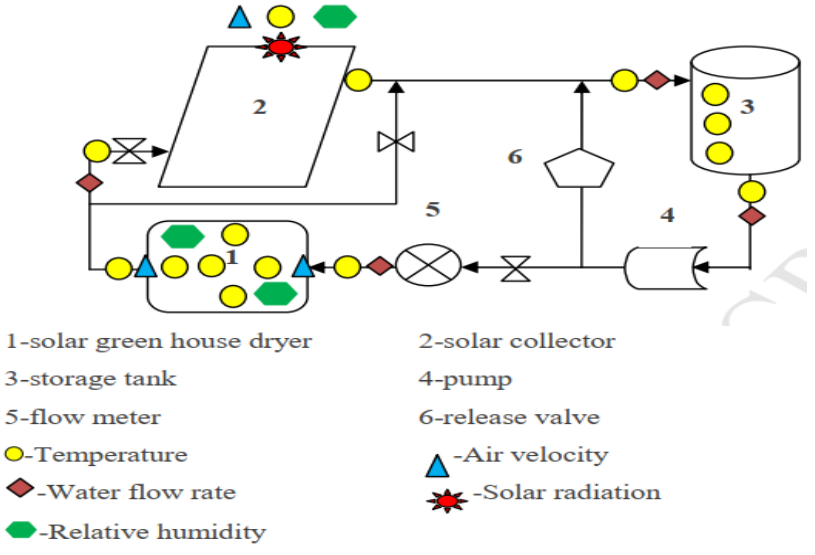

Figure 2. 24 Schematic setup for GSD modified with a solar collector and heat storage unit (Deeto et al., 2018)

Kıyan et al., (2013) proposed a hybrid greenhouse attached with a hot water storage unit and fossil fuel heater as shown in figure 2.25. A mathematical model was developed for the proposed setup. The models were solved by simulation software MATLAB/ Simulink. A case study was done on the GSD to check the feasibility of the developed models.

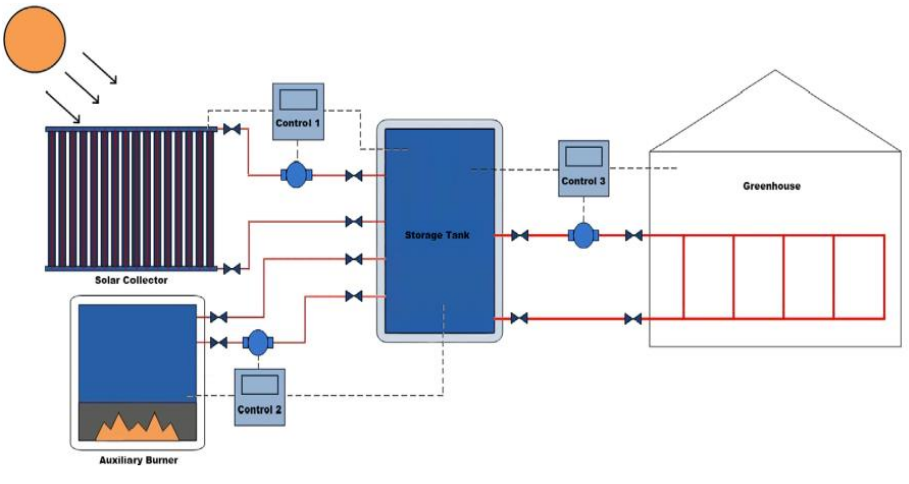

Figure 2. 25 Schematic layout of the GSD modified with hot water storage unit and fossil fuel heater (Kıyan et al., 2013)

Janjai, (2012) constructed the parabolic shaped greenhouse shown in the figure 2.26 attached with a liquefied petroleum gas (LPG) gas burner. The dryer had a ground area of 160 m^2 and was enclosed with a polycarbonate sheet. PV panels operated nine DC fans provided the air circulation. The GSD was used to dry tomatoes and the highest temperature recorded inside the dryer was 65 °C. The solar greenhouse dryer was easy to construct and was suitable for commercial-scale applications because of the fast-drying rate. However, a cheaper source of auxiliary energy than LPG gas could reduce the operational cost of the dryer.

Figure 2. 26 GSD modified with a LPG burner (Janjai, 2012)

2.6.1.4 Knowledge gap on improvements of GSD

It is evident from the above literature review that preheating air for drying reduces the drying time. Most research work is done on PV/T and flat plate collectors, hence the need to carry out more research work on concentrating/focusing solar thermal collectors. This research study therefore, looks into an improved GSD with parabolic trough solar concentrator air preheater.

2.7 Major Factors Affecting Solar Drying

Solar drying is a continuous process where moisture content, air and product temperature change simultaneously along with the two basic inputs to the system, i.e. the solar insolation and the ambient temperature. The drying rate is affected by ambient climatic conditions.

2.7.1.1 Solar Radiation

Solar radiation is composed of three components; the direct, indirect and reflected solar irradiance. These components of the global solar irradiance all determine the total amount of energy that will be received on a collector's surface and can be measured by a pyranometer. It varies depending on the geographic location, climatic conditions, the clearness of the sky, position of the sun, and the day of the year. Higher readings can be recorded on a clear and sunny day than on cloudy day or when the sun is down. The higher the available solar irradiance, the higher the temperature and therefore the higher the drying rate.

2.7.1.2 Temperature

The drying rate of products depends on the air temperature. Solar radiation received by the GSD or a solar collector is converted to heat which increases the temperature of the air in the drying chamber. This increase in temperature of the air in turn heats up the crop surface which causes the moisture in the crop to migrate to the surface and is vaporized. Usually, the higher the temperatures in the chamber, the higher the drying rates. However, some crops have specific maximum temperature under which they can be dried and if exceeded might lead to their deterioration.

In direct solar dryers, the drying material absorbs solar radiation and transfers a portion of the heat to the drying air entering the dryer. This air in turn carries away evaporated moisture from the drying material while in the case of an indirectly heated solar dryer, the air is preheated in the collector and then enters the drying unit.

2.7.1.3 Relative Humidity

The drying potential of a GSD depends on the difference between the moisture content of the product and the equilibrium moisture content of the drying material determined by the temperature and relative humidity of the drying air. If the relative humidity is higher, the drying potential is lower and hence a lower drying rate.

The ability of a crop to dry is dependent on the ratio of the amount of moisture in the crop to that of the immediate surrounding air. If the surrounding air has a lower relative humidity, it means that the surrounding air can accommodate moisture migrating from the crop. Therefore, the lower the relative humidity inside the GSD, the higher the drying rate and vice versa.

2.7.1.4 Moisture Content

The selection of the design of solar dryers is guided by the initial moisture content and the amount of moisture to be removed from the agricultural products. The amount of moisture of the product to be removed is dictated by the expected storage period of the dried product. The lower the final moisture content, the higher is the expected storage life of the product. Again, the drying rate of the product is also influenced by the moisture content of the product.

Most agricultural food products which require drying contain some amount of water in their fresh state. This water which is also termed moisture, when present might render the products unsafe for storage as it might lead to deterioration. The moisture content of any product being dried has the potential of directly affecting the drying time. The amount of moisture content in the product is likely to determine the type of solar dryer to be selected. Two phases have been identified to characterize the drying process and they are the constant rate and the falling rate phase. The initial phase where water is evaporated directly from the produce surface is the constant rate. As the drying progresses it requires more energy to evaporate the water that is embedded in the produce. This phase is called the falling rate and the final moisture content of produce usually falls within this phase of the drying process.

2.7.1.5 Air mass Flow Rate

The air flow rate through a solar dryer is generally a measure of the quantity of air that pass through a dryer within a specified time. The quantity of air mass flowrate is usually measured in

kilogram. Therefore, the air mass flow rate is the mass of air flowing through dyer in a unit time. Higher mass flow rates denote good ventilation, and therefore increases the drying rates and efficiency of the GSD

2.8 Chapter Summary

This chapter has covered in details how solar energy resource is harnessed using various technologies and ultimately applied in drying applications of agricultural products. The next chapter three deals with the methods used in this research.

CHAPTER THREE: RESEARCH METHODOLOGY

3.0 Introduction

This chapter describes how the entire research work was carried out in order to fulfill the aforementioned objectives of the study. It gives a detailed account of the systematic procedures, processes and the types of equipment that were used for the research work.

3.1 Research Design

The research study was quantitative in nature and utilized experimental research design method. Experimental design as a subset of scientific investigation is a popular and widely used research approach. Through accurate and precise empirical measurement and control, an experimental design increases the ability to determine causal relationships and state causal conclusions of the research.

3.2 Variables

The research work utilized both independent and dependent variables. The independent variables for analysis were collected through experiments and they included: air temperature, relative humidity, solar irradiation, mass of the products being dried, time of drying and air speed of the air inside and outside the greenhouse solar dryer. Dependent variables were the performance indicators of the research being conducted the included moisture content of products being dried, drying rates of products, specific moisture extraction rate, specific energy consumption and the efficiencies of the dryer and the parabolic trough solar collector.

3.3 Study Area/Site

The research study was carried out at the Agricultural Field Station of The University of Zambia, Great East Road campus.

3.3.1 Climatic and geographical data

Agricultural Field Station, at The University of Zambia is a place in Lusaka district of Republic of Zambia. It is located at a latitude of 15º23’38’’S and longitude of 28º20’05’’E. The average solar radiation/insolation on the surface of the Agricultural Field Station is 900 W/m^2. The geographical and climatic data of the location is suitable for drying fruits and vegetables. The figure 3.1 shows the google map of the location where the greenhouse solar dryer was situated.

Figure 3. 1 Map Location (Google, 2022)

3.4 Design of the PTSC Air Heater for a GSD

3.4.1 Philosophy of the design

The basic idea of the entire research entails the application of parabolic trough collector systems in GSD, particularly those that focus and concentrate solar energy at a focal line using air as the heat transfer fluid. The GSD was modified with a PTSC with a goal of increasing the drying efficiency and reducing drying time. Figure 3.2 below shows a line focus parabolic trough solar collector.

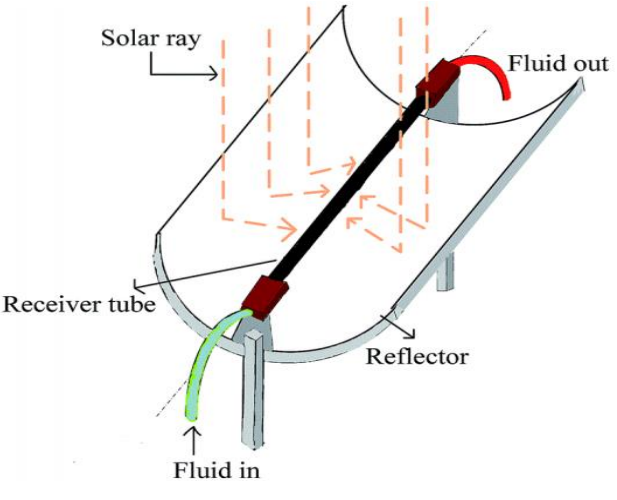

Figure 3. 2 A line focus parabolic trough collector (Dabiri & Rahimi, 2016)

3.4.2 Working principle of the modified GSD with the PTSC

The modified GSD operated under mixed -mode forced convection operation principle. A mixed-mode forced convection GSD is designed for the maximum harnessing of solar radiation. It

utilizes the direct heat from solar radiation through greenhouse plastic cover as well as preheated air from PTSC air heater connected to the GSD.

3.4.3 Laboratory Determination of Initial Moisture Content for Tomatoes

Preliminary investigations were conducted on the tomatoes considered for drying to determine their initial moisture content. This exercise informed the approximate amount of moisture that was to be removed from the tomatoes during dried.

Tomatoes for carrying out experiments were bought from the local market, Soweto and directly from farms. The tomatoes were initially washed with running water to remove any dirt. No chemical pre-treatment of the tomatoes was done before and during drying. A vegetable cutting knife was used to cut the tomato samples to slices of approximate 4mm thickness.

The oven-method procedure of the hot air oven method according to AOAC 1990 for determination of moisture content of sliced tomato was followed. Two small pieces were cut from one randomly selected tomato and the average of their moisture contents calculated. The initial weight of each tomato piece samples with their dishes were recorded after determining the weight of the empty dishes. Then, the weights of the samples were measured and recorded using the time scale given in table 3.1 while drying in the oven. The two samples of the tomato were placed in oven set at 60^0 and dried for the first 2 hours and their weights were measured and recorded. The tomato samples were dried again for 2 hours after which their weights were measured at an interval of 1 hour to monitor the weight change with time and the results recorded as given in table 3.1.

The decreasing masses of the sample pieces were monitored until a final stable weight was reached by means of a calibrated digital balance. The end of drying for the tomatoes samples was reckoned by constant weight readings. Visual inspection of colour and texture was also relied upon to confirm the dried status of the tomato samples.

Table 3. 1 Change in Weights of Tomato samples with time

Sample Weights (g)		**Time Interval**			
		10:00-12:00 (hrs)	12:00-14:00 (hrs)	14:00-15:00 (hrs)	15:00-16:00 (hrs)
Sample G1	Initial Wt.	10.3	8.1	7.6	7.6
	Final Wt.	8.1	7.6	7.6	7.6
Sample G2	Initial Wt.	9.3	7.8	7.5	7.5
	Final Wt.	7.8	7.5	7.5	7.5

There being no reasonable change in the weight of the tomato samples with time, the final weights at 16:00hrs were taken as the final weights of the tomato samples.

The initial and final weights of the tomato samples and aluminum pans were taken and recorded as in table 3.2 below.

Table 3. 2 Initial and Final Weights of the Tomato Samples

Weight (grams)	**Sample G1**	**Sample G2**
Weight of aluminum pans (W_0)	7.4	7.4
Weight of pans + wet tomato (W_1)	10.3	9.3
Weight of wet tomato ($W_2=W_1-W_0$)	2.9	1.9
Weight of pans + dry tomato(W_3)	7.6	7.5
Weight of dry tomato ($W_4=W_3-W_0$)	0.2	0.1

The loss in weight of the tomato samples was recorded using a digital weighing balance (Mettler Instruments BV, Switzerland, mode PE 3000, maximum weighing capacity:3,100g, sensitivity: 0.1g, accuracy of ± 0.1 g) expressed as their initial moisture content values on wet basis (percentage) and dry basis (decimal) as calculated by equations 3.1 and 3.2, respectively.

$$M_{0wb} = \frac{W_1 - W_3}{W_2} \times 100\% \quad \text{..... (3.1)}$$

$$M_{0db} = \frac{W_1 - W_3}{W_4} \quad \text{..... (3.2)}$$

Where:

M_{0wb}= initial moisture content of tomato sample on wet basis, percentage (%)

W_1= weight of fresh undried tomato sample + weight of aluminum pan, g

W_2= weight of wet tomato sample, g

W_0=weight of aluminum pan, g

M_{0db}= initial moisture content of tomato sample on dry basis, decimal

W_3= weight of dried tomato sample + weight of aluminum pan, g

W_4 = weight of dried tomato sample, g

Equations 1 and 2 were used to compute the wet basis and dry basis of the tomato samples. Their averages were calculated and recorded as shown in table 3.3.

Table 3. 3 Wet Basis and Dry basis Average values of Tomato Samples

	Sample G1	***Sample G2***	***Average***
Wet basis $(\boldsymbol{M_{0wb}})$	93.1%	94.7%	93.9% ≈ 94%
Dry basis $(\boldsymbol{M_{0db}})$	13.5	18.0	15.75

Moisture content was calculated as the ratio of weight loss during the drying period with the weight of the wet or the dry weight of the tomato samples. The value of moisture content usually expressed in percentage, %, was thus presented both on a wet basis, *wb*, or dry basis, *db*. The moisture contents, wet-basis, and dry-basis, given in table 3.3 were evaluated as shown below by utilizing the equations *(3.3)* and *(3.4)* (Benedict et al., 2019a):

$$M_{wb} = \left(\frac{W_o - w_d}{W_o}\right) x\ 100 \quad \ldots\ldots\ldots\ldots\ldots\ldots\ldots\ldots\ldots\ldots\ldots\ldots\ldots\ldots (3.3)$$

$$M_{db} = \left(\frac{\boldsymbol{w_o - w_d}}{\boldsymbol{w_d}}\right) \quad \ldots\ldots\ldots\ldots\ldots\ldots\ldots\ldots\ldots\ldots\ldots\ldots\ldots\ldots\ldots\ldots (3.4)$$

The moisture content at any time t during drying, M_t, was be evaluated by:

$$M_t = \frac{W_t - W_{dm}}{W_t} \quad \ldots\ldots\ldots\ldots\ldots\ldots\ldots\ldots\ldots\ldots\ldots\ldots\ldots\ldots\ldots\ldots (3.5)$$

Where:

M_t was the moisture content at any time (t)

w_t was the mass of the tomato sample at time any given time (t)

W_{dm} was the mass of the dry matter of the tomato sample

3.4.4 **Parabolic Trough Collector Area Determination**

This section describes using equations, how to calculate the size of the parabolic trough solar collector that was used to preheat air for drying.

Step 1: Mass of water to be evaporated (M_w)

The mass of the moisture to be removed from the food product was calculated by equation 3.*6* (Fudholi et al., 2013):

$$M_w = \frac{m_p(m_i - m_f)}{100 - m_f} \quad \ldots\ldots\ldots\ldots\ldots\ldots\ldots\ldots\ldots\ldots\ldots\ldots\ldots\ldots \quad (3.6)$$

where, M_w is the mass of water to be removed from the fresh tomatoes, m_p is the initial mass of the tomatoes to be dried, m_i is the initial moisture content of fresh tomatoes, % wet basis, m_f is the final moisture content of dried tomatoes, % wet basis.

Step 2: Enthalpy Required, h

The enthalpy *h* of air was approximated by equation below (Benedict et al., 2019b):

$$h = 1006.9T + w(2512131 + 1552.4T) \ldots\ldots\ldots\ldots\ldots (3.7)$$

where:

T was the temperature of drying air, °C, and

w is the humidity ratio of water vapor, in one kg of dry air.

Step 3: Drying rate, d_r

The average drying rate d_r for drying the tomatoes was evaluated by equation *3.8*:

$$d_r = \frac{m_w}{t_d} \ldots\ldots\ldots\ldots\ldots\ldots\ldots\ldots\ldots\ldots\ldots\ldots\ldots\ldots\ldots\ldots\ldots\ldots (3.8)$$

where m_w is the mass of moisture removed from the tomatoes and t_d is the estimated drying time in hours (21 hrs).

Step 4: Mass flow rate, m_a

The mass flow rate, m_a of the air needed for drying, was calculated by equation *3.9*:

$$m_a = \frac{d_r}{w_f - w_i} \ldots\ldots\ldots\ldots\ldots\ldots\ldots\ldots\ldots\ldots\ldots\ldots\ldots\ldots\ldots\ldots (3.9)$$

where d_r is the average drying rate, w_i is the initial humidity ratio, kg H_2O/kg dry air, w_f is the final humidity ratio, kg H_2O/kg dry air.

Step 5: Volumetric airflow rate, V_a

The volumetric airflow rate V_a in m^3/hr will be evaluated by equation *3.10*:

$$v_a = \frac{m_a}{\rho_a} \ldots\ldots\ldots\ldots\ldots\ldots\ldots\ldots\ldots\ldots\ldots\ldots\ldots\ldots\ldots\ldots\ldots\ldots (3.10)$$

Step 6: Total useful thermal energy, E

The total useful thermal energy of the drying air, *E* in Joules, required to evaporate the water was calculated by equation *3.11* (Akoy et al., n.d.):

$$E = m_a(h_f - h_i)t_d \quad \ldots\ldots\ldots\ldots\ldots\ldots\ldots\ldots\ldots\ldots\ldots\ldots\ldots\ldots\ldots\ldots(3.11)$$

Where:

m_a is the air mass flow rate in kg/hr,

h_i and h_f are the final and initial enthalpy of drying air and ambient air respectively in J/kg of dry air and,

t_d is the estimated drying time in hours**.**

Step 7: Collector area, A_a

The total area required under solar radiation was calculated from equation *3.12* (Seveda, 2012):

$$E = A_a.I.n_{PTSC} \quad \ldots\ldots\ldots\ldots\ldots\ldots\ldots\ldots\ldots\ldots\ldots\ldots\ldots\ldots\ldots\ldots\ldots (3.12)$$

Where:

E is the total useful thermal energy, in Joules,

A_a is the parabolic trough solar collector aperture area is in m^2,

I is the total incident radiation on the parabolic trough solar collector surface during the drying period, and

η_{PTSC} was the PTSC aluminium foil reflectance efficiency.

3.4.5 **PTSC Design**

3.4.5.1 Analysis of sun movement: Declination angle(δ)

This refers to the elevated angle between equatorial plane and sun's direction. It is formulated using the day 'n' in the year, where n varies from 1 to 365.
The general equation for optimum slope of the parabolic trough solar collector (β) with respect to the horizontal is defined with the angle of declination (δ), and the latitude of the agricultural field station at The University of Zambia, Great East Road campus. The solar collector was tilted at an angle (β) of 15^o North.
Mathematically,

$$\beta = \delta + \text{latitude angle } (\Theta) \ldots\ldots\ldots\ldots\ldots\ldots\ldots\ldots\ldots\ldots\ldots\ldots\ldots\ldots(3.13)$$

3.4.5.2 Geometry Modelling of the PTSC

The geometry of the parabolic trough solar collector was significant as it informed the precise fabrication process. The parabolic shape geometry was described by the parabola equation *3.14* (Naranchala et al., 2020),(Çağlar, 2016),

$$y = \frac{x^2}{4f} \quad \text{………………………………………………………………(3.14)}$$

The total collector aperture area (Aa) was the product of the width (W_a) and the length (L):

$$Aa = W_a.L \quad \text{……………………………………………………………(3.15)}$$

using the area of the parabolic trough collector as 2.614 m^2, and choosing the aperture width as 1.2 m, the length of the PTSC was obtained as follows:

$$L = \frac{A_a}{W_a}$$

Note: (2m was used in the fabrication as the standard length of the galvanized iron sheet)

The rim angle (φ_r) was calculated using the aperture width (W_a) and the focal distance (f) as shown below(Arunkumar & Ramesh, 2022a):

$$\varphi_r = \tan^{-1}\left[\frac{8\frac{f}{w}}{16\left(\frac{f}{w}\right)^2 - 1}\right] \quad \text{…………………………………………………(3.16)}$$

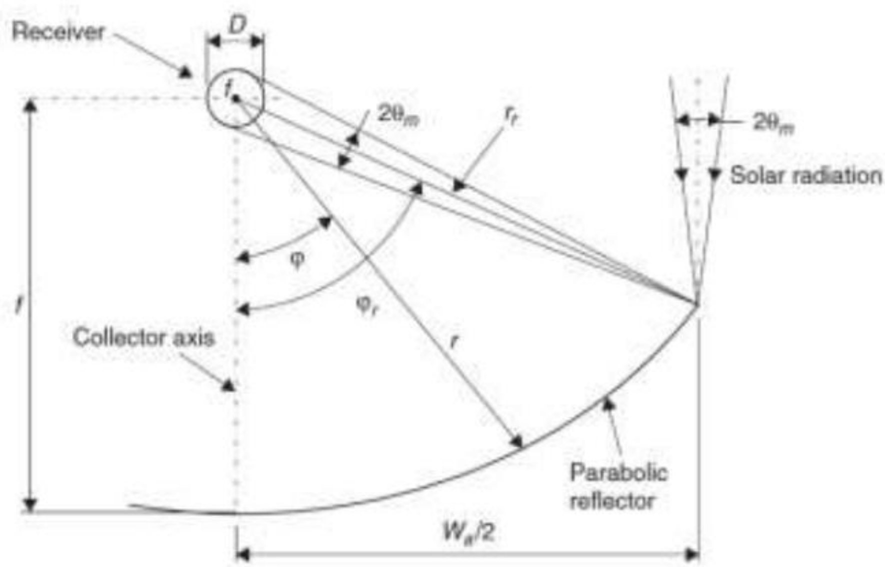

Figure 3. 3 Traversal cut of the solar collector(Macedo-Valencia et al., 2014)

Considering the parameters from the figure above, the focal length and the radius of the parabola, was calculated using equations *3.17* to *3.20* (Macedo-Valencia et al., 2014):

$$f = \frac{W_a}{4tan\left(\frac{\varphi}{2}\right)}$$ (Taking the rim angle as 98°)……..*(3.17)*

$$r = \frac{2f}{1+cos(\varphi)}$$……*(3.18)*

The depth or height of the parabolic trough collector was given by;

$$h = \frac{W_a^2}{16f}$$……*(3.19)*

Also, the focal length of the PTSC was defined and verified mathematically as follows(Arunkumar & Ramesh, 2022b).

$$f = \frac{Y_S^2}{4h}$$……*(3.20)*

Where:

f = the focal length of parabolic trough solar collector

Y_s = the half length of collector aperture

h = the height/depth of the PTC

φ = the rim angle

Parabola arc length was calculated using equation *(3.21)* (Valan Arasu & Sornakumar, 2007):

$$S = 2f\left\{sec\left(\frac{\varphi}{2}\right)tan\left(\frac{\varphi}{2}\right) + ln\left[sec\left(\frac{\varphi}{2}\right) + tan\left(\frac{\varphi}{2}\right)\right]\right\}$$*....(3.21)*

The absorber area (A_{ro}) was the outer area of the tube (Using the ¾'' GI pipe) given by(Bellos & Tzivanidis, 2019):

$A_{ro} = \pi.D_{ro}.L$……*(3.22)*

The geometrical concentration ratio (CR) is defined as the collector aperture area (A_a) to the absorber area (A_{ro}) by(Bellos & Tzivanidis, 2019):

$$CR = \frac{A_a}{A_{ro}}$$……*(3.23)*

3.4.6 **Performance Evaluation of the PTSC Air Heater**

3.4.6.1 Thermal efficiency

Under a steady state condition, the thermal efficiency of a parabolic trough solar collector (η_{th}) was evaluated by the following equation(Duffie & Beckman, 2013):

$$\eta_{th} = \frac{Q_u}{A_{ap}I_D}$$……*(3.24)*

where:

Q_u is the useful energy transferred to the heat transfer fluid defined as follows;

$$Q_u = \dot{m}C_{p.f}(T_{out} - T_{in})\ldots\ldots\ldots\ldots\ldots\ldots\ldots(3.25)$$

$\dot{m}$ = constant air flow rate

$C_{p.f}$ = specific heat capacity of the air

T_{out} = the maximum outlet temperature

T_{in} = average inlet ambient temperature

A_{ap} = Collector aperture area

I_D = average normal solar radiation on the PTSC surface

3.4.6.2 Heat losses from the absorber tube

According to (Motwani, et al., 2020), heat losses from the absorber tube are the combination of conduction, convection and radiation losses. Energy balance describing the heat losses by the heat transfer fluid to the outer surface of the tube and then to ambient was given by:

$$Q_f = Q_{cond} + Q_{conv} + Q_{rad}\ldots\ldots\ldots\ldots\ldots\ldots(3.26)$$

Where:

Q_f = total heat losses by the HTF (air) to the surrounding

Q_{cond} = heat loss through conduction

Q_{conv} = heat loss through convection

Q_{rad} = heat loss through radiation

Neglecting heat loss by conduction, the above equation can be re-written as:

$$Q_f = Q_{conv} + Q_{rad}\ldots\ldots\ldots\ldots\ldots\ldots\ldots\ldots(3.27)$$

Convective heat transfer loss (Q_{conv}) from the surface of the absorber tube to the surrounding was calculated theoretically using the equation below:

$$Q_{conv} = h_c\,(T_s - T_a)\,A_s\ldots\ldots\ldots\ldots\ldots\ldots\ldots\ldots(3.28)$$

Where:

T_s = average absorber tube surface temperature, K

T_a = average ambient temperature, K

A_s = Surface area of the absorber tube given by $\pi\, d_o L\ (m^2)$

h_c = the convective heat transfer coefficient of air, which was calculated from(Yaghoubi et al., 2013):

$$h_c = 4d^{-0.42} v_w^{0.5} \ldots\ldots\ldots\ldots\ldots\ldots\ldots\ldots\ldots\ldots (3.29)$$

where V_w was the average wind velocity in m/s and d was the outer diameter of the absorber tube in m.

Radiation heat loss from the surface of the absorber tube to the surrounding were calculated theoretically by using the below equation:

$$Q_{rad} = \sigma\, \varepsilon_{ab}\, A_s (T_s^4 - T_a^4) \ldots\ldots\ldots\ldots\ldots\ldots\ldots (3.30)$$

Where:

σ = Stefan Boltzmann constant in W/m^2K^4

ε_{ab}= emissivity of the matt black painted GI pipe

$A_s = \pi\, d_o L\ (m^2)$

T_s = average absorber tube surface temperature, K

T_a = ambient temperature, K

Therefore, total heat losses from the surface of the absorber tube are the sum of convection and radiation losses,

$$Q_f = Q_{conv} + Q_{rad} \ldots\ldots\ldots\ldots\ldots\ldots\ldots\ldots\ldots\ldots (3.31)$$

3.4.6.3 Exergetic Performance

The useful thermal input in PTSC is a dominant parameter that could be evaluated by an exergetic performance analysis, which demonstrated the production capacity of the PTSC to generate hot air.

The rate of absorber tube exergy was calculated by equation given by (MacPhee & Dincer, 2009):

$$Ex_u = \dot{m}\, C_{p.f} \left[(T_{out} - T_{in}) - T_{amb} ln \left(\frac{T_{out}}{T_{in}} \right) \right] \ldots\ldots (3.32)$$

The solar radiation exergy absorbed by the receiver tube and reflector is written as (Petela, 2003):

$$Ex_a = A_{ap} I_D \left[1 + \frac{1}{3}\left(\frac{T_{amb}}{T_s}\right)^4 - \frac{4T_{amb}}{3T_s}\right] \ldots\ldots\ldots\ldots\ldots (3.33)$$

where Ts = 5762K is the apparent sun temperature.

The exergy efficiency can be written as:

$$\eta_{exr} = \frac{Ex_u}{Ex_a} = \frac{\dot{m}\, Cp.f\left[(T_{out} - T_{in}) - T_{amb} ln\left(\frac{T_{out}}{T_{in}}\right)\right]}{A_{ap} I_D \left[1 + \frac{1}{3}\left(\frac{T_{amb}}{T_s}\right)^4 - \frac{4T_{amb}}{3T_s}\right]} \ldots\ldots (3.34)$$

3.5 Fabrication of the parabolic trough solar collector air heater

After the initial design of the parabolic trough solar collector, the parameters arrived at were used in its construction. The PTSC was essentially made up of the following major components:

- Parabolic trough concentrator
- Receiver absorber tube
- Axial fan
- Support structure
- Adjustable stands

3.5.1 Parabolic Trough Concentrator

The parabolic trough collector was made up of galvanized iron sheets, aluminium foil, two shutter ply wood and self-tapping screws.

A shutter plywood of dimensions 1000mm x 1200mm x 18mm was used. Using the PTSC parameters of aperture width 1200mm and height of 345mm, two equivalent pieces were cut. A manilla paper with the shape of the parabola accurately drawn was superposed onto each piece of the plywood and curves were drawn using a pencil. A jig saw was used to cut the parabolic solid from the shutter ply wood. A through hole of dimeter 0.027m was drilled at the focal point of each ply wood where the absorber tube was to pass. Also, taking into account the locking mechanism of the PTSC when tracking the sun, a total of 17 through holes of diameter 4.5mm were drilled at a radius of 20cm from the focal point, separated with 10^o from each other.

Two galvanized iron sheets of dimensions 2 m x 0.9 m were acquired from the hardware in Kalingalinga shopping area. To achieve the parabola arc length of 1.4 m, a piece of galvanized iron sheet of dimensions 2m x 0.52m was cut using a tin snip and joined to a full iron sheet of dimension 2m x 0.9m by the use of diameter 4mm rivets. The distance between the rivets was arbitrarily chosen as 0.1m to maintain uniformity.

With the galvanized iron sheet of dimensions 2m x 1.4m, aluminium kitchen foil was fitted with contact adhesive called Tuff Stuff. The dull side of the aluminium foil was the one in contact with the galvanized sheet with the contact adhesive in between. The shiny part of the aluminium foil was the one that formed the inside of the parabolic trough because of its high reflectivity.

The galvanized sheet fitted with the aluminium foil was joined using self-tapping screws of diameter 4mm by 20mm onto the curved surface of the shutter plywood material to take the shape of the parabola.

The parabolic trough collector was reinforced with four parallel mild steel square tubes of dimensions 2000mm x 20mm x 20mm. Square tubes along the straight edges were extended by 100mm from both ends to facilitate easy carrying of the trough during mounting for the experiment.

Figure 3. 4 Fabricated PTSC

3.5.2 Receiver

The primary purpose of the designed parabolic trough solar collector was to heat air from ambient to a higher temperature. The desired process was carried out in the receiver placed concentrically along the focal line of the collector where the reflected and diffused solar beams were concentrated and converted to heat energy. Different shapes from circular to square could be used, however, circular section was chosen. The chief reason being easily available and less area coverage to avoid shading on the reflector. A galvanized iron (GI) circular pipe of inner and outer diameter of 0.0216m and 0.0253m respectively was used for the purpose. The absorber tube was painted with matt black paint to ensure maximum absorptance of concentrated heat. A pre-fabricated axial fan with a reducer was joined to the absorber tube using a two inch to three quarter reducer as shown in figure 3.5 below.

Figure 3. 5 Absorber tube connected to the axial fan

3.5.3 Duct System

A polyvinyl chloride (PVC) pipe of outer diameter (0.0292m) and inner diameter (0.0217m) was connected at the exit end of the absorber tube. It was strategically connected near one air inlet vent opening of the GSD to direct hot air under the drying tables in the GSD chamber.

3.5.4 PTSC Support Structure and Adjustable Stands

For the collector's stability and accuracy, a rigid supporting structure (figure 3.6) was designed and fabricated with rigid flat and square tubes made of mild steel. Precise length measurements were done using a metre rule and a tape measure. A grinding machine was used to cut the flat and square tubes to the desired lengths. The joining mechanism of the individual parts employed use of diameter 4mm rivets and M6 x 50mm bolt and nuts. The drilling of through holes was first done by drilling pilot holes with a 4.5mm drill bit and then enlarged with a 6.5mm diameter drill bit. Tightening of the bolts and nuts was done using a pliers and a spanner size 10mm. A file was used to create a smooth surface finish at the ends of the mild steel flat plates and square tubes to guarantee safe handling at all times. Adjustable stands were used to slant the PTSC to the desired angle of slope and inclination.

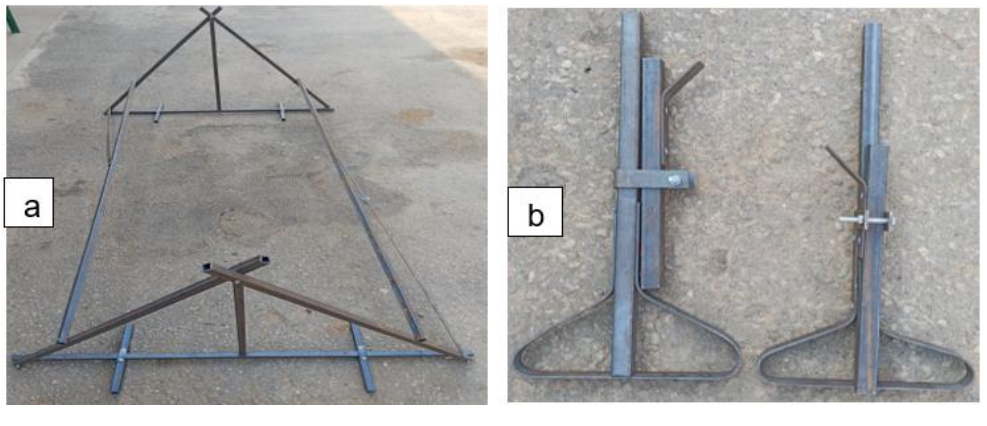

Figure 3. 6 (a) Support structure (b) Adjustable stands

3.6 Attachment of the parabolic trough concentrator air heater to the greenhouse dryer

An existing GSD at the University of Zambia Agricultural Field Station was used for the research study. The greenhouse solar tunnel drying chamber was constructed on a concrete slab. Square tube metal sections were welded and screwed together to form a metal structure shape of a tunnel. A translucent polyethylene ultra-violet film cover was used as the greenhouse material cover. Inside the GSD, there were two drying tables of dimensions 3.93 m x 0.85 m x 0.93 m made up of steel square tubes and a plastic mesh where tomatoes were placed during drying. Four DC exhaust fans of the same rating (12V and 0.6A) were fitted at the top of the front side of the greenhouse dryer to expel the warm drying air from the greenhouse thereby creating a forced convection. Entry to the inside of the greenhouse dryer was accessed by opening the door in the front side.

The designed and fabricated parabolic trough concentrator air heater was positioned strategically at the rear side next to the greenhouse solar dryer. A PVC pipe was connected at the air outlet side of the absorber tube to introduce the hot air into the greenhouse dryer.

3.7 Experimentation

3.7.1 GSD without PTSC Test

Two different kinds of experiments were conducted. These were no load tests and loaded tests of the GSD without the PTSC. The no load test experiments were conducted under different test conditions specifically with air vents fully closed, fully open and partially open. Loaded tests of the GSD were conducted with 4mm sliced tomatoes well spread on top of the drying tables with air vents fully open to allow ambient air to enter from below the trays. In addition, for the loaded GSD test, a 100W rated AC fan was used to create an artificial wind effect inside the GSD. Figure 3.7, 3.8, 3.9 and 3.10 shows GSD without the PTSC, the rear side of the GSD not connected with the PTSC with air vents fully closed, fully open and partially open respectively. Figure 3.11 shows the setup of the loaded GSD with tomatoes with equal amount being dried using the Open Sun Drying (OSD) method.

Figure 3. 7 GSD without the PTSC

Figure 3. 8 GSD with air vents fully closed

Figure 3. 9 GSD with air vents fully open

Figure 3. 10 GSD with air vents partially open

Figure 3. 11 Load test of the GSD with tomatoes with equal amounts being dried using OSD method (tray positioned outside the GSD under the open sun).

3.7.2 PTSC Performance Test

This test assessed the performance of the fabricated PTSC air heater under objective three in terms of temperatures variations. The experimental setup of the PTSC consisted of a collector, a receiver galvanized iron pipe painted matt black of length 2.15 m, an AC powered axial fan connected to one end of the receiver absorber tube and a support structure. The major parameter of interest was the temperature, and therefore the ambient temperature of air entering through the axial fan, temperature of the absorber tube surface and temperature of the exiting heated air was measured using thermocouple sensors and a hand-held infrared thermometer. Also, the solar radiation and the wind were also measured using a pyranometer and airflow meter respectively. All the measuring instruments apart from the infrared thermometer were connected to a multichannel data logger that recorded readings at an interval of one minute.

The outdoor experimentation was carried out in the month of September and October 2022. The testing system was oriented North-South direction at an angle 15^{o} equal to the latitude of the test location to capture maximum insolation as shown in figure 3.12.

Figure 3. 12 PTSC experimental setup

3.7.3 GSD Connected with PTSC Performance Test

Site assessment of the GSD was done. For maximum tracking of the sun, the PTSC was oriented on true North-South direction and rotated East-West direction after every 30 minutes. Additionally, the PTSC was inclined at 15^0 to ensure normal or perpendicular hitting of the collector by solar rays. Figure 3.13 and figure 3.14 shows the experimental setup of the GSD connected with the PTSC before noon and afternoon respectively.

Figure 3. 13 Experimental setup of GSD connected with PTSC before noon

Figure 3. 14 Experimental setup of GSD connected with PTSC after noon

3.8 Performance Analysis of GSD With and Without PTSC Air Heater

3.8.1 Determination of moisture content

The initial moisture content on wet basis (M_{wb}) was calculated using the equation (3.1 and 3.3) hitherto described.

3.8.2 Saving in drying time

The percentage of time saved for drying the tomato products in the modified GSD in comparison with GSD without the PTSC and OSD method was calculated using the following the equation below as reported by (Fudholi, et al., 2013):

$$S = \left(\frac{t_{OS} - t_{SD}}{t_{OS}}\right) x\ 100 \ldots\ldots\ldots\ldots\ldots\ldots\ldots\ldots\ldots\ldots (3.35)$$

Where;

S was the percentage of saved drying time,

t_{OS} was time taken to dry the tomatoes in open sun in hours, and

t_{SD} was time taken to dry tomatoes in the greenhouse solar dryer in hours.

3.8.3 Specific Energy Consumption (SEC)

Specific Energy Consumption (SEC) was the amount of energy required by the GSD to extract one kilogram of moisture from the tomato product. It was one of the key performance parameters of the GSD. The specific energy consumption (SEC), was calculated using the following equation:

$$SEC = \frac{P_t}{W}\ (kWh/kg) \ldots\ldots\ldots\ldots\ldots\ldots\ldots (3.36)$$

Where;

SEC was the specific energy consumption in (kWh/kg),

W was the mass of water evaporated from the tomatoes in (kg), and

P_t was the total energy input to the GSD in (kWh).

3.8.4 Specific Moisture Extraction Rate (SMER)

Specific Moisture Extraction Rate (SMER) was another performance index, which was used to describe the efficiency of energy or the effectiveness of energy used in the drying process in the GSD. It was in effect, the inverse of specific energy consumption and was given by the ratio between the total moisture removed to the total energy input. The specific moisture extraction rate (SMER) was calculated by the below equation:

$$SMER = \frac{W}{P_t}\ (\frac{kg}{kWh}) \ldots\ldots\ldots\ldots\ldots\ldots\ldots (3.37)$$

Where;

SMER was the specific moisture extraction rate in (kg/kWh),

W was the mass of water evaporated from the product in (kg), and

P_t was the total energy input to the GSD in (kWh).

3.8.5 Determination of GSD thermal efficiency:

The thermal drying efficiency of the GSD was estimated using the equation defined below given as:

$$\eta_{GSD} = \left(\frac{WL}{A_c I_D + P_f}\right) * 100 \ldots\ldots\ldots\ldots\ldots\ldots (3.38)$$

where;

η_{GSD} was the thermal drying efficiency of the GSD,

L is the latent heat of vaporization of water at drying air temperature (J/kg),

W is the mass of water evaporated from the product (kg),

A_c is the collector area (m^2),

I_D is the solar radiation intensity (W/m^2), and

P_f is the power of the fans (W).

3.9 Instrumentation and Measurements of Variables

During the running of experiments, manual and computerized data collection and recording methods were done with the help of a number of instruments as discussed below.

3.9.1 Mass Measurement

The masses of the tomatoes before, during and after drying were measured using a digital weighing balance with a measuring range of 0.1g. The fresh tomato samples were dried in an oven with a maximum temperature of 60°C. The mass of the PTSC components was measured using an analogue spring balance.

3.9.2 Relative Humidity Measurement

A relative humidity probe (Campbell Scientific Inc., model: HMP35D; accuracy at +20◦C was ±2% RH (0–90% RH) and ±3% RH (90–100% RH)) capable of measuring relative humidity in the range of 0 and 100% was used to measure relative humidity of air inside the greenhouse solar dryer. At all times the relative humidity probe was placed at the centre of the GSD and just slightly above the drying trays.

A Hygrometer instrument was also used to measure the ambient dry bulb and wet bulb temperature. Additionally, it was used to measure relative humidity using the dry bulb and wet bulb temperature. However, some values of relative humidity could not be read from the hygrometer when the dry bulb temperatures were too high. Instead, psychometric chart was used as well as inputting the dry bulb and wet bulb temperatures values in an already programmed website (Holsoft, 2022) which had higher accuracy.

3.9.3 Temperature Measurement

During no load test and load test of the drying process, three temperature probes (Campbell Scientific Inc., model: 108– L accuracy ±0.01 ºC) and one combined temperature and humidity probe were used to monitor temperature and humidity performance parameters of the greenhouse solar dryer. All the four probes were positioned inside the GSD drying chamber. Both the temperature and the humidity readings were recorded at one minute interval. Ambient temperature was recorded using an analogue hygrometer. In addition, an infrared handheld thermo-gun was used to measure the temperatures of the heated absorber tube

3.9.4 Solar Radiation Measurement

A pyranometer (Kipp & Zonen Delft BV, model: CM11, irradiance range: 0–1,400 W/m^2, sensitivity: between 4 and 6 μV/Wm^{-2}) was used in measuring the solar radiation incident on the parabolic trough solar collector surface and the greenhouse solar dryer. It was placed on a flat horizontal surface near the greenhouse solar dryer and the PTSC during the experiments.

3.9.5 Air Fan Speeds and Windspeed Measurement

An air speed meter that had capabilities of measuring wind speed and temperature digitally at the same time was used. Table 3.4 gives a summary of all the measuring instruments used in data collection exercise of the research study.

Table 3. 4 The specifications of the measuring instruments

S/No.	Instrument	Quantity	Range	Accuracy	Use
1	Infrared thermo gun	1	-18 ^{o}C – 350 ^{o}C	0.1 ^{o}C	Temperature
2	Thermocouple temperature probes	4	-5 to +95 ^{o}C	±0.01 ^{o}C	Temperature
3	Relative humidity probes	1	0 - 90% RH	±2%	Relative humidity
4	Hygrometer	1	-10 ^{o}C – 50 ^{o}C	1 ^{o}C	Temperature and Humidity
5	Pyranometer	1	0 – 1,400 W/m^2	0.1 W/m^2	Solar Radiation
6	Digital weighing balance	1	0 – 3 Kg	0.1 g	Mass measurement
7	Air speedometer	1	0 - 30 m/s -20 ^{o}C – 60 ^{o}C	0.1 m/s 0.1 ^{o}C	Air & wind speed and Temperature

3.10 Chapter Summary

This chapter covered in details the research design used, study area, design of the PTSC, fabrication of the designed PTSC, attachment of the PTSC to the already existing GSD, experimentation, instrumentation and measurements of parameters. The data collected using the hitherto discussed approaches is discussed in chapter four of results and discussions.

CHAPTER FOUR: RESULTS AND DISCUSSION

4.0 Introduction

This chapter, guided by the objectives, presents systematically the results and discussions of the research study. The chapter covers the following items in details: design parameters of the PTSC, fabricated PTSC air heater, results of the fabricated PTSC, results and comparison of the GSD with and without the PTSC air heater.

4.1 *Objective I:* To design the proposed parabolic trough concentrator for preheating air

The already existing dryer was studied to establish the ideal size of the PTSC that was to be constructed. Literature review on tomatoes that was to be dried was done. It was established from the literature review that the initial moisture content of tomatoes ranged from 90% to 96% and the final safe moisture content ranged from 10% to 18%. Using two drying tables inside the GSD, each with a holding capacity of approximately 15kg, initial and final moisture content on wet basis as 94% and 10% respectively, design calculations were formulated as outlined in Chapter 3 section 3.4.5. Table 4.1 below shows the system characteristics of the designed PTSC air heater.

Table 4. 1 System characteristics of the PTSC air heater

Rim angle	98^o
Focal length	0.261 m
Height	0.345 m
Aperture width	1.2 m
Total length	2 m
Total aperture area	2.4 m^2
Absorber tube area	0.15899 m^2
Absorber pipe inner/outer diameter	0.0216 m/0.0253 m
Concentration ratio	15.1
Tracking axis orientation	North – South
Receiver absorptivity	1
Mirror material	Galvanised sheet covered with aluminium foil
Frame material	Steel square tubes and flat plates
Heat Transfer Fluid	Air

4.2 *Objective II:* To fabricate the proposed parabolic trough solar concentrator

4.2.1 PTSC Air Heater Assembly

A new PTSC module was designed and constructed. It had a rapid integration and assembly method on site. It was assembled in just less than 60 minutes with the use of a screwdrivers, spanners number 10mm and a pair of pliers. The individual components like the parabolic trough collector, receiver absorber tube, axial fan, support structure and adjustable stands were fabricated and assembled to make a complete unit. The figure 4.1 below shows the assembled PTSC air heater.

Figure 4. 1: PTSC assembly

4.2.2 Tracking System

The PTSC was designed to have an orientation axis of North-South direction and rotation direction of East-West direction to track the sun. The PTSC was designed to have a manual tracking system. Seventeen through holes, 10^0 apart, were drilled onto the shutter plywood. The locking mechanism utilized a locking pin such as a nail onto the vertical line of the support structure. The parabolic trough was rotated after every 30 minutes. Notably, the trough was freely suspended using the receiver absorber tube. The figure 4.2 below shows the tracking system and locking mechanism of the fabricated PTSC.

Figure 4. 2 Manual tracking system of the fabricated PTSC

4.2.3 Mass of the PTSC

A complete module weighed 38.6 kg, and can be transported in a compact car due to its modular concept. It is also possible to scale the system in a series or parallel arrangement, according to user needs. The table 4.2 below shows the mass in kilograms of the PTSC air heater specific components.

Table 4. 2 Mass of the specific components of the PTSC air heater

S/No.	Component	Mass (Kg)
1	PTC	20.8
2	Receiver absorber tube	3.2
3	Reducer	3.5
4	Support structure	8.3
5	Two adjustable stands	0.8
6	Axial fan	2
Total		**38.6**

4.3 *Objective III:* To test the performance of the parabolic trough solar collector

4.3.1 Temperatures

The PTSC air heater was tested on a clear day with the experimental setup described in Chapter 3 section 3.7.2. Figure 4.3 shows the temperature variations analyzed from the data collected.

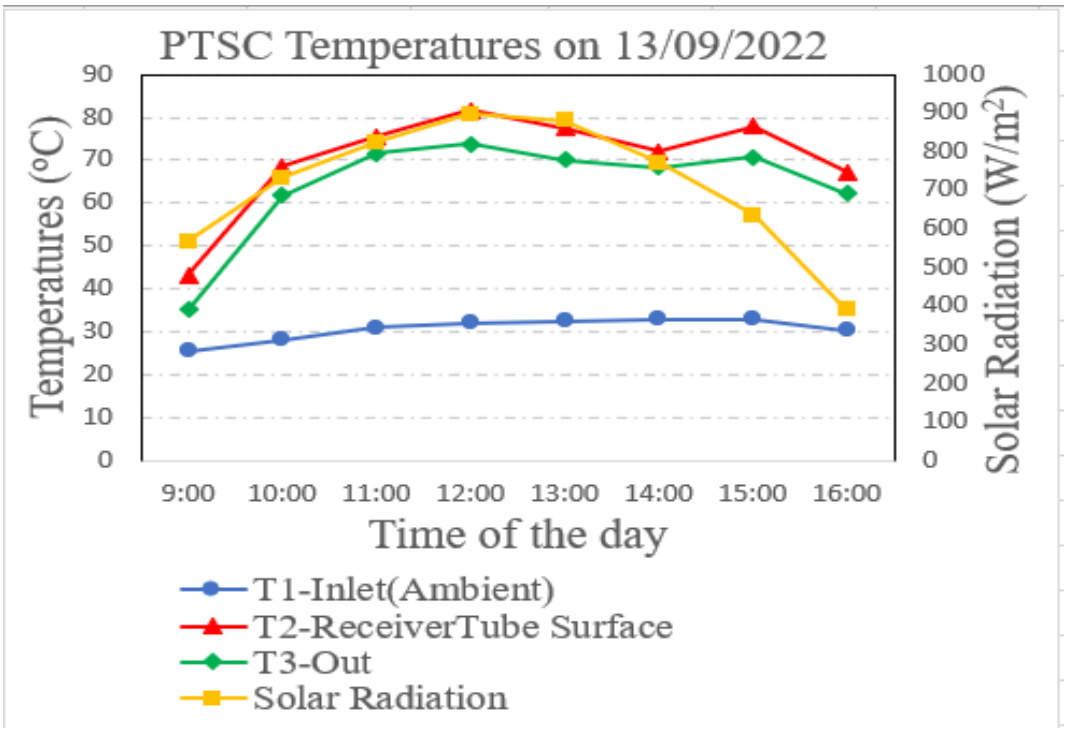

Figure 4. 3 A graph of temperatures against time of the day during testing of the PTSC

The minimum, maximum and average solar radiation during the experiment was 346 W/m^2, 906 W/m^2 and 736 W/m^2 respectively. From the figure 4.3 above, it is observed that temperatures had a direct relationship with the solar radiation, that is, temperatures increased as the solar radiation increased and vice versa.

The ambient air recorded a minimum, maximum and an average temperature of 25.5 ^{o}C, 34.4 ^{o}C and 31.1 ^{o}C respectively. The absorber tube temperatures depended on timely manual rotation of the PTSC to track the sun, the accuracy and precision of the fabricated parabolic trough. A delay in rotating the PTSC could cause temperatures to start decreasing. The minimum temperature of the absorber tube was recorded as 31 ^{o}C at 0900hrs when the experiment was starting. The maximum temperature recorded from the absorber tube was 85.6 ^{o}C at 1334hrs. It was certain beyond doubt that there could be heat transfer between the absorber tube and the heat transfer fluid(air). The minimum and maximum temperature of the hot air at the exit of the absorber tube was 35.1 ^{o}C and 80.1 ^{o}C respectively. As per the expectations, it was observed that the temperature of hot air at the exit of the absorber tube was always less than that of the absorber tube surface. This was due to the fact that there was heat loss from the bare absorber tube surface to the surrounding. The measured wind effect of 3.5m/s during the experiment contributed to significant heat loss from the bare absorber tube surface.

The testing of the PTSC gave impressive reliable results of raising air temperatures by 45.6 ^{o}C above the ambient temperature. It was evident that the PTSC could preheat the ambient air to considerable high temperatures (45 ^{o}C to 60 ^{o}C) suitable for drying tomatoes inside the GSD.

4.3.2 Thermal Efficiency

The thermal efficiency of the fabricated PTSC air heater was evaluated as 5.3% as shown in appendix II. It was satisfactory with design parameters particularly the low airflow rate of 0.11346 kg/min and climatic condition of the test location. Key factors that affected the thermal efficiency of the PTSC air heater was the air flow rate inside the absorber tube and respective temperatures. In addition, the type of the HTF also significantly determine the thermal efficiency. HTF with low specific heat capacities lead to low thermal efficiencies of PTSC and vice versa. Air as the HTF, due to low value of specific heat capacity lead, to low thermal efficiencies of PTSC in contrast to HTFs like water, oil, salts and nanofluids that have high specific heat capacities. In a similar study, a PTSC was designed and fabricated to preheat air for drying apple slices in a drying chamber. A thermal efficiency of 8% to 25% was achieved with varying airflow rates of 0.6 kg/min to 1.72 kg/min respectively (Khan, et al., 2013).

Another similar study, a PTSC air heater was constructed for a GSD to dry Paddy rice. A thermal efficiency of the fabricated parabolic trough of 8.73% was found (Sookramoon, 2016b) which is slightly higher than what has been found in the current study.

4.3.3 Heat Losses from the Absorber Tube

The convection and radiation heat losses from the absorber tube were 306.6 W and 72.49 W respectively giving a total of 379.09 W as shown in appendix III. It was evident that there was significant heat loss from the air as the heat transfer fluid to the surrounding majorly through the convection and lesser through radiation. The high value of convective heat loss was attributed to wind effect. Cold air that passed over the bare absorber tube carried significant heat away. Such result was expected since the design and fabrication of the PTSC did not consider the use of transparent glass to cover the parabolic groove where the absorber tube was located. In addition, the absorber tube was not insulated in any way hence the significant heat losses. Arunkumar & Ramesh, (2022c) reported that evacuated absorber tubes were more efficient for the collector's overall performance.

4.3.4 Exergetic Performance

The evaluated exergetic performance was 0.346% as shown in appendix IV. The useful thermal input in PTSC is a dominant parameter that could be evaluated by an exergetic performance analysis, which demonstrated the production capacity of the PTSC to generate hot air. Many studies have been conducted on thermal performance improvement of PTSC, based on their energetic and exergetic performances.

4.4 *Objective IV:* To compare the performance of the greenhouse solar tunnel dryer with and without the attached parabolic trough solar collector

4.4.1 No Load Test of the GSD With and Without the PTSC Air Heater

No load test means that the GSD was tested without drying tomatoes inside it. It was important to run a no-load test to establish the values of highest temperatures of the air that could be reached in preparation of drying tomatoes. The major temperatures of interests were temperatures at the inlet air vents and at the middle of the GSD. Also, the values of the relative humidity were of interest to be monitored before the actual drying of tomatoes.

4.4.1.1 Temperatures

Figure 4.4 shows the temperatures of the GSD without PTSC in operation and with the air vents closed. It was observed that the temperatures near the air vents inlets were higher than the ambient air temperatures. This confirms that no cool ambient air was entering the GSD. The minimum, maximum and average temperatures recorded inside the GSD and above the drying tables were 44.5 ºC 54.7 ºC and 51 ºC respectively.

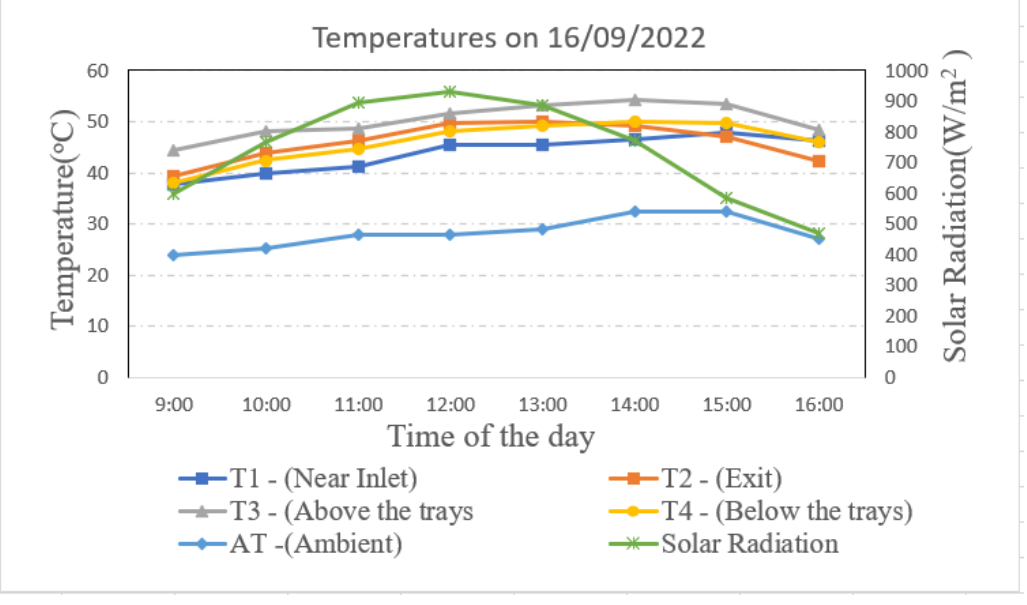

Figure 4. 4 Temperatures of the GSD without PTSC and with air vents closed

Figure 4.5 shows the temperatures variations inside the GSD with no PTSC and with air vents fully open. Temperatures at the inlet of the GSD were almost equal to the ambient temperatures. This observation confirmed that truly cool ambient air entered the GSD which was undesirable during drying. The minimum, maximum and average temperatures at the middle of the GSD and above the drying tables were 38.6 ºC, 50.3 ºC and 44.5 ºC respectively.

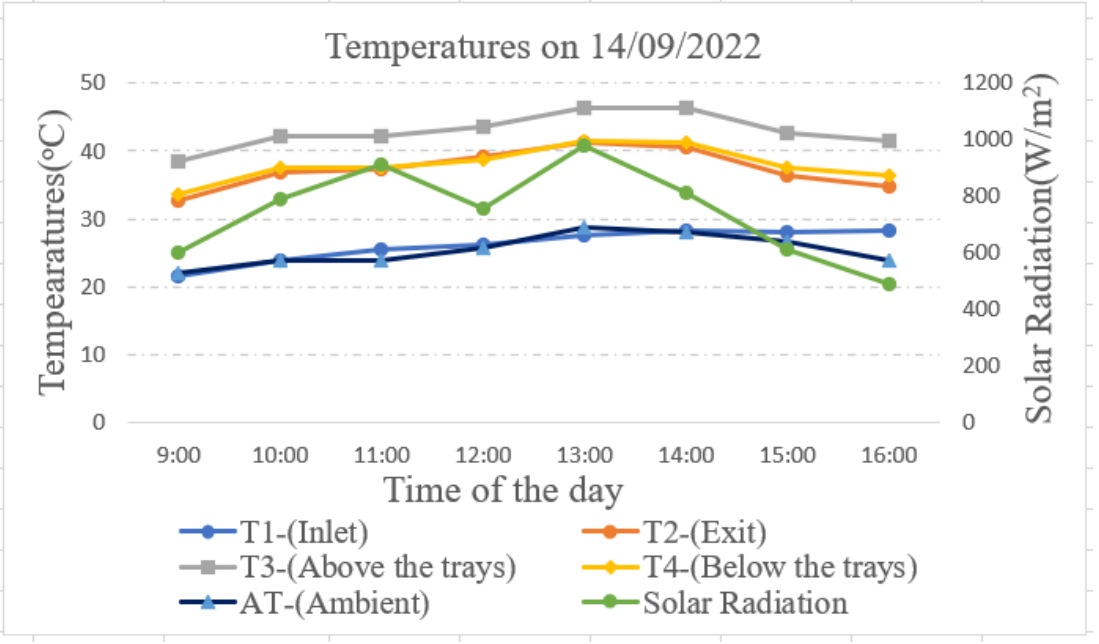

Figure 4. 5 Temperatures of the GSD without the PTSC and with air vents open

Figure 4.6 shows the temperatures variation inside the GSD with PTSC connected and in operation of preheating air. The minimum, maximum and average temperatures of hot air entering the GSD from 0900hrs to 1600hrs were 39.9 ^{o}C, 60.4 ^{o}C and 50.9 ^{o}C respectively. The minimum, maximum and average temperatures at the middle and above the drying tables were 43.5 ^{o}C, 54.8 ^{o}C and 49.7 ^{o}C respectively. From the data analysed in the figure 4.6, the PTSC stabilized temperatures inside the GSD above 49.7 ^{o}C (i.e by 19.5 ^{o}C above ambient temperature) from 0900hrs to 1600hrs. The PTSC, with varying solar intensity throughout the day and considering thermal losses, it managed to raise the ambient air temperatures by 23.6 ^{o}C , that is, from 34 ^{o}C to 57.6 ^{o}C.

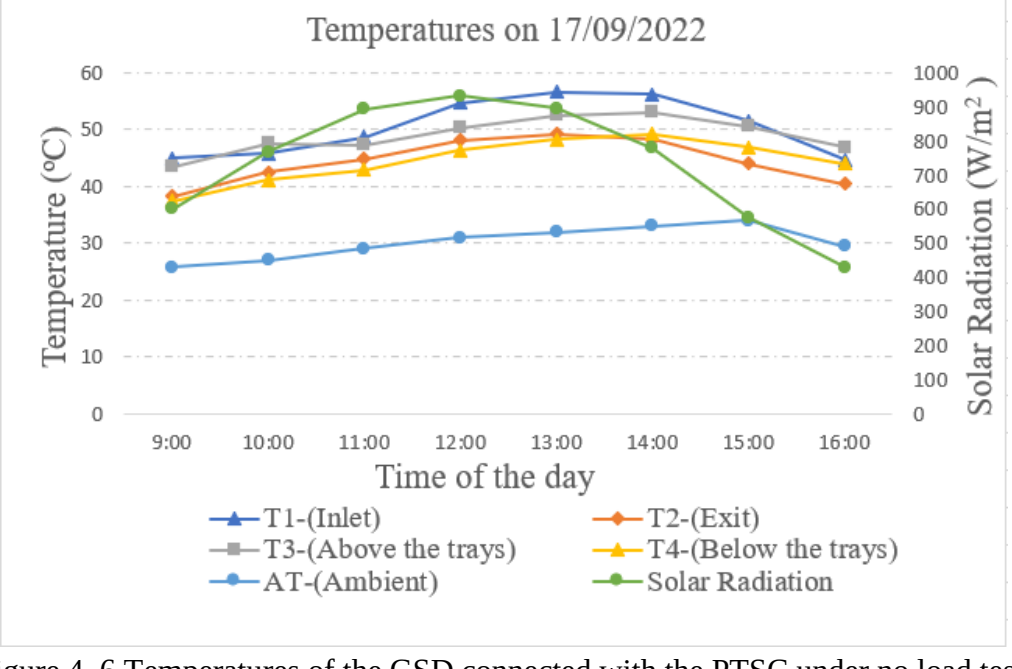

Figure 4. 6 Temperatures of the GSD connected with the PTSC under no load test.

The dry run experiments showed that there was a direct relationship between the ambient air entering the GSD and the temperatures inside the GSD. Cool ambient air entering the GSD via the air inlet vents lowered the temperatures by 7 ^{o}C on average i.e from an average of 51 ^{o}C to 44 ^{o}C.

4.4.1.2 Relative humidity

Relative humidity is another factor that significantly affects the drying of tomatoes as discussed in Chapter 2 during the testing of the GSD. It was therefore imperative to measure relative humidity at ambient conditions and inside the GSD. Also, solar radiation was measured to establish the relationship therein.

Figure 4.7 shows the variations of relative humidity at ambient conditions and inside the GSD. Generally, relative humidity decreased with increase in solar radiation that caused air temperature to rise. For the first day, air vents for the GSD at inlet were completely closed as shown in figure 3.8, for the second day, air vents for the GSD were completely open as shown in figure 3.9 and for the third day, GSD was connected to PTSC in operation as shown in figure 3.13 and figure 3.14.

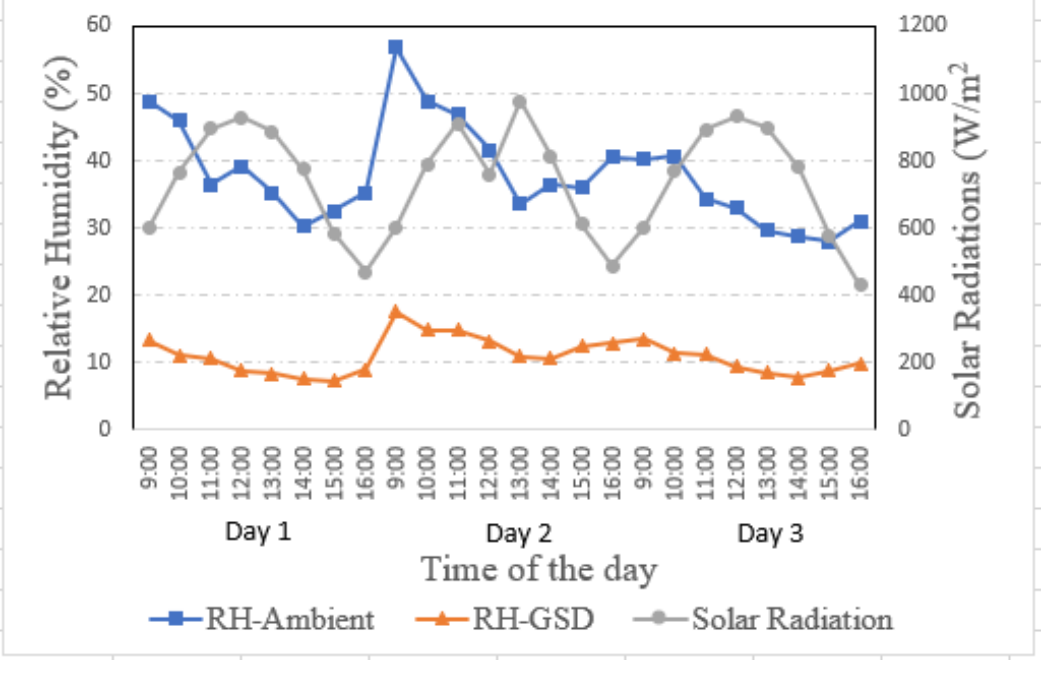

Figure 4. 7 Relative humidity inside the GSD and at ambient conditions (no load test)

For the first day, the minimum, maximum and average relative humidity inside the GSD were 7%, 13.4.% and 9.2% respectively. The ambient relative humidity registered on average was 38%.

For the second day, the minimum, maximum and average relative humidity inside the GSD were 9%, 17% and 13% respectively. The ambient relative humidity registered on average was 43%.

For the third day, the minimum, maximum and average relative humidity inside the GSD were 7%, 13.5% and 9% respectively. The ambient relative humidity registered on average was 33%.

It was observed that, relative humidity values inside the GSD were almost the same when air vents were fully closed and when the PTSC was connected with air vents closed and open. The values of the relative humidity inside the GSD when the air vents were open were high compared to the other cases discussed, demonstrating the effect of ambient cool air inside the GSD. The effect thereof is to slower drying inside the GSD.

Ambient relative humidity measured to be in the range of 33% to 43% are unsuitable for drying of agricultural products like tomatoes that have high moisture content of more than 90% on wet basis.

It was predicted that, the integration of the PTSC air heater to the GSD could significantly lower relative humidity inside the GSD to support faster drying of tomatoes compared to the ambient relative humidity with OSD method.

4.4.2 **Load Test of the GSD with PTSC Air Heater**

4.4.2.1 Solar radiations

The variations of solar radiation for typical experimental runs during drying of tomatoes are shown in the figure 4.8 below.

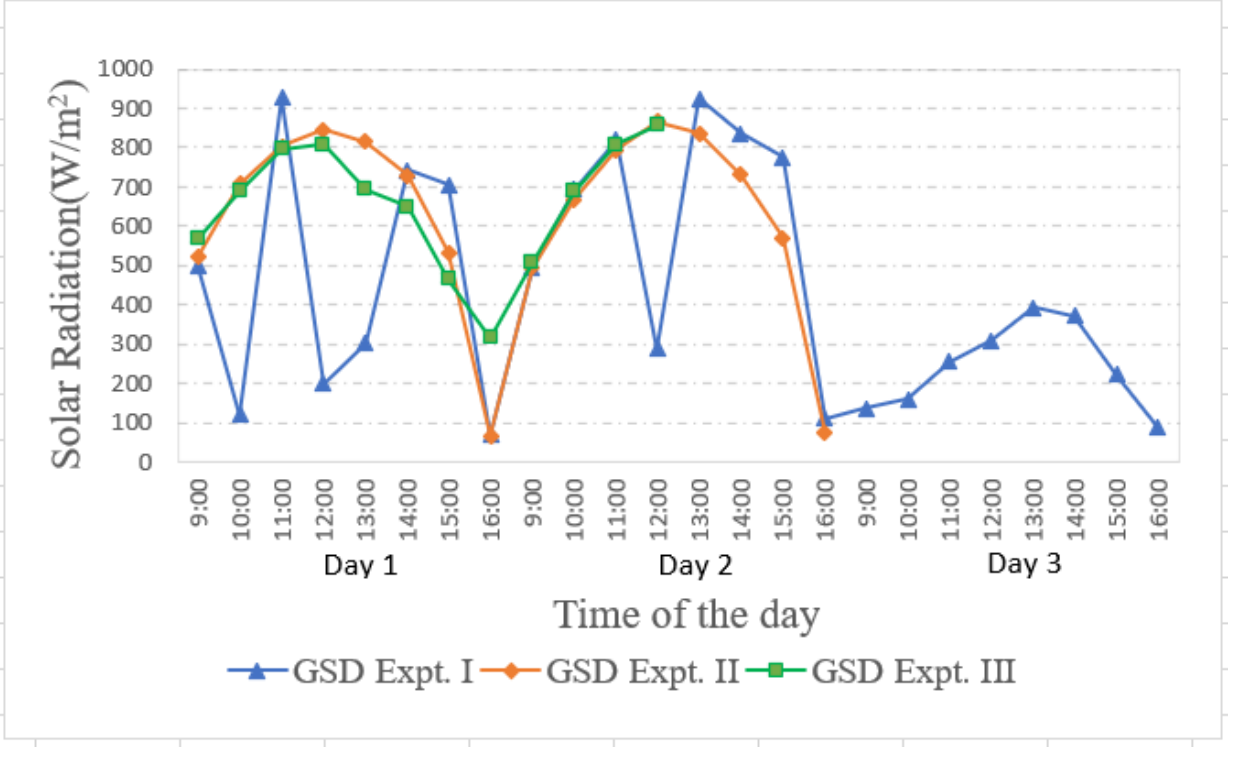

Figure 4. 8 Solar radiation for experiment I, II & III

Experiment I, which was conducted from 29/05/2022 to 3/06/2022 suffered from heavy intermittent cloud cover as shown on the graph. It explains why the drying took longer than other experiments. The highest solar radiation recorded was 928W/m^2 during day one of the experiment.

Experiment II, which was conducted on 7/08/2022 to 8/08/2022 was carried out when the sky was clear for the two days. The highest solar radiation was 866 W/m^2 recorded at noon for the two days.

Experiment III, which was conducted on 20/09/2022 and 21/09/2022 involved the drying of tomatoes in a GSD connected with a PTSC in the month of September, the solar radiations varied from 315 W/m^2 as the minimum and 868 W/m^2 as the maximum for the 10 hours the experiment was run.

4.4.2.2 Temperatures

The temperature was an important parameter monitored inside and outside the GSD. An increase in temperature increased the drying rate. Ambient temperature was constantly measured using an analogue hygrometer and recorded manually after every one hour.

Temperatures inside the GSD were measured using thermocouples and recorded in a multichannel data logger after every one minute. Four different thermocouples were at all times strategically positioned inside the GSD as follows:

- T1 – measured temperatures of air entering the GSD
- T2 – measured temperatures of air exiting or leaving the GSD at the exhaust fans
- T3 – measured temperatures of air at the middle of the GSD and above the drying tables
- T4 – measured temperatures of air below the drying tables and close the floor

The figure 4.9 shows the temperature variations of air inside and outside the GSD during experiment I. The maximum temperature reached was 45 ^oC. Fast drying of tomatoes require temperatures in the range of 45 ^oC to 60 ^oC, and therefore ambient cold air that entered the GSD limited the rise of temperatures above 45 ^oC.

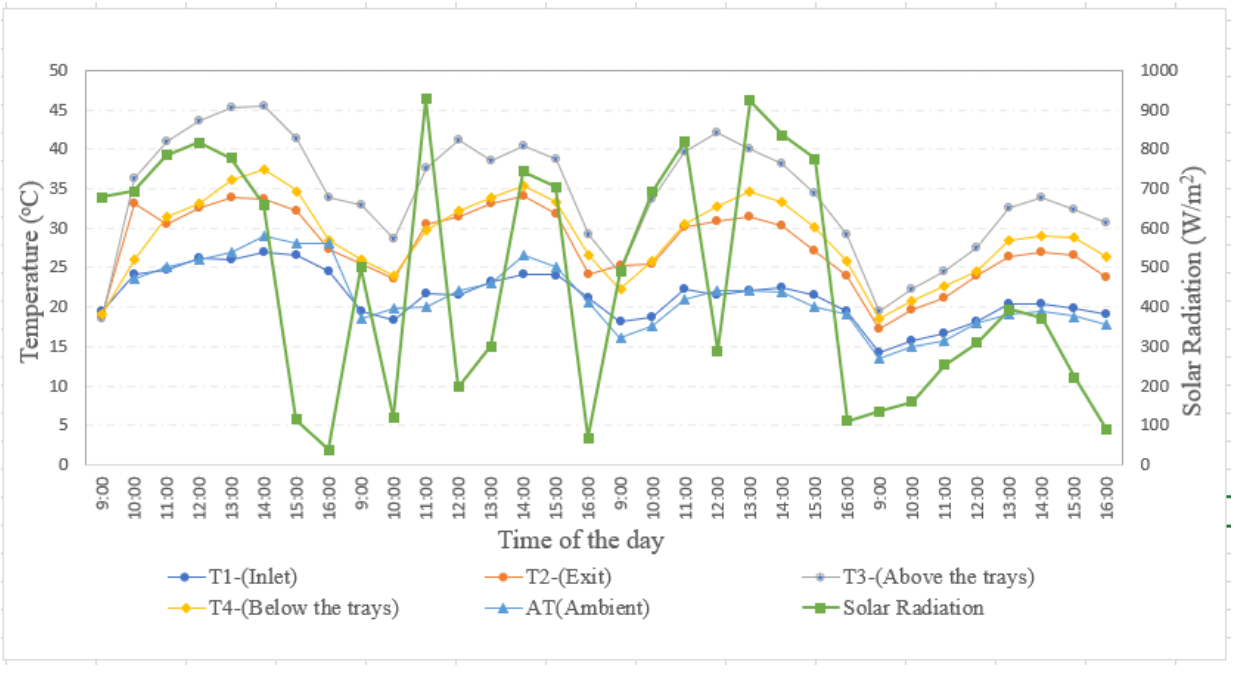

Figure 4. 9 Temperature variations for experiment I

Figure 4.10 shows the temperature variations inside and outside the GSD during experiment II of drying tomatoes without the PTSC in action.

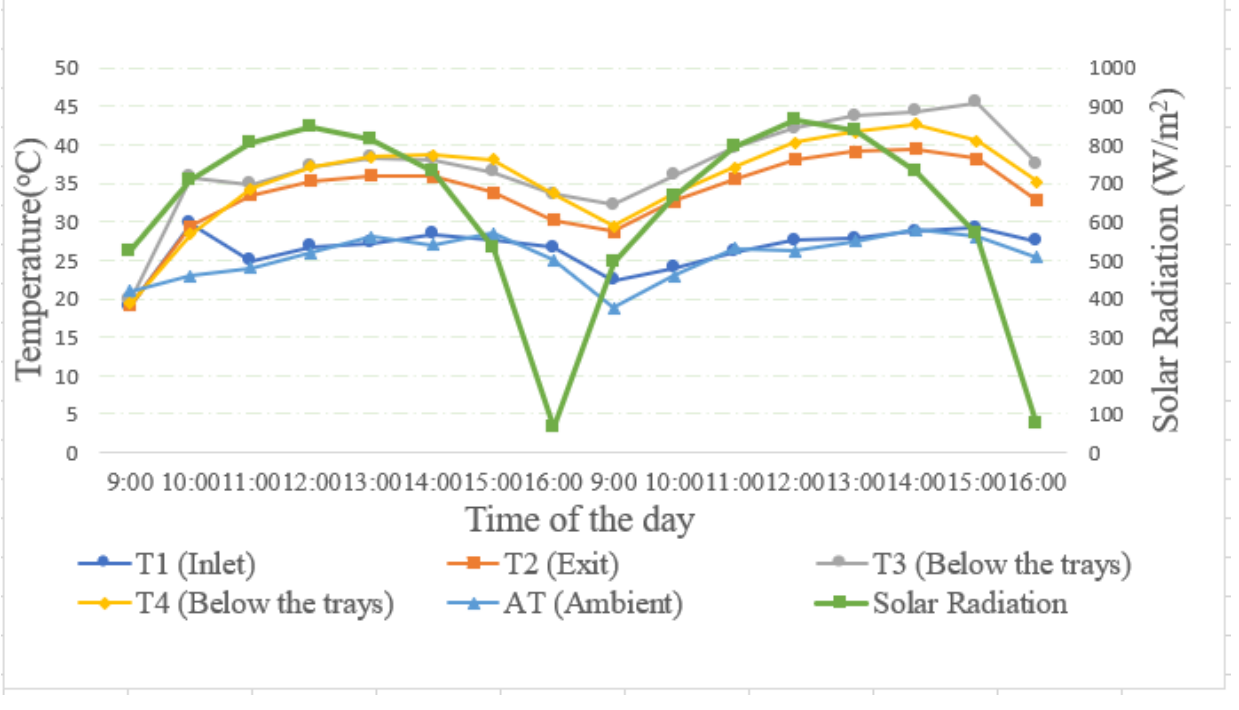

Figure 4. 10 Temperature variations for experiment II

Temperatures of ambient air and air entering the GSD were almost the same. This implied that cool ambient air entered the GSD during the drying of tomatoes. High temperatures at the middle of the GSD but above the drying tables was observed presumably because hot air is lighter and therefore rose up as cool or cold air was being heated up by the greenhouse effect. Temperatures

of air below the drying tables was always significantly higher compared to the air entering the GSD. This was because concrete the floor covered with a black polythene paper aided in maximum absorption of solar radiation inside the GSD. Temperatures of air exiting the GSD was always less compared to the temperature below and above the drying tables. This could be explained by the fact it carried moisture evaporated from the tomatoes.

Figure 4.11 below shows the variation of the ambient air temperature and temperatures inside the GSD at different positions of experiment III during the solar drying of tomatoes with the PTSC connected.

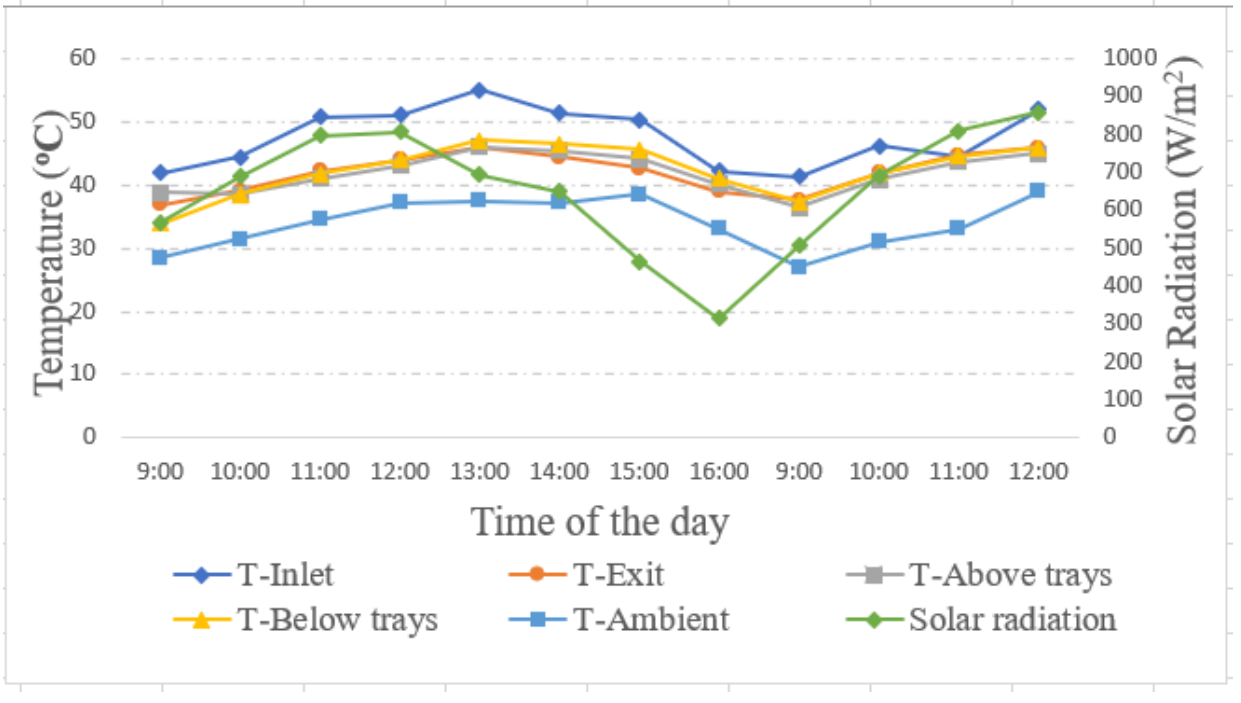

Figure 4. 11 Temperature variations for experiment III

The ambient temperature varied from 27 ^{o}C as the minimum at 1600Hrs of the first day and 39 ^{o}C as the maximum at 1200hrs of the second day. From figure 4.11, ambient temperature had a direct proportional relationship with solar radiation. Temperatures inside the GSD exhibited the same trend of increasing with the solar insolation. Temperatures at inlet from the PTSC were always above the ambient and other positions in the GSD in the range of 9 ^{o}C to 20 ^{o}C. Temperatures below and above the trays as wells as at the exit where fans were positioned, are observed to be very close to each other. This was as a result of the electric fan that was strategically located to circulate air inside the GSD.

The high temperatures increased and favoured the drying rate of tomatoes inside the GSD. However, they were monitored constantly not to exceed the optimum temperature of 60 ^{o}C. Temperatures above the optimum in drying of tomatoes cause case hardening.

4.4.2.3 Relative Humidity

Figure 4.12 shows the relative humidity variation of experiment I. Ambient air recorded high relative humidity compared to RH inside the GSD. This was as a result of cold weather experienced during the month the experiment was carried out.

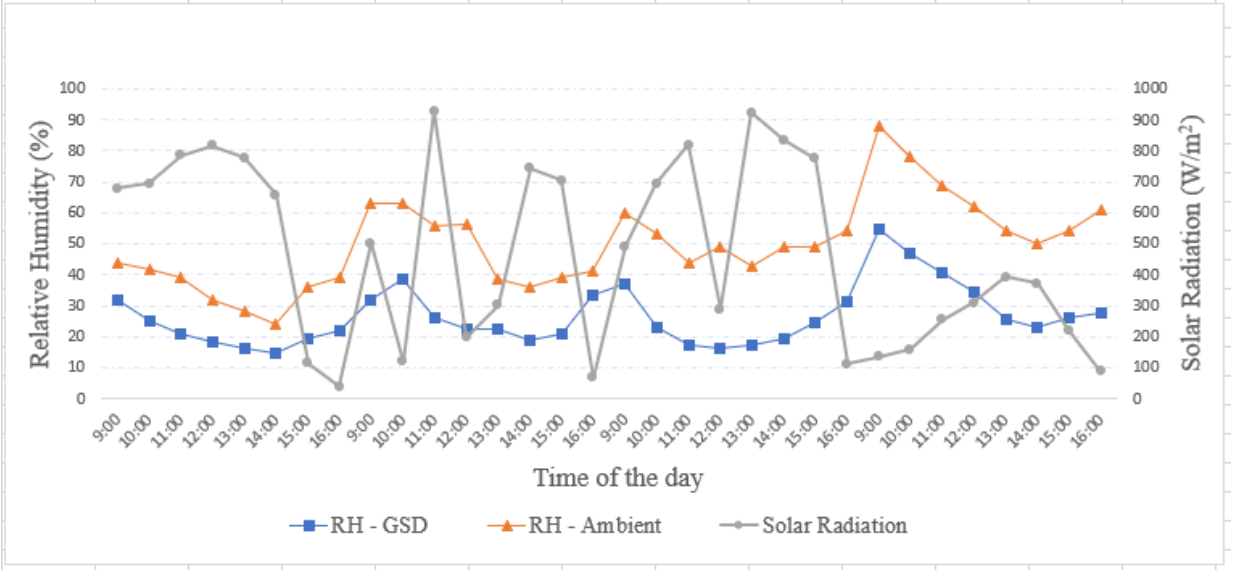

Figure 4. 12 Relative humidity variations of experiment I

Figure 4.13 shows the variations of the ambient air relative humidity and air relative humidity inside the GSD for experiment II and III.

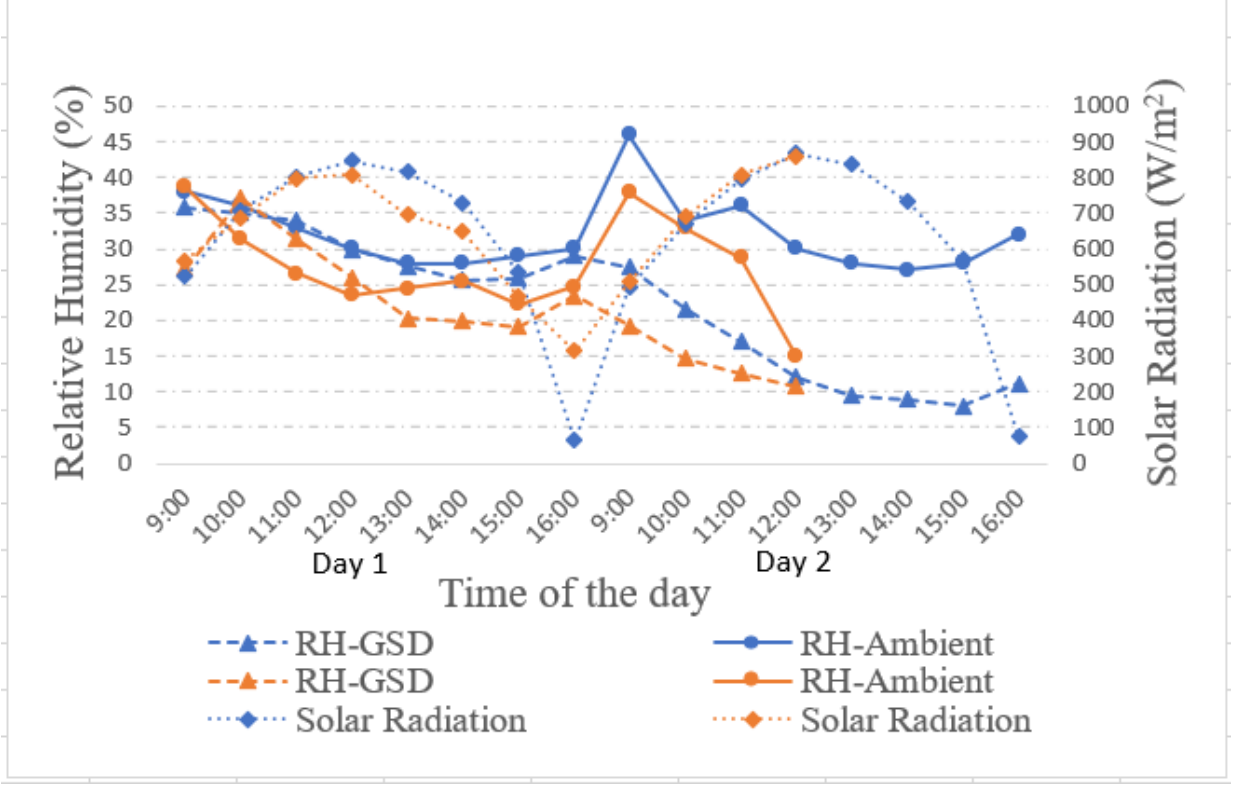

Figure 4. 13 Relative humidity variations during experiment II & III

The ambient relative humidity decreased with the increase in the solar radiation which also caused the ambient temperature to increase. Air relative humidity inside the GSD sharply increased from 27.2% to 37.2% between 0900Hrs and 1000Hrs on the first day for experiment III. This was as a result of loading fresh sliced tomatoes at the start of the experiment. From 1000hrs, air RH inside the GSD started to decrease as the temperatures rose inside and also fast removal of moist air by the four solar PV powered dc fans. From 1500Hrs to 1600Hrs, it is observed that both ambient air RH and RH inside the GSD gradually started increasing. This was due to insignificant moisture loss from the tomatoes and also reduced volume of air being evacuated by the dc fans that relied on solar radiation intensity

4.4.2.4 Masses

Masses of the tomatoes dried during the three experiments was continually and constantly monitored by weighing the samples using a digital weighing balance on an hourly basis. Tomatoes were considered fully dry from the constant digital weighing scale readings.

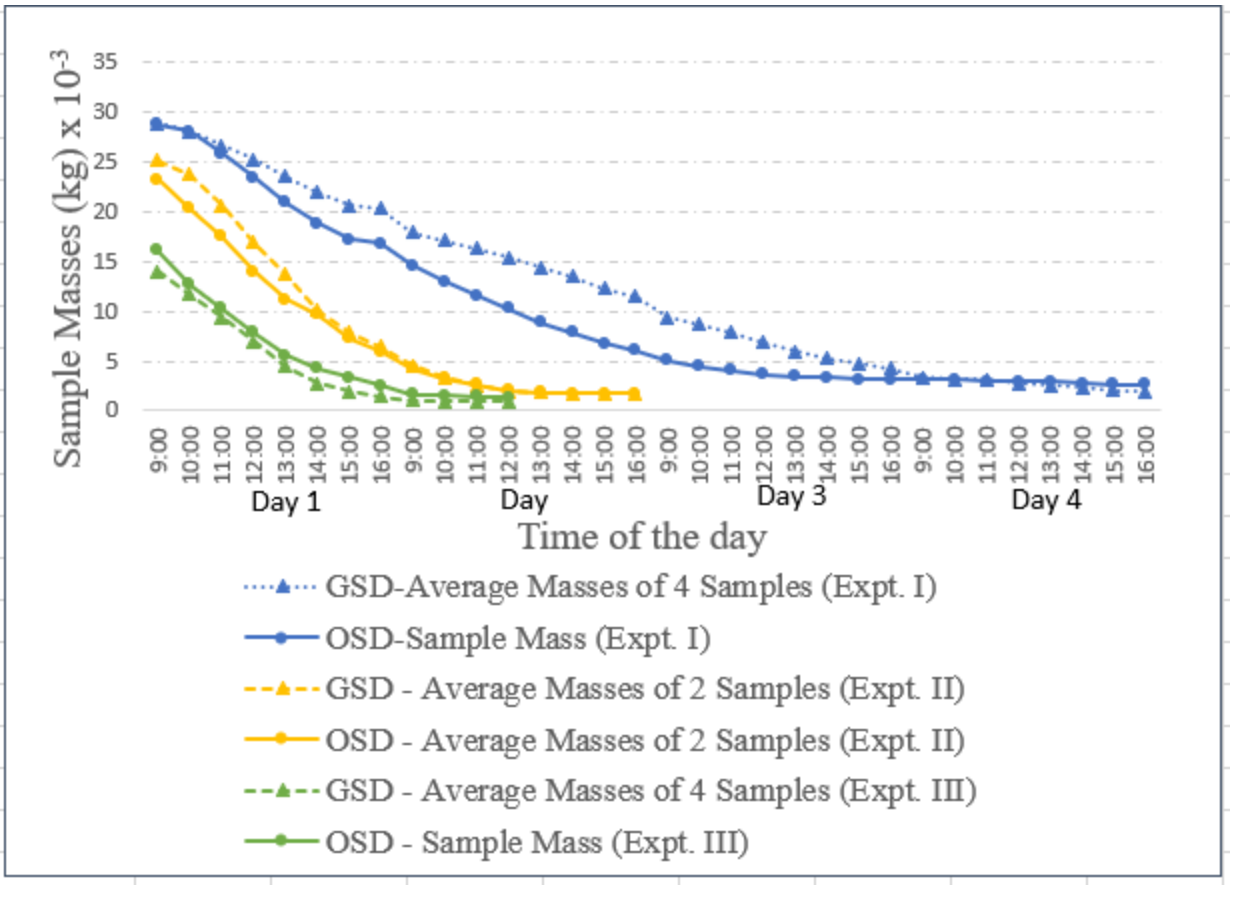

Figure 4. 14 Mass reduction of tomatoes samples dried in experiment I, II & III

In experiment I which was conducted from 29/05/2022 to 3/06/2022, there were four random samples inside the GSD, two on each drying table and one OSD sample whose masses were measured and manually recorded after one hour. The average mass of the four samples inside the GSD was evaluated. The mass of the OSD sample and the averaged mass of the samples inside the GSD were plotted in a graph as shown in the figure 4.14 with the colour code blue.

In experiment II which was conducted on 7/08/2022 to 8/08/2022, OSD and GSD methods were used to dry 12 kg and 14.5 kg of tomatoes respectively. Therefore, one drying table was used inside the GSD and one drying table was used outside for OSD. Two randomly selected samples from each drying table were constantly measured on hourly basis and their masses recorded. The figure 4.14 above shows the mass reduction of averaged masses of tomatoes samples from both OSD and GSD method with the colour code yellow.

In experiment III which was conducted on 20/09/2022 & 21/09/2022, one drying table was used inside the GSD. Two samples were randomly selected from the drying table and were constantly measured. For OSD method, one sample was used as the control experiment. The figure 4.14 above, shows the graph of sample masses from OSD and GSD method against time of drying with the colour code green.

Mass reduction of tomato samples was not the best method to determine the effectiveness of using GSD with and without the PTSC against the OSD. Instead, moisture content graph in the figure 4.18 was used to establish the best drying method.

4.4.2.5 Airflow

Airflow as discussed in chapter two was an important factor that determined drying of tomatoes in all the three experiments carried out. The GSD used for experiments was designed to have two air inlet vents and four exhaust openings where the dc fans were mounted to help remove hot air used after drying. The size of each of the two air inlet vents/openings was 0.24 m x 0.12 m giving an area opening of 0.0288 m^2. The total area of the two inlet openings combined was 0.0576 m^2 (2 x 0.0288 m^2). The volume of air entering the GSD depended on the average wind velocity of the test location. The wind speed of the ambient air was measured and recorded manually at an interval of one hour.

Removing warm air from the GSD was done by the use of four dc axial fans rated 12V and 0.6A which were powered by three solar photovoltaic modules each rated 30W. Each dc fan had a diameter of 0.12m with a cross-sectional area of 0.01131m^2. The total area of the openings combined at the exit was 0.04524m^2 (4 x 0.01131m^2). Warm air escaping from GSD through any small openings or opening of the door during entering the GSD was assumed negligible. The

volume of air removed by the fans from the GSD at any given time depended on the intensity of solar radiation.

The figure 4.15 below shows a graph of average dc exhaust fan speeds against time of the day during the drying period of experiment I. The four dc exhaust fans speeds measurement were done after every one hour using an air speedometer and their average computed. Respective solar radiations were obtained from hourly time stamps recorded in the multichannel data logger. It can be observed from the graph that the dc fan speeds had a direct proportion relationship with the solar radiation. In other words, as the solar radiation increased, the fan speeds increased hence removing larger amounts of moist air and vice versa. The sharp fluctuations of the fan speeds were as a result of the intermittent cloud cover during the particular days of drying. The fourth day of drying was quite cloudy and registered the least measurements of fan speeds. The minimum, maximum and average mass flow rates values of air removed from the GSD were 0.04224 kg/s, 0.23244 kg/s and 0.12528 kg/s, respectively.

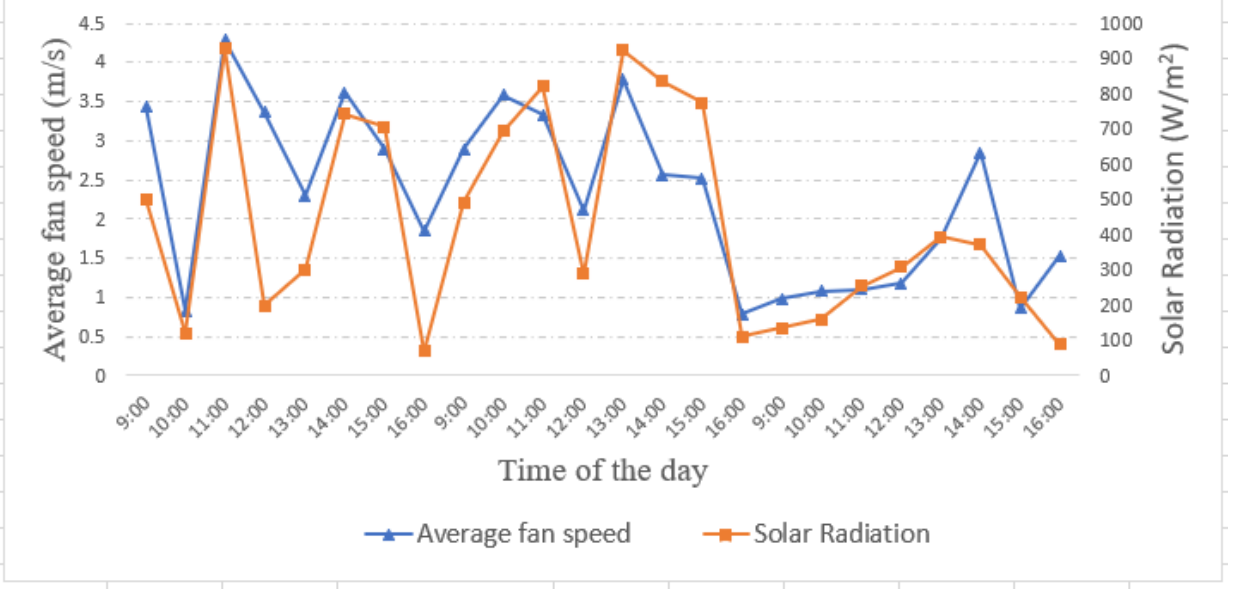

Figure 4. 15 Average exhaust fan speeds at the exit of the GSD with respective solar radiation for experiment I

Figure 4.16 shows the graph of mass flow rates of air entering and exiting the GSD against the time of the day from the data obtained during experiment II of drying tomatoes. The drying period had sunny and clear skies. It is observed that the solar radiation was consistent and had no major fluctuations. It resulted to almost a smooth curve of exhaust mass flow rates against the time of day. Similar observation was noted of direct relationship between the solar radiation and exhaust fan speeds. The power output of the photovoltaic modules increased with increase in solar radiation and vice versa. The minimum, maximum and average mass flow rate of air exiting the GSD was 0.08367 kg/s, 0.2368 kg/s and 0.1860 kg/s respectively.

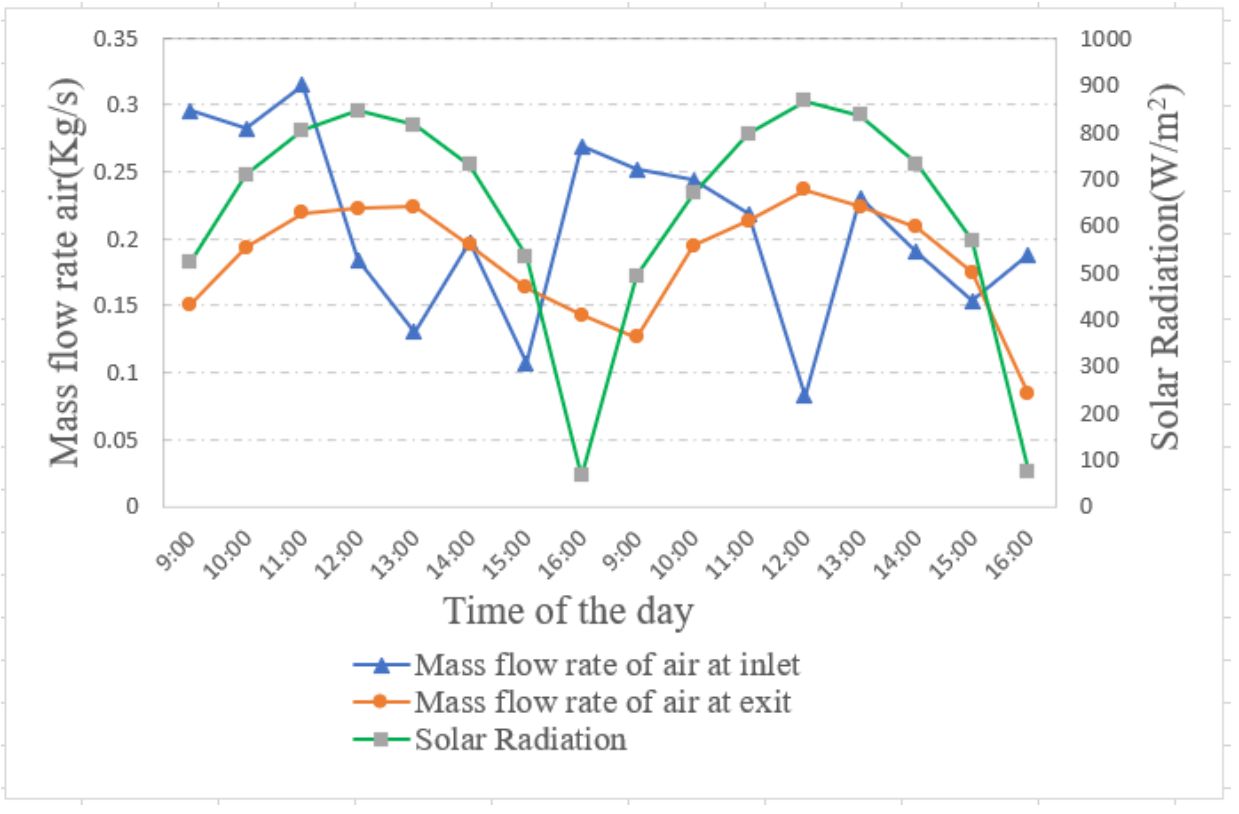

Figure 4. 16 Mass flow rates of air in and out of the GSD for experiment II

Figure 4.17 shows the variations of the ambient wind speed and the average fan speeds. It is observed that the fan speeds increased with increase in solar radiation. The wind speed during the experiment did not depend with the solar radiation. The ambient wind increased the rate of water removal from tomatoes dried using OSD method. The fan speeds indicated the removal rate of the warm and moist air from the GSD.

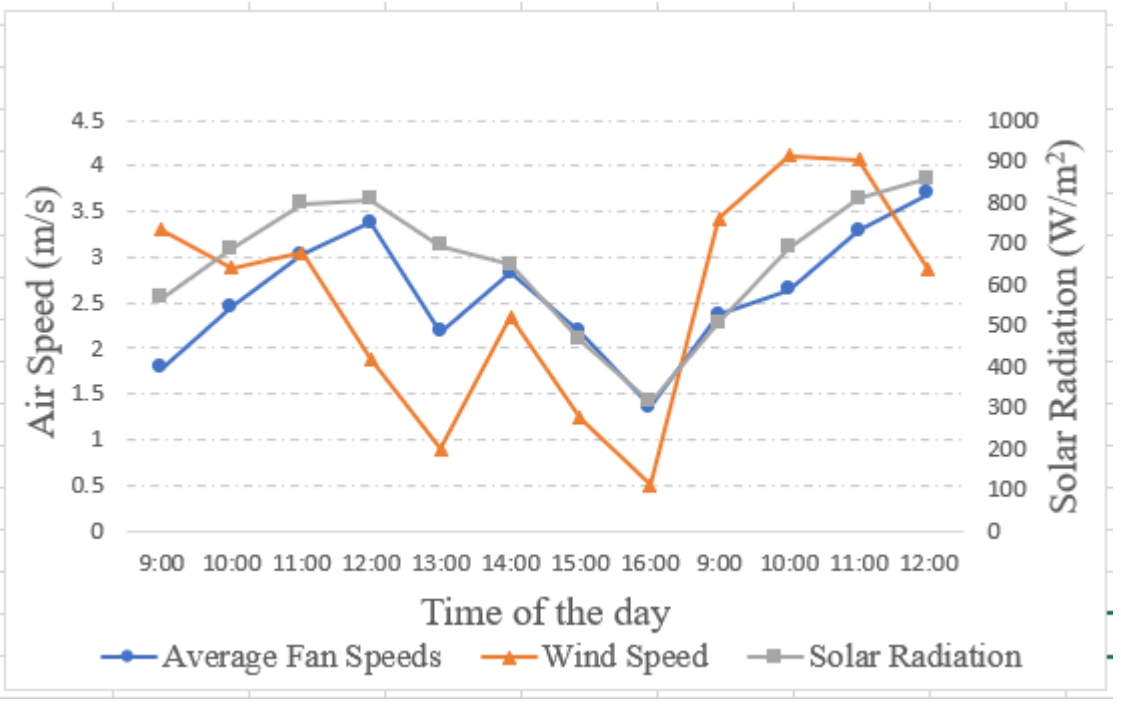

Figure 4. 17 Average exhaust fan speeds at the exit of the GSD with respective solar radiations for experiment III

4.4.3 **Performance Analysis**

In this section, performance analysis of the GSD with and without PTSC was done. It's worth mentioning that only experiment II and III were considered for this exercise as they were conducted with similar test conditions of clear sunny days and use of circulation fan inside the GSD. However, moisture content for the tomatoes used for experiment I was reported.

4.4.3.1 Determination of moisture content

Three experiments were conducted in testing the operation of the GSD. The tomatoes were used as the agricultural products for drying. Before drying of the tomatoes in the GSD, initial moisture content was determined experimentally and mathematically using a drying oven.

The table 4.3 below shows the initial moisture content on wet basis of the tomatoes used in testing the GSD. Hitherto, similar studies on tomatoes drying from different researchers reported initial moisture content of 96% (Benedict et al., 2019a) and 94% (Ringeisen et al., 2014).

Table 4. 3 Initial moisture contents of tomatoes used in the three experiments

Initial moisture content wet basis			
Experiment	***Sample G1(%)***	***Sample G2(%)***	**Average(%)**
I	93.1	94.7	93.9
II	94.9	92.3	93.6
III	95.0	93.4	94.2

The final safe storage moisture content of the dried tomatoes especially from the GSD was established from the numerical calculations as 14%. The result figure was validated using electrical oven method and was found and confirmed to agree to be 14%. Previous similar research studies on drying of tomatoes reported final moisture content of 10%(Ringeisen et al., 2014) 12% (Benedict et al., 2019a). The result obtained was within the acceptable range of safe storage moisture content of dried tomatoes.

The figure 4.18 shows a graph of the moisture contents by percentages of the averaged mass of tomato samples from experiment II and III. For experiment II, the GSD was not connected to the PTSC air heater whereas for experiment III, the GSD was connected to the PTSC air heater. In both experiments, control samples were randomly selected and dried using OSD method.

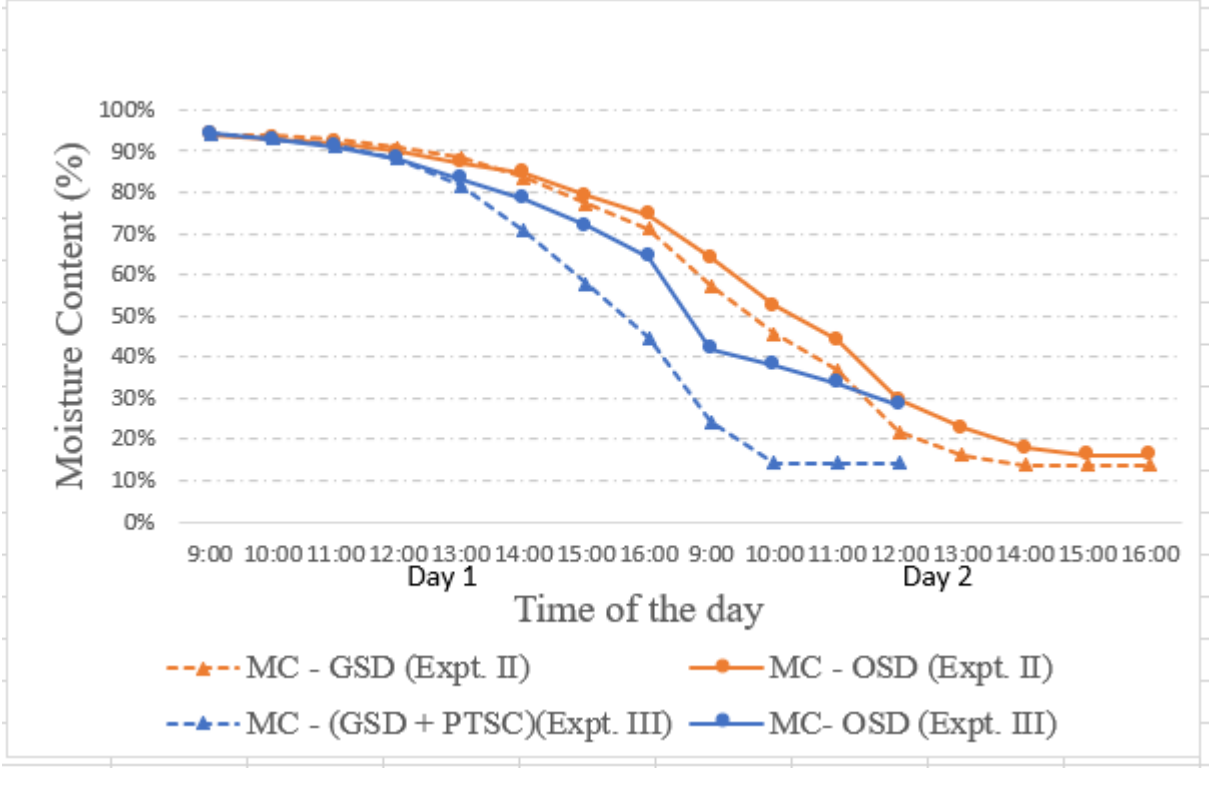

Figure 4. 18 Moisture contents by percentage of tomato samples from experiment II and III.

From figure 4.18, moisture contents for the period 09:00hrs to 14:00hrs of both samples in experiment II and from 09:00hrs to 12:00hrs for experiment III was almost equal respectively as

the drying was taking part. This was attributed to the easy removal of concentrated or saturated moisture at the surface of the freshly cut tomatoes. From 14:00hrs of experiment II and 12:00hrs of experiment III for the first day of drying, the moisture content difference commenced to be significantly noted. It was appreciated that drying of tomatoes involved movement of moisture content from the interior to the outer surface part of the tomato samples. Removing moisture from the interior part of the tomatoes required more heat energy and that was where PTSC air heater came into play.

At 14:00hrs of the first day for experiment II, moisture content from both sample (GSD and OSD) was exactly 83% and 85%. respectively. At 16:00hrs of the same first day of drying, moisture contents of tomato samples from GSD and OSD were 71% and 75% respectively giving a moisture content difference of 4%. At 1200hrs of the first day for experiment III, moisture content from both sample (GSD and OSD) was exactly the same at 88%. At 16hrs of the same first day of drying, moisture contents of tomato samples from GSD and OSD were 45% and 64% respectively giving a moisture content difference of 19%. The moisture content difference of 19% and 4% were obtained, when the GSD was connected with and without PTSC air heater respectively. It was observed that PTSC air heater connected to the GSD improved drying process by providing additional heat energy from preheated air. Both experiments were closed at 1600hrs and OSD samples were kept inside the GSD.

After closure of experiments on day one, the graph shows that drying continued inside the GSD after sunset despite the fact there was no sunshine. This drying was facilitated by the heat absorbed and stored by the concrete floor not covered with a black polythene paper in experiment II and covered with a black polythene paper in experiment III. The concrete floor served as a thermal energy storage system. The heat stored ensured continuous drying of tomatoes inside the GSD from 16hrs to 0900hrs the second day of drying for both experiments without tomatoes regaining moisture. This drying that utilized stored heat energy, reduced moisture content of GSD samples from 71% to 57% and from 75% to 64% for OSD in experiment II, from 45% to 24% for GSD, and from 64% to 42% for OSD in experiment III.

The second day of drying for experiment II, tomatoes inside the GSD took only five hours from 0900hrs to 1300hrs to reduce the moisture content from 57% to the desired safe storage moisture content of 14%. No more drying took place after this moisture content level of 14% and weighed masses of tomatoes samples gave constant readings. At 1400hrs of the second day, all the tomatoes inside the GSD were considered dry. The OSD samples took eight hours from 0900hrs to 1700hrs to reduce the moisture content from 64% to the desired safe storage moisture content of 14%.

The second day of drying for experiment III with GSD connected with PTSC air heater, tomatoes inside the GSD took only one hour from 0900hrs to 1000hrs to reduce the moisture content from 24% to the desired safe storage moisture content of 14%. This fast drying of tomatoes inside the GSD in the morning when solar radiation was not intense was as a result of the hot air from the PTSC. No more drying took place after this moisture content level of 14% and weighed masses of tomatoes samples gave constant readings. At 1000hrs of the second day, all the tomatoes inside the GSD were considered dry. However, for the OSD sample it was different. At 0900hrs of the second day, the moisture content level was at 42% and this required drying to continue to achieve the desired safe storage moisture content of less than15%. At 1200hrs of the second day, the OSD sample had reached a moisture content of approximately 28%. The drying was too slow such that the tomato sample lost 0.1 gram of moisture per hour. From the calculations, it was expected that the final mass of the completely dried OSD sample combined with the tray could weigh 6.5 grams. At 1200hrs of the second day, it was weighing 6.7 grams and from extrapolation, it required two more hours to completely dry the sample to reach the total final and expected mass of 6.5 grams.

Overall, and from the figure 4.18, GSD combined with the PTSC was faster and more efficient compared to the GSD without the PTSC air heater. In addition, it was observed that the use of GSD with and without the PTSC was better method of drying tomatoes compared to OSD method. It therefore, for experiment II, took 12 hours and 15 hours for GSD without PTSC air heater and OSD respectively, and for experiment III, took 8 hours and 12 hours for GSD combined with PTSC and OSD respectively to dry the tomatoes samples to the desired moisture content of 14%.

4.4.3.2 Determination of drying rates

The mass of water evaporated or removed from the wet tomato products was calculated using equation 3.6 as described in Chapter 3:

The drying rate of the GSD was evaluated using equation 3.8 in chapter 3. Drying rates were evaluated from the two experiments conducted of drying tomatoes. The table 4.4 shows the method of drying, initial mass of tomatoes, the amount of moisture removed from tomatoes, time taken and the respective drying rates in kg/hr.

Table 4. 4 Drying rates from different drying methods

Expt.	Method of drying	Initial mass of tomatoes (m_p) in kg	Mass of moisture removed (M_w) in (kg)	Time taken to dry tomatoes (Hrs)	Drying rate (kg/hr)
II	GSD	14.5	13.5	11	1.227
	OSD	12	11.2	15	0.747
III	GSD + PTSC	14.9	13.9	8	1.738

From the drying rates evaluated above, OSD showed to have the lowest drying rate of 0.747 kg/hr and hence unsuitable for drying tomatoes in large scale. GSD modified with PTSC showed to have higher drying rate of 1.738 kg/hr compared to GSD without the PTSC with 1.227 Kg/hr. The highest drying rate was realized due to the constant supply of hot air into the GSD.

4.4.3.3 Saving in drying time

Drying time was an important performance parameter of the dryer which represented the time taken by the GSD for removing the moisture content from initial level 94% to the final safe storage moisture level of 14%. Equation 3.35 was used in evaluating the saving in drying time. The same equation was modified to compare the modified GSD with the GSD without the PTSC in terms of saving in drying time.

a. Experiment II: GSD and OSD

Time taken to dry tomatoes in OSD was 15 hours and time taken to dry tomatoes in the GSD without the PTSC was 11 hours. Substituting in the equation 3.35, we get the percentage of saved drying time as 26.7%:

b. Experiment III: (GSD + PTSC) and OSD

Time taken to dry tomatoes in OSD was 12 hours and time taken to dry tomatoes in the modified GSD with the PTSC was 8 hours. Substituting in the equation 3.35, we get percentage of saved drying time as 33.3%

c. Comparison of (GSD + PTSC) with GSD

Percentage of saved drying time of the modified GSD with the PTSC (experiment III) compared to GSD without the PTSC (experiment II) with circulation fan in both cases was evaluated. Time taken to dry tomatoes in GSD without the PTSC from experiment (II) was 11 hours and time taken to dry tomatoes in the modified GSD with the PTSC from experiment (III) was 8 hours. Substituting in the equation 3.35, we get percentage of saved drying time as 27.3%.

The modified greenhouse solar dryer with a parabolic trough solar collector considerably reduced the drying time compared to GSD without PTSC and OSD. Drying of tomatoes using GSD with and without PTSC compared to OSD showed to have utilized less hours of drying with respective percentages of saved time as 33.3% and 26.7%. Modified GSD with PTSC showed to perform better than the GSD without PTSC with a percentage saved time of 27.3%. Similar study was carried to dry tomatoes in a GSD modified with concave concentrator. The tomatoes in the dryer with the concentrator reached the 10% moisture content level at 22.3% faster than those in the control dryer.

4.4.3.4 Specific Energy Consumption (SEC)

From the detailed calculations in Appendix V using equation 3.36, the SEC for the GSD in drying the tomatoes with and without the PTSC air heater were 5.54 kWh/kg and 7.627 kWh/kg respectively. When the PTSC air heater was connected to the GSD to provide hot air, drying of equal amounts of tomatoes took fewer hours compared to GSD without the PTSC, hence the low value of SEC.

4.4.3.5 Specific Moisture Extraction Rate (SMER)

SMER was evaluated as 0.1778 kg/kWh and 0.1311 kg/kWh using equation 3.37 and shown in appendix VI for the GSD with and without the PTSC air heater. In this performance analysis, it was demonstrated that GSD connected with the PTSC air heater extracted higher amount of moisture per hour compared with the GSD without the PTSC air heater.

4.4.3.6 Determination of GSD Thermal Efficiency

The thermal efficiency of the GSD without the PTSC air heater was evaluated as 11.3% from appendix VII. It significantly depended with the amounts of tomatoes being dried. Thus, the higher the amounts of tomatoes being dried in kilograms, the higher the thermal drying efficiency.

4.5 Challenges Encountered

There were two main challenges faced during the setup of experiments. First one, when the PTSC was supported and inclined with the adjustable stands, the absorber inlet position was way too high above the already fabricated drying tables. The effect could be that hot air generated could not have a chance to come into direct contact with the tomatoes that were being dried. This required the adjustable stands to be adjusted to their lowest position, the slanting position was eliminated. Consequently, the ground was dug just below the side of the PTSC where air was entering the absorber tube to a depth that could make the PTSC have a slope angle of 15^{o} to 20^{o}.

The second challenge was the shading effect of the GSD on the PTSC. Appreciating the fact that the GSD was not oriented on a true North-South direction, it produced a shade at the rear side in the afternoon. This required a considerable distance to be left between the GSD and the PTSC. Consequently, there was a chance of significant heat loss from the hot air to the pipe and the surrounding air. This resulted to temperatures of hot air entering the GSD reducing from above 80 ^{o}C to a range of 55 ^{o}C to 65 ^{o}C, which in sense, was suitable for drying the tomatoes.

4.6 Chapter Summary

Results and findings of the intended research study were presented and exhaustively discussed. Clearly and without any doubt, the objectives of the study were sufficiently met. However, there were significant areas of research that called for more work to be done as presented in the next chapter.

CHAPTER FIVE: CONCLUSIONS AND RECOMMENDATIONS

This chapter presents in summary, the conclusions and the recommendations drawn from the research study.

5.0 Conclusions

Outlined below, under each objective are the conclusions arrived at after the research study was completed.

Objective I: **To design the proposed parabolic trough concentrator for pre-heating air.**

- A PTSC for preheating air of a GSD was designed using relevant mathematical models from literature. Key geometrical parameters of the PTSC are rim angle of 98^{o}, focal length of 0.261m, height of 0.345m, aperture width of 1.2m, total length of 2m, and a concentration ratio of 15.1.

Objective II: **To fabricate the proposed parabolic trough solar concentrator.**

The PTSC was fabricated using locally available materials and local labour. The total cost of the fabricated PTSC was K2,285, as outlined in Appendix 1 of this dissertation.

Objective III: **To test the performance of the parabolic trough solar collector.**

- Focusing/concentrating solar collectors are suitable in modifying the GSD. The PTSC was very reliable in preheating drying air for the GSD. The average surface temperature of the receiver was 85.6 ^{o}C and the temperature at the collector outlet was 80.1 ^{o}C on average.
- Heat transfer losses through convection and radiation were determined as 306.6 W and 72.49 W respectively giving a total of 379.09 W.
- PTSC thermal efficiency of 5.3% was achieved which was comparable to other similar research studies by different researchers.

Objective IV: **To test the performance of the greenhouse solar tunnel dryer with and without the attached parabolic trough solar collector.**

- From the literature review conducted, PHLs of agro-based products particularly the tomatoes is a serious challenge in the agricultural sector.
- Drying of agro-products like tomatoes to increase their shelf life is a mature and a proven technology in the agricultural sector.

- Greenhouse solar drying is a reliable technology in drying agro-based products like tomatoes used in the test experiments.
- Fresh and dried tomatoes were experimentally found to have an initial and final moisture contents of 94% and 14% respectively.
- GSD modified with a PTSC air heater dried 15kg equal amount of tomatoes faster than the same GSD without the PTSC air heater. Practically, GSD with and without the PTSC air preheater took 8 hours and 11 hours respectively to dry 15kg equal amount of sliced tomatoes. As a result, the percentage saved time was 27.3%.
- Drying rates of the GSD with and without the PTSC air heater was 1.738 kg/hr and 1.227 kg/hr, respectively.
- Specific Energy Consumption (SEC) of the GSD with and without the PTSC air heater was 5.54 kWh/kg and 7.627 kWh/kg respectively.
- Specific Moisture Extraction Rate (SMER) of the GSD with and without the PTSC air heater was found to be 0.1778 kg/kWh and 0.1311 kg/kWh respectively.
- Thermal efficiency of the GSD was found to be 11.3%, which was dependent on the amount of tomatoes dried in kg.
- An air circulation fan inside the GSD with and without the PTSC air heater accelerated drying of tomatoes.

5.1 Recommendations

Despite the fact that the objectives of the research study were sufficiently covered, the following are some of the recommendations to further enrich the work that was done:

Objective II

- Replacement of the ply wood on the PTSC with a more durable material like plastic.

Objective III

- Automatic tracking system for the sun to be considered as it will be more accurate than manual tracking. Automatic tracking system of the sun for the PTSC will ensure increasing high temperatures of the hot drying air throughout the sunshine hours.
- Use of the glass cover with the PTSC to reduce on heat losses through convection mode of heat transfer catalyzed by the wind effect.
- Use of bigger fan to push air into the GSD, either axial or centrifugal to match the air flow requirements of the already fabricated GSD.

Objective IV

- Mechanized cutting of tomato slices to ensure uniform thickness. Consequently, all the tomatoes will dry at the same time.
- To ensure maximum drying efficiency, the GSD to be always loaded to the full capacity under which it was designed.
- More efficient thermal energy storage system inside the GSD to be considered for research to complement the concrete slab.

5.2 Chapter Summary

Conclusions presented in this chapter have tried to demonstrate the satisfactorily end results that were realized from each objective whereas the recommendations have tried to point out some gaps that would be filled by future researchers.

REFERENCES

1. Abdulhamed, A. J., Adam, N. M., Ab-Kadir, M. Z. A., & Hairuddin, A. A. (2018). Review of solar parabolic-trough collector geometrical and thermal analyses, performance, and applications. *Renewable and Sustainable Energy Reviews*, *91*, 822–831. https://doi.org/10.1016/j.rser.2018.04.085
2. Akoy, E.-A., Ismail, M., Ahmed, E.-F., & Luecke, W. (n.d.). *Design and Construction of A Solar Dryer for Mango Slices*. 7.
3. Arunkumar, S., & Ramesh, K. (2022a). Design and optimization of solar parabolic trough collector with evacuated absorber by grey relational analysis. *Current Science*, *122*(4), 410. https://doi.org/10.18520/cs/v122/i4/410-418
4. Arunkumar, S., & Ramesh, K. (2022b). Design and optimization of solar parabolic trough collector with evacuated absorber by grey relational analysis. *Current Science*, *122*(4), 410. https://doi.org/10.18520/cs/v122/i4/410-418
5. Arunkumar, S., & Ramesh, K. (2022c). Design and optimization of solar parabolic trough collector with evacuated absorber by grey relational analysis. *Current Science*, *122*(4), 410. https://doi.org/10.18520/cs/v122/i4/410-418
6. Barnwal, P., & Tiwari, G. N. (2008). Grape drying by using hybrid photovoltaic-thermal (PV/T) greenhouse dryer: An experimental study. *Solar Energy*, *82*(12), 1131–1144. https://doi.org/10.1016/j.solener.2008.05.012
7. Bellos, E., & Tzivanidis, C. (2019). Alternative designs of parabolic trough solar collectors. *Progress in Energy and Combustion Science*, *71*, 81–117. https://doi.org/10.1016/j.pecs.2018.11.001
8. Benedict, E. O., Edward, D., & Oboetswe, M. S. (2019a). *Development of a Cost-effective Design of a P-V Ventilated Greenhouse Solar Dryer for Commercial Preservation of Tomatoes in a Rural Setting*. *4*(4), 12.

9. Benedict, E. O., Edward, D., & Oboetswe, M. S. (2019b). *Development of a Cost-effective Design of a P-V Ventilated Greenhouse Solar Dryer for Commercial Preservation of Tomatoes in a Rural Setting*. *4*(4).
10. Çağlar, A. (2016, July). *Design of a Parabolic Trough Solar Collector Using a Concentrator with High Reflectivity*. The 2nd World Congress on Mechanical, Chemical, and Material Engineering. https://doi.org/10.11159/htff16.152
11. Chauhan, P. S., & Kumar, A. (2016). Performance analysis of greenhouse dryer by using insulated north-wall under natural convection mode. *Energy Reports*, *2*, 107–116. https://doi.org/10.1016/j.egyr.2016.05.004
12. Crabtree, G. W., Lewis, N. S., Hafemeister, D., Levi, B., Levine, M., & Schwartz, P. (2008). Solar Energy Conversion. *AIP Conference Proceedings*, *1044*, 309–321. https://doi.org/10.1063/1.2993729
13. Dabiri, S., & Rahimi, M. F. (2016). *Basic introduction of solar collectors and energy and exergy analysis of a heliostat plant*. 8.
14. Deeto, S., Thepa, S., Monyakul, V., & Songprakorp, R. (2018). The experimental new hybrid solar dryer and hot water storage system of thin layer coffee bean dehumidification. *Renewable Energy*, *115*, 954–968. https://doi.org/10.1016/j.renene.2017.09.009
15. Duffie, J. A., & Beckman, W. A. (2013). *Solar Engineering of Thermal Processes*. 928.
16. ELkhadraoui, A., Kooli, S., Hamdi, I., & Farhat, A. (2015). Experimental investigation and economic evaluation of a new mixed-mode solar greenhouse dryer for drying of red pepper and grape. *Renewable Energy*, *77*, 1–8. https://doi.org/10.1016/j.renene.2014.11.090
17. Eltawil, M. A., Azam, M. M., & Alghannam, A. O. (2018). Energy analysis of hybrid solar tunnel dryer with PV system and solar collector for drying mint (MenthaViridis).

Journal of Cleaner Production, *181*, 352–364. https://doi.org/10.1016/j.jclepro.2018.01.229

18. Fudholi, A., Othman, M. Y., Ruslan, M. H., & Sopian, K. (2013). Drying of Malaysian *Capsicum annuum* L. (Red Chili) Dried by Open and Solar Drying. *International Journal of Photoenergy*, *2013*, 1–9. https://doi.org/10.1155/2013/167895
19. Hamdani, Rizal, T. A., & Muhammad, Z. (2018). Fabrication and testing of hybrid solar-biomass dryer for drying fish. *Case Studies in Thermal Engineering*, *12*, 489–496. https://doi.org/10.1016/j.csite.2018.06.008
20. Kamarulzaman, A., Hasanuzzaman, M., & Rahim, N. A. (2021a). Global advancement of solar drying technologies and its future prospects: A review. *Solar Energy*, *221*, 559–582. https://doi.org/10.1016/j.solener.2021.04.056
21. Kamarulzaman, A., Hasanuzzaman, M., & Rahim, N. A. (2021b). Global advancement of solar drying technologies and its future prospects: A review. *Solar Energy*, *221*, 559–582. https://doi.org/10.1016/j.solener.2021.04.056
22. Kıyan, M., Bingöl, E., Melikoğlu, M., & Albostan, A. (2013). Modelling and simulation of a hybrid solar heating system for greenhouse applications using Matlab/Simulink. *Energy Conversion and Management*, *72*, 147–155. https://doi.org/10.1016/j.enconman.2012.09.036
23. Kumar, M., Sansaniwal, S. K., & Khatak, P. (2016). Progress in solar dryers for drying various commodities. *Renewable and Sustainable Energy Reviews*, *55*, 346–360. https://doi.org/10.1016/j.rser.2015.10.158
24. Macedo-Valencia, J., Ramírez-Ávila, J., Acosta, R., Jaramillo, O. A., & Aguilar, J. O. (2014). Design, Construction and Evaluation of Parabolic Trough Collector as Demonstrative Prototype. *Energy Procedia*, *57*, 989–998. https://doi.org/10.1016/j.egypro.2014.10.082

25. MacPhee, D., & Dincer, I. (2009). Thermal modeling of a packed bed thermal energy storage system during charging. *Applied Thermal Engineering*, *29*(4), 695–705. https://doi.org/10.1016/j.applthermaleng.2008.03.041

26. Mehta, P., Samaddar, S., Patel, P., Markam, B., & Maiti, S. (2018). Design and performance analysis of a mixed mode tent-type solar dryer for fish-drying in coastal areas. *Solar Energy*, *170*, 671–681. https://doi.org/10.1016/j.solener.2018.05.095

27. Mohsin, A. S. M., Maruf, Md. N. I., Sayem, A. H. M., Mojumdar, Md. R. R., & Shamim Farhad, H. M. (2011). Prospect & Future of Solar Dryer: Perspective Bangladesh. *International Journal of Engineering and Technology*, *3*(2), 165–170. https://doi.org/10.7763/IJET.2011.V3.217

28. Naranchala, K., Senangkanikorn, N., Krawklom, U., & Choomfon, C. (2020). *A development of solar dryer using parabolic mirror plates*. *8*(2), 5.

29. Petela, R. (2003). Exergy of undiluted thermal radiation. *Solar Energy*, *74*(6), 469–488. https://doi.org/10.1016/S0038-092X(03)00226-3

30. Ringeisen, B., M. Barrett, D., & Stroeve, P. (2014). Concentrated solar drying of tomatoes. *Energy for Sustainable Development*, *19*, 47–55. https://doi.org/10.1016/j.esd.2013.11.006

31. Seveda, M. S. (2012). Design and Development of Walk-In Type Hemicylindrical Solar Tunnel Dryer for Industrial Use. *ISRN Renewable Energy*, *2012*, 1–9. https://doi.org/10.5402/2012/890820

32. Simate, I., & Simukonda, K. (2022). Photovoltaic Forced Convection Greenhouse Solar Dryer with an Integrated Vertical Solar Collector for Mango Drying. *Advances in Image and Video Processing*, *10*(2). https://doi.org/10.14738/aivp.102.12077

33. Singh, P., & Gaur, M. K. (2022). A review on thermal analysis of hybrid greenhouse solar dryer (HGSD). *Journal of Thermal Engineering*, 103–119. https://doi.org/10.18186/thermal.1067047

34. Slimani, M. E. A., Amirat, M., Bahria, S., Kurucz, I., Aouli, M., & Sellami, R. (2016). Study and modeling of energy performance of a hybrid photovoltaic/thermal solar collector: Configuration suitable for an indirect solar dryer. *Energy Conversion and Management*, *125*, 209–221. https://doi.org/10.1016/j.enconman.2016.03.059
35. Sookramoon, K. (2016a). Design of a Solar Tunnel Dryer Combined Heat with a Parabolic Trough for Paddy Drying. *Applied Mechanics and Materials*, *851*, 239–243. https://doi.org/10.4028/www.scientific.net/AMM.851.239
36. Sookramoon, K. (2016b). Design of a Solar Tunnel Dryer Combined Heat with a Parabolic Trough for Paddy Drying. *Applied Mechanics and Materials*, *851*, 239–243. https://doi.org/10.4028/www.scientific.net/AMM.851.239
37. Srinivasan, G., & Muthukumar, P. (2021). A review on solar greenhouse dryer: Design, thermal modelling, energy, economic and environmental aspects. *Solar Energy*, *229*, 3–21. https://doi.org/10.1016/j.solener.2021.04.058
38. Tiwari, S., Tiwari, G. N., & Al-Helal, I. M. (2016). Performance analysis of photovoltaic–thermal (PVT) mixed mode greenhouse solar dryer. *Solar Energy*, *133*, 421–428. https://doi.org/10.1016/j.solener.2016.04.033
39. Valan Arasu, A., & Sornakumar, T. (2007). Design, manufacture and testing of fiberglass reinforced parabola trough for parabolic trough solar collectors. *Solar Energy*, *81*(10), 1273–1279. https://doi.org/10.1016/j.solener.2007.01.005
40. Vijayan, S., Arjunan, T. V., & Kumar, A. (2020). Exergo-environmental analysis of an indirect forced convection solar dryer for drying bitter gourd slices. *Renewable Energy*, *146*, 2210–2223. https://doi.org/10.1016/j.renene.2019.08.066
41. Yaghoubi, M., Ahmadi, F., & Bandehee, M. (2013). Analysis of Heat Losses of Absorber Tubes of Parabolic through Collector of Shiraz (Iran) Solar Power Plant. *Journal of Clean Energy Technologies*, 33–37. https://doi.org/10.7763/JOCET.2013.V1.8

42. Youcef-Ali, S., Messaoudi, H., Desmons, J. Y., & Abene, A. (2001). Determination of the average coefficient of internal moisture transfer during the drying of a thin bed of potato slices. *Journal of Food Engineering*, 7.

43. Andritso, N., Dalampakis, P. & Kolios, N., 2003. Use of geothermal energy for tomato drying. *Oregon Institute of Technology Geo-Heat Center Bulletin.*

44. Bala, B. et al., 2003. Solar drying of pineapple using solar tunnel drier. *Renewable Energy,* Volume 28, pp. 183-190.

45. Belessiotis, V. & Delyannis, E., 2011. Solar drying. *Solar Energy,* 85(8), pp. 165-169.

46. Benedict, E. O., Dintwa, E. & Oboetswe, M. S., 2019. Development of a Cost-effective Design of a P-V Ventilated Greenhouse Solar Dryer for Commercial Preservation of Tomatoes in a Rural Setting. *Advances in Technology Innovation,* 4(4), pp. 222-233.

47. ELkhadraoui, A., Kooli, S., Hamdi, I. & Farhat, A., 2015. Experimental investigation and economic evaluation of a new mixed-mode solar greenhouse dryer for drying of red pepper and grape. *Renewable Energy,* Volume 77, pp. 1-8.

48. FAO, 2022. *Food Loss and Waste Database.* [Online]
Available at: https://www.fao.org/platform-food-loss-waste/flw-data/en/
[Accessed 2 August 2022].

49. Feng, H., Yin, Y. & Tang, J., 2012. Microwave drying of food and agricultural materials: basics and heat and mass transfer modelling. *Food Engineering Reviews,* 4(2), pp. 89-106.

50. Fudholi, A., Othman, M. Y., Ruslan, M. H. & Sopian, K., 2013. Drying of Malaysian Capsicum annuum L. (Red Chili) Dried by Open and Solar Drying. *international journal of photoenergy,* Volume 2013, p. 9.

51. Google, 2022. *Google Earth.* [Online]
Available at: https://earth.google.com/web/@-15.39428409,28.33589434,1261.38449009a,999.49549581d,30y,0h,0t,0r/data=MikKJw

olCiExZG9Pb3RZQnVPZG9IQmswTFFCcTVvTDIwVkpOdHI0UmsgAQ

[Accessed 15 September 2022].

52. Gutti, B., Kiman, S. & Murtala, A. M., 2012. Solar Dryer- An effective tool for agricultural products preservation. *Journal of Applied technology in Environmental Sanitation,* 2(1), pp. 31-38.
53. Hasan, M. & Langrish, T., 2017. *Clean Energy for Sustainable Development.* 2nd ed. Australia: Elsevier.
54. Hodges, J. R., J., C. & Bennett, B., 2011. Post harvest losses and waste in developed and less developed countries: opportunities to improve resource use. *The Journal of Agricultural Science,* Volume 149, pp. 37-45.
55. Holsoft, 2022. *Holsoft Humidity Calculator.* [Online]

Available at: https://www.holsoft.nl/physics/rhcalc1.htm

[Accessed 29 September 2022].
56. Janjai, S., 2012. A greenhouse type solar dryer for small-scale dried food industries: development and dissemination. *International Journal of Energy and Environment,* Volume 3, pp. 383-398.
57. Joy, C., George, P. & Jose, K., 2001. Solar tunnel drying of red chillis (Capsicum annum L.). *Journal of food science and technology (Mysore),* 38(3), pp. 213-216.
58. Karim, M. & Hawlader, M., 2004. Development of solar air collectors for drying applications. *Energy Conversion and Management,* 45(3), pp. 329-344.
59. Khan, M. A. et al., 2013. Development of a Small Scale Concentrating Parabolic Trough Solar Collector for Drying Purposes. *Engineering International,* 1(1), p. 11.
60. Kumar, D. & Kalita, P., 2017. Reducing Postharvest Losses during Storage of Grain Crops to Strengthen Food Security in Developing Countries. *Foods,* 6(1), p. 8.

61. Motwani, K., Chotai, N., Patel, J. & Hadiya, R., 2020. Design and experimental investigation on cut tube absorber for solar parabolic trough collector. *Energy Sources, Part A: Recovery, Utilization, and Environmental Effects.*

62. Mujumdar, A., 2014. *Handbook ofIndustrial Drying.* fourth ed. s.l.:s.n.

63. Okos, M., Campanella, O., Narsimhan, G. & Singh, R., 2006. *Food Dehydration, Handbook of Food Engineering.* s.l.:CRC Press.

64. Prakash, O. & Kumar, A., 2013. Historical review and recent trends in solar drying systems. *International Journal of Green Energy,* Volume 10, pp. 690-738.

65. Simate, I. N., 2001. SIMULATION OF THE MIXED-MODE NATURAL-CONVECTION SOLAR DRYING OF MAIZE. *Drying Technology: An International Journal,* 19(6), pp. 1137-1155.

66. Weisman, J. & Eckart, R., 1985. *Modern Power Plant Engineering.* s.l.:Prentice-Hall.

67. Zhang, F., Zhang, M. & Mujumdar, A. S., 2011. Drying characteristics and quality of restructured wild cabbage chips. *Drying Technology,* 29(6), pp. 682-688.

68. Zobaa, A. f. & Bansal, R. C., 2011. *Handbook of renewable energy technology.* 1st ed. Singapore: World Scientific Publishing Co. Pte Ltd.

APPENDICES

Appendix I: Materials used for the PTSC air heater

S/No.	Material	Unit	Qty	Unit Cost (K)	Total Cost (K)
1	GI Iron sheet	2m x 0.9m	2	250	500
2	Aluminium kitchen Foil	5m x 0.3m	2	30	60
3	Tuff Stuff Contact Adhesive	0.5 L	1	60	60
4	¾'' GI Pipe	6m	3m	100	300
5	Mild steel square tube sections	6m	20m	15	15
6	Thread seal	5m x 0.015m	1	0.5	20
7	Shutter plywood	3m x 1.2m	1	400	400
8	M6 x 50 Bolt & Nut	-	25	4	100
9	M4 x 20 Bolt & Nut	-	30	1	30
10	Axial fan/blower	1	1	800	800
	Total				**2,285**

Appendix II: Thermal Efficiency Calculation of the PTSC Air Heater

The thermal efficiency of the PTSC air heater was calculated using the equation below:

$$\eta_{th} = \frac{Q_u}{A_{ap} I_D}$$

where:

Q_u is the useful energy transferred to the heat transfer fluid defined as follows;

$$Q_u = \dot{m} C_{p.f} (T_{out} - T_{in})$$

$\dot{m}$ = constant air flow rate of 0.001891 kg/s

$C_{p.f}$ = specific heat capacity of the air as 1006J/KgK

T_{out} = the maximum outlet temperature was 80.1 ˚C

T_{in} = average inlet ambient temperature of 31.1 ˚C

A_{ap} = Collector aperture area of 2.4m^2

I_D = average normal solar radiation on the PTSC surface as 736 W/m^2

Substituting the values in the equation above, the thermal efficiency of the PTSC was calculated as:

$$\eta_{th} = \frac{0.001891 \; x \; 1006 \; x \; (80.1 - 31.1)}{2.4 \; x \; 736}$$

$$= 5.3\%$$

Appendix III: Heat losses from the absorber tube

Calculation of convective heat losses

Convective heat transfer loss (Q_{conv}) from the surface of the absorber tube to the surrounding was calculated theoretically using the equation below:

$$Q_{conv} = h_c\,(T_s - T_a)\,A_s$$

Where:

T_s = (85.6 + 273), average absorber tube surface temperature, K

T_a = (30.6 + 273), average ambient temperature, K

A_s = 0.159, Surface area of the absorber tube given by $\pi\, d_o L\ (m^2)$

h_c = the convective heat transfer coefficient of air, which was calculated:

$$h_c = 4d^{-0.42}v_w^{0.5}$$

$$= 4x0.0253^{-0.42}x3.5^{0.5}$$

$$= 35.06 W/m^2K$$

where V_w was the average wind velocity in m/s and d was the outer diameter of the absorber tube in m.

Substituting in Q_{conv},

$$= 35.06\,(358.6 - 303.6)\,0.159$$

$$= 306.6\ W$$

Calculation of radiation heat losses

Radiation heat loss from the surface of the absorber tube to the surrounding were calculated theoretically by using the below equation:

$$Q_{rad} = \sigma\,\varepsilon_{ab}\,A_s(T_s^4 - T_a^4)$$

Where:

σ = 5.6704 x 10^{-8}, Stefan Boltzmann constant in W/m^2K^4

ε_{ab}= 1, emissivity of the matt black painted GI pipe

$A_s = \pi\, d_o L\ (m^2)$

$= 3.142 \times 0.0253 \times 2$

$= 0.1590\ m^2$

T_s = (85.6 + 273) average absorber tube surface temperature, K

T_a = (30.6 + 273), ambient temperature, K

Substituting the values in the equation;

$= 5.6704 \times 10^{-8} \times 1 \times 0.159 \times (358.6^4 - 303.6^4)$

$= 72.49\ W$

Therefore, total heat losses from the surface of the absorber tube were the sum of convection and radiation losses,

$Q_f = Q_{conv} + Q_{rad}$

$= 306.6\ W + 72.49\ W$

$= 379.09\ W$

Appendix IV: Calculation of the Exergetic Performance

The rate of absorber tube exergy was calculated by equation given by:

$$Ex_u = \dot{m}\, C_{p.f}\left[(T_{out} - T_{in}) - T_{amb} ln\left(\frac{T_{out}}{T_{in}}\right)\right]$$

$$= 0.001891 \text{ x } 1006\left[(353.9 - 304.1) - 304.1 ln\left(\frac{353.9}{304.1}\right)\right]$$

$$= 7.002$$

The solar radiation exergy absorbed by the receiver tube and reflector is written as:

$$Ex_a = A_{ap} I_D\left[1 + \frac{1}{3}\left(\frac{T_{amb}}{T_s}\right)^4 - \frac{4T_{amb}}{3T_s}\right]$$

where Ts = 5762K is the apparent sun temperature.

Substituting;

$$Ex_a = 2.4 \text{ x} 906\left[1 + \frac{1}{3}\left(\frac{304.1}{5762}\right)^4 - \frac{4x304.1}{3x5762}\right]$$

$$= 2021.33$$

The exergy efficiency can be written as:

$$\eta_{exr} = \frac{Ex_u}{Ex_a} = \frac{\dot{m}\, Cp.f\left[(T_{out} - T_{in}) - T_{amb} ln\left(\frac{T_{out}}{T_{in}}\right)\right]}{A_{ap} I_D\left[1 + \frac{1}{3}\left(\frac{T_{amb}}{T_S}\right)^4 - \frac{4T_{amb}}{3T_S}\right]}$$

$$= \frac{7.002}{2021.33}$$

$$= 0.00346$$

$$= 0.346\ \%$$

Appendix V: Specific Energy Consumption (SEC) Calculations

Analysis of Experiment II

Total energy input:

Average solar radiation = 628 W/m^2

Total area of the GSD = (3m x 4.9m)

= 14.7 m^2

Total solar power into the GSD = 628/1000 kW/m^2 x 14.7m^2

= 9.2316kW

Total energy = (9.2316 kW x 11 hrs)

= 101.55 kWh

Energy from the AC fan inside the GSD = 100W x 11hrs

= 1.1kWh

Energy from the four exhaust DC fans

Power = VI

= (12V X 0.6 A) x 4

= 28.8 Watts

Energy = 28.8W x 11hrs

= 316.8 Wh

= 0.3168 kWh

Total energy for the GSD = 101.55Kwh + 1.1Kwh + 0.3168 kWh

= 102.97 kWh

Mass of moisture removed from the tomatoes:

M_w = 13.5kg (from the table 4.3)

Therefore,

SEC = 102.97 kWh / 13.5 kg

= **7.627 kWh/kg**

Analysis of Experiment III

Total energy input:

Average solar radiation = 653.75 W/m^2

Total area of the GSD = (3m x 4.9m)

=14.7 m^2

Total solar power into the GSD = (653.75/1000 Kw/m^2 x 14.7m^2)

= 9.61 kW

GSD Energy = (9.61 Kw x 8 hrs)

= 76.88Kwh

Energy from the hot air

$Q_{Hot\ Air} = \dot{m}C_{p\ air}(T_{in} - T_{amb})$

= 1.75872 Kg/hr x 1006 J/KgK x (331.6 – 303.2) K x 8hrs

= 401978.6711 J

=401.979 KJ

From;

1 kWh = 3.6MJ = 3600KJ

Then, energy in kwh from the hot air is:

$$= \frac{1\ \text{Kwh x } 401.979\ \text{KJ}}{3600\ \text{KJ}}$$

= 0.1117 kWh

Therefore, total energy input to the GSD is,

= 76.88kWh + 0.1117 kWh

= 76.99 kWh

= 77 kWh

Mass of moisture removed from the tomatoes

M_w = 13.9 kg (From table 4.3)

Therefore,

SEC = 77 kWh / 13.9 kg

= 5.54 kWh/kg

Appendix VI: Specific Moisture Extraction Rate (SMER)

Analysis of Experiment II

$$SMER = \frac{13.5\ kg}{102.97\ kWh}$$

$$= \textbf{\textit{0.1311 kg/kWh}}$$

Analysis of Experiment III

$$SMER = \frac{13.9\ kg}{78.1697\ kWh}$$

$$= \textbf{\textit{0.1778 kg/kWh}}$$

Appendix VII: Determination of GSD thermal efficiency:

Particular parameters were as follows:

W**:** Mass of water evaporated from the product = 13.9 kg (from table 4.3)

L_v**:** Latent heat of vaporization of water at drying temperature using equation below (Youcef-Ali et al., 2001):

$= 4.186 \times 10^3(597 - 0.57T_{dr})$ (T_{dr} = 56 ^oC and is temperature for drying)

$= 4.186 \times 10^3(597 - 0.57 \times 56)$

=2365.425 KJ/kg

A_c**:** Area of the dryer = 14.7 m^2

I_D**:** Average solar insolation = 0.678 kW/m^2

P_f**:** Total power from the fans = 0.1288 kW

Substituting,

$$\eta_{GSD} = \left(\frac{13.9Kg \times 2365.425KJ/Kg}{\{(14.7m^2 \times 0.678\ kW)+0.1288kW\}8hrs \times 3600KJ/kWh}\right) \times 100$$

$$= 11.3\%$$

Appendix VIII: Solidworks Models and Engineering Drawing

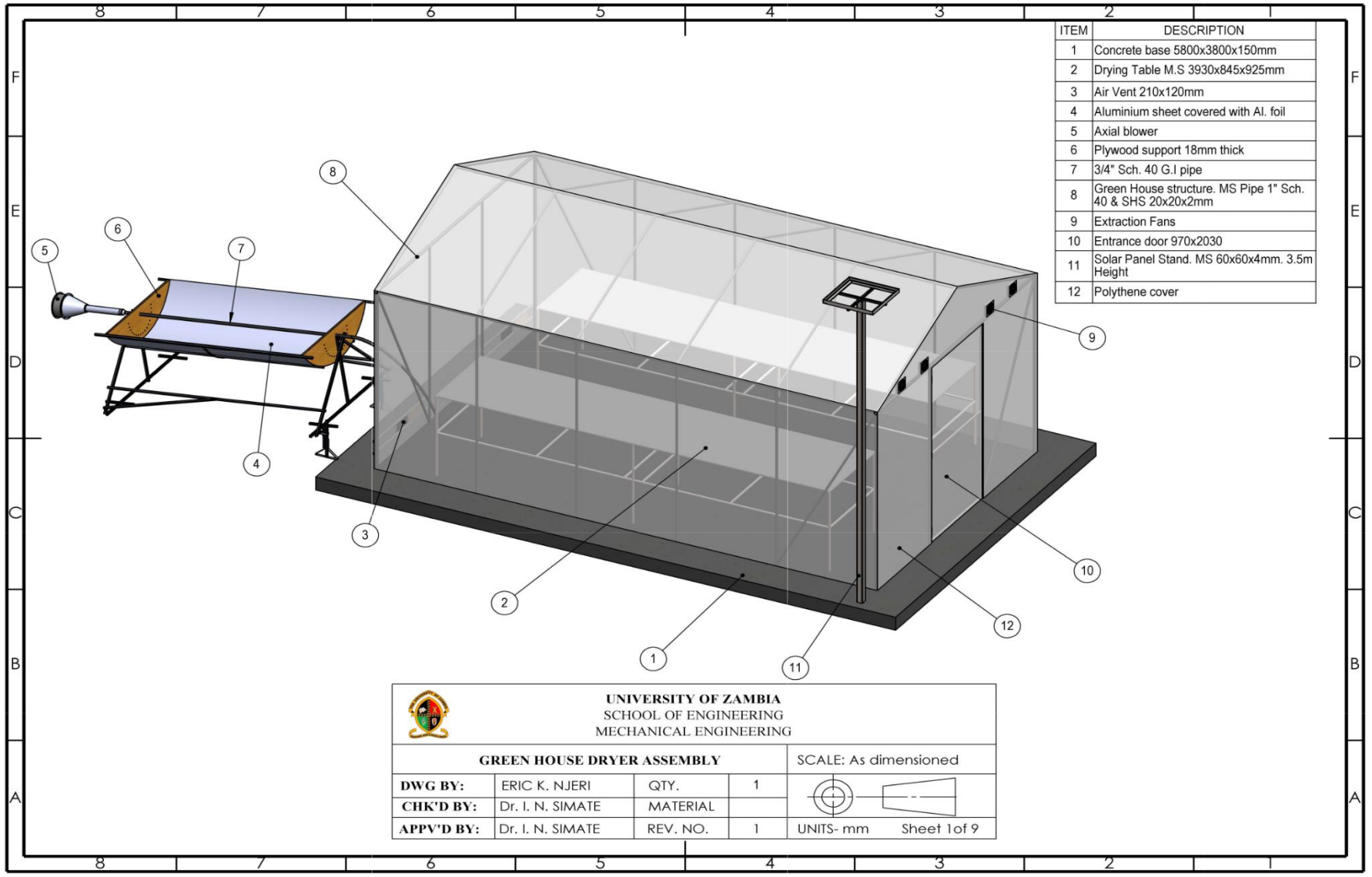

ITEM	DESCRIPTION
1	Concrete base 5800x3800x150mm
2	Drying Table M.S 3930x845x925mm
3	Air Vent 210x120mm
4	Aluminium sheet covered with Al. foil
5	Axial blower
6	Plywood support 18mm thick
7	3/4" Sch. 40 G.I pipe
8	Green House structure. MS Pipe 1" Sch. 40 & SHS 20x20x2mm
9	Extraction Fans
10	Entrance door 970x2030
11	Solar Panel Stand. MS 60x60x4mm. 3.5m Height
12	Polythene cover

UNIVERSITY OF ZAMBIA
SCHOOL OF ENGINEERING
MECHANICAL ENGINEERING

GREEN HOUSE DRYER ASSEMBLY				SCALE: As dimensioned
DWG BY:	ERIC K. NJERI	QTY.	1	
CHK'D BY:	Dr. I. N. SIMATE	MATERIAL		
APPV'D BY:	Dr. I. N. SIMATE	REV. NO.	1	UNITS- mm Sheet 1of 9

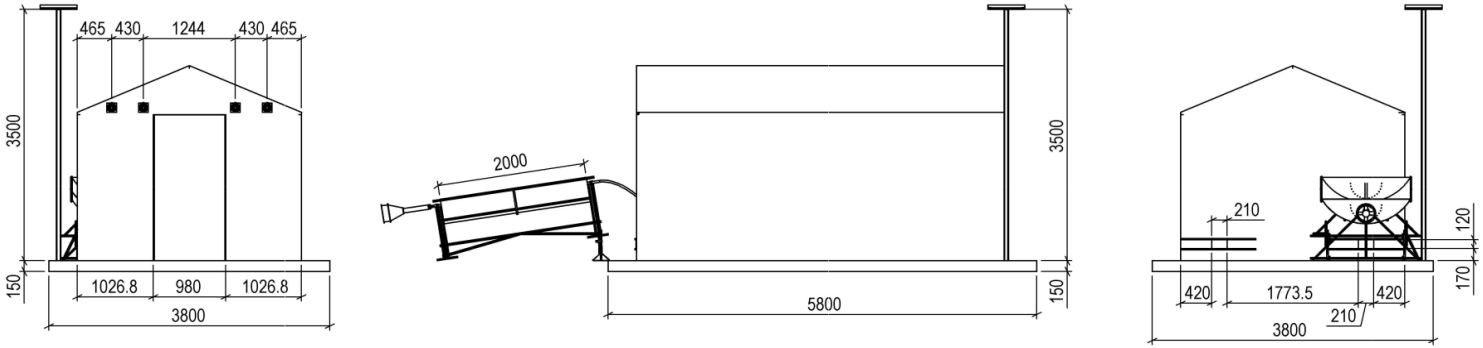

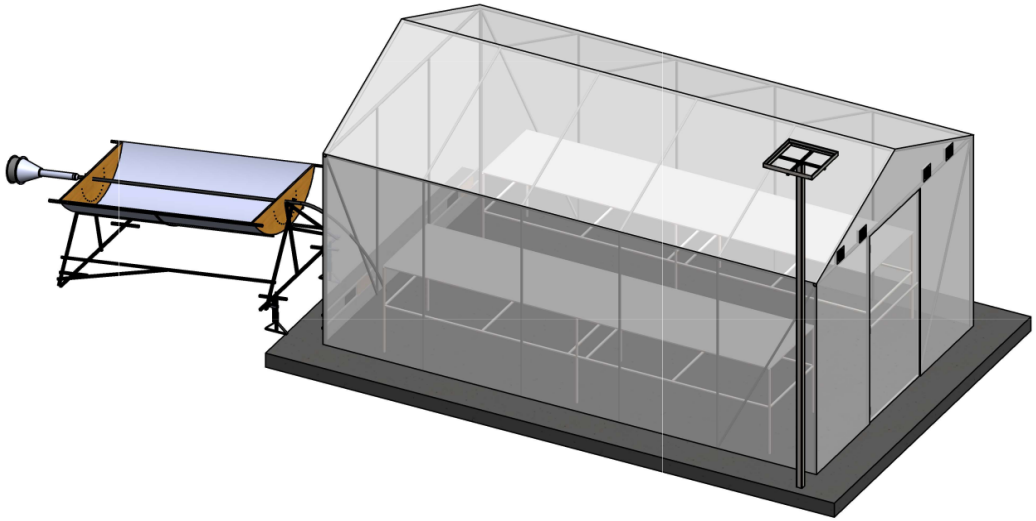

UNIVERSITY OF ZAMBIA SCHOOL OF ENGINEERING MECHANICAL ENGINEERING				
ASSEMBLY VIEWS				SCALE: As dimensioned
DWG BY:	ERIC K. NJERI	QTY.	1	
CHK'D BY:	Dr. I. N. SIMATE	MATERIAL		
APPV'D BY:	Dr. I. N. SIMATE	REV. NO.	1	UNITS- mm Sheet 2of 9

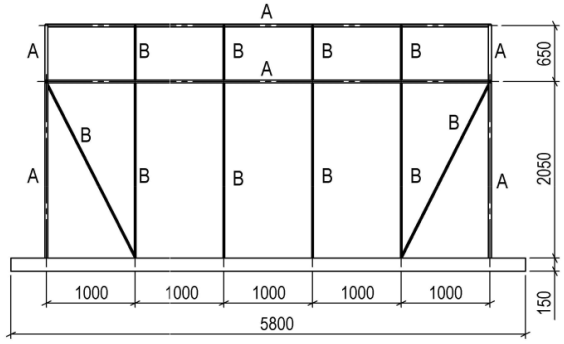

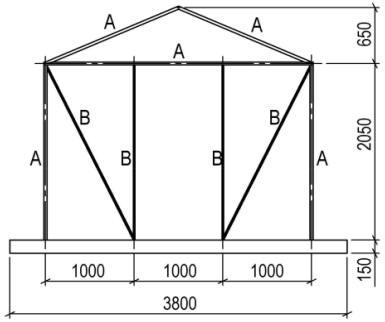

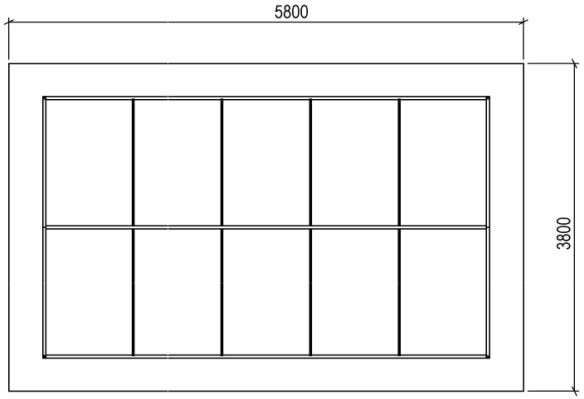

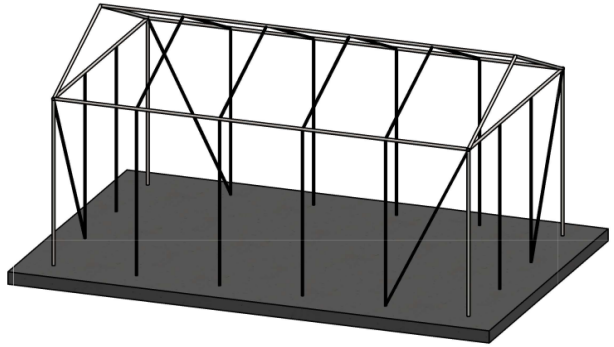

A- Ms Pipe 1" Sch. 40
B- Ms SHS 20x20x2mm

UNIVERSITY OF ZAMBIA SCHOOL OF ENGINEERING MECHANICAL ENGINEERING				
GREEN HOUSE STRUCTURE				SCALE: As dimensioned
DWG BY:	ERIC K. NJERI	QTY.	1	
CHK'D BY:	Dr. I. N. SIMATE	MATERIAL	MS	
APPV'D BY:	Dr. I. N. SIMATE	REV. NO.	1	UNITS- mm Sheet 3of 9

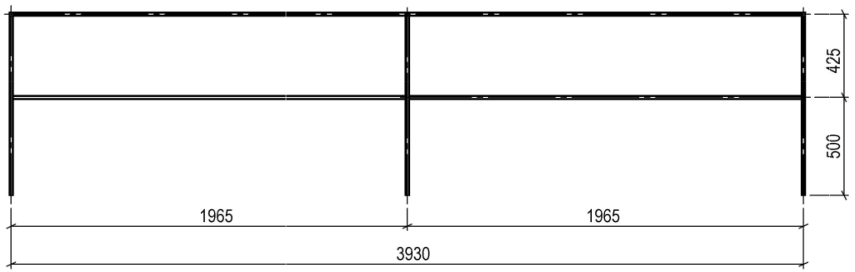

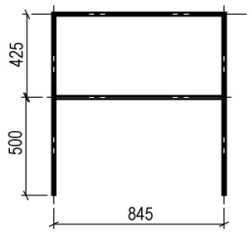

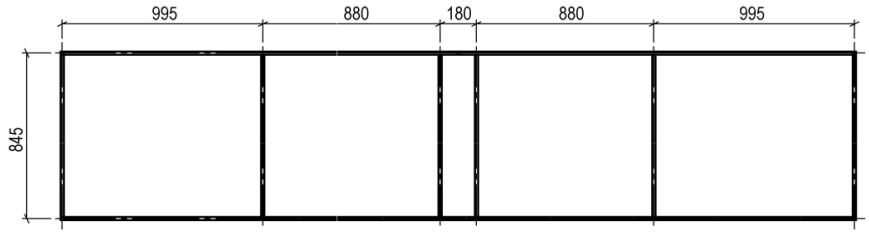

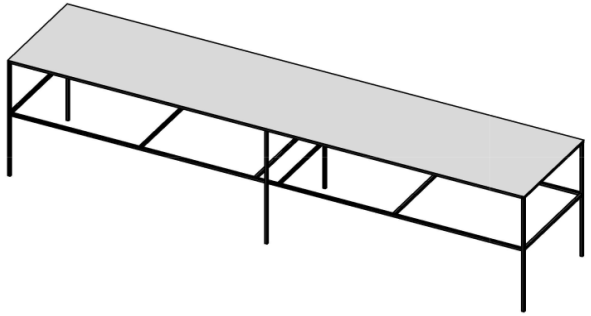

All profiles are MS SHS 20x20x2mm

UNIVERSITY OF ZAMBIA SCHOOL OF ENGINEERING MECHANICAL ENGINEERING				
DRYING TABLE				SCALE: As dimensioned
DWG BY:	ERIC K. NJERI	QTY.	2	
CHK'D BY:	Dr. I. N. SIMATE	MATERIAL	M.S	
APPV'D BY:	Dr. I. N. SIMATE	REV. NO.	1	UNITS- mm Sheet 4of 9

ITEM	DESCRIPTION
1	2" Sch.5 Pipe
2	Axial blower
3	Concentric reducer
4	MS SHS 20x20x2 Trough reinforcers
5	Aluminium foil cover
6	3/4" GI Sch.5 pipe
7	Wooden block
8	Flexible PVC pipe
9	Adjustible Stand
10	Fixed Stand

UNIVERSITY OF ZAMBIA
SCHOOL OF ENGINEERING
MECHANICAL ENGINEERING

PARABOLIC TROUGH ASSEMBLY				SCALE: As dimensioned
DWG BY:	ERIC K. NJERI	QTY.	1	
CHK'D BY:	Dr. I. N. SIMATE	MATERIAL		
APPV'D BY:	Dr. I. N. SIMATE	REV. NO.	1	UNITS- mm Sheet 5of 9

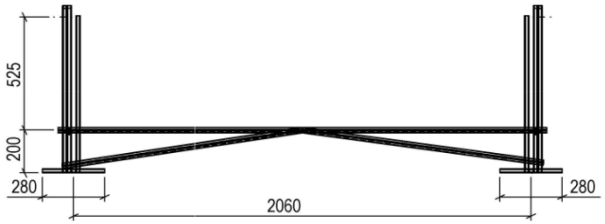

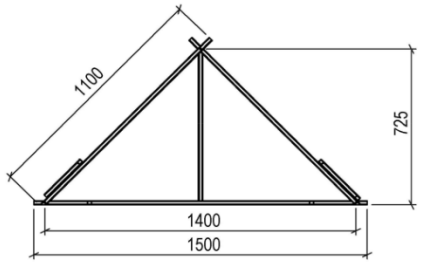

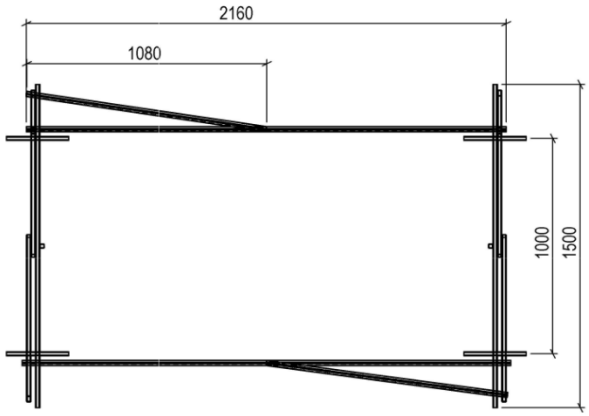

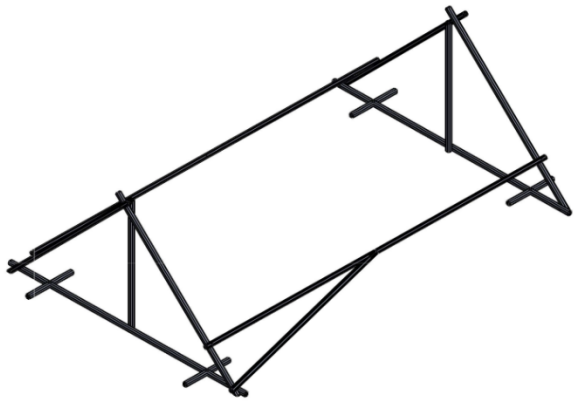

UNIVERSITY OF ZAMBIA SCHOOL OF ENGINEERING MECHANICAL ENGINEERING				
PARABOLIC TROUGH STAND				SCALE: As dimensioned
DWG BY:	ERIC K. NJERI	QTY.	1	
CHK'D BY:	Dr. I. N. SIMATE	MATERIAL	M.S	
APPV'D BY:	Dr. I. N. SIMATE	REV. NO.	1	UNITS- mm Sheet 6of 9

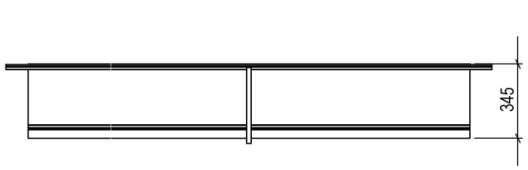

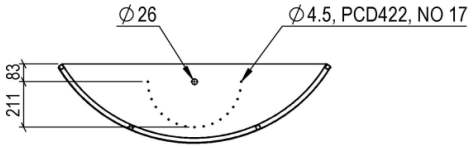

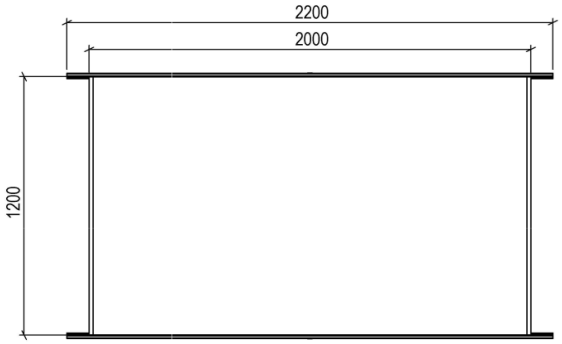

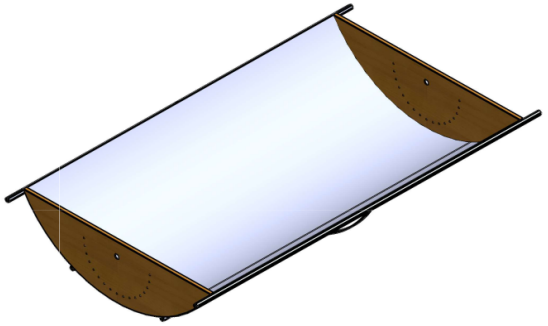

UNIVERSITY OF ZAMBIA SCHOOL OF ENGINEERING MECHANICAL ENGINEERING				
PARABOLIC TROUGH ASSEMBLY				SCALE: As dimensioned
DWG BY:	ERIC K. NJERI	QTY.	1	
CHK'D BY:	Dr. I. N. SIMATE	MATERIAL		
APPV'D BY:	Dr. I. N. SIMATE	REV. NO.	1	UNITS- mm Sheet 7of 9

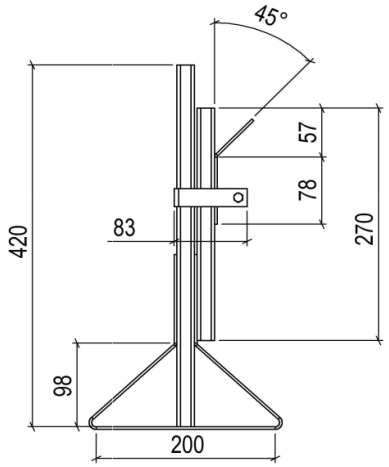

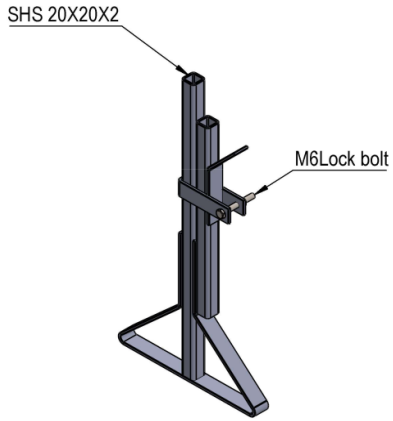

UNIVERSITY OF ZAMBIA SCHOOL OF ENGINEERING MECHANICAL ENGINEERING				
ADJUSTIBLE STAND				SCALE: As dimensioned
DWG BY:	ERIC K. NJERI	QTY.	2	
CHK'D BY:	Dr. I. N. SIMATE	MATERIAL	M.S	
APPV'D BY:	Dr. I. N. SIMATE	REV. NO.	1	UNITS- mm Sheet 8of 9

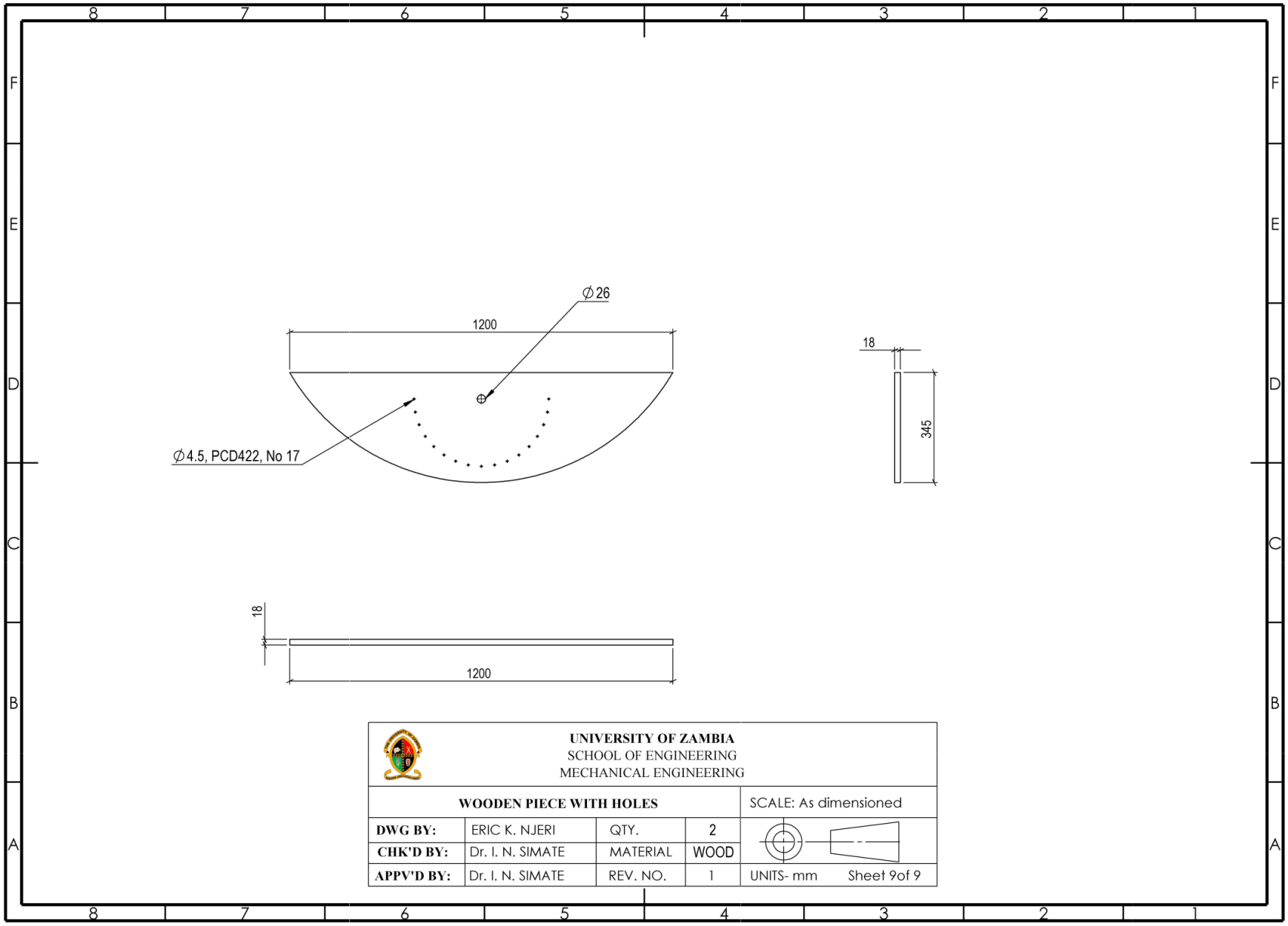

UNIVERSITY OF ZAMBIA
SCHOOL OF ENGINEERING
MECHANICAL ENGINEERING

WOODEN PIECE WITH HOLES				SCALE: As dimensioned
DWG BY:	ERIC K. NJERI	QTY.	2	
CHK'D BY:	Dr. I. N. SIMATE	MATERIAL	WOOD	
APPV'D BY:	Dr. I. N. SIMATE	REV. NO.	1	UNITS- mm Sheet 9of 9

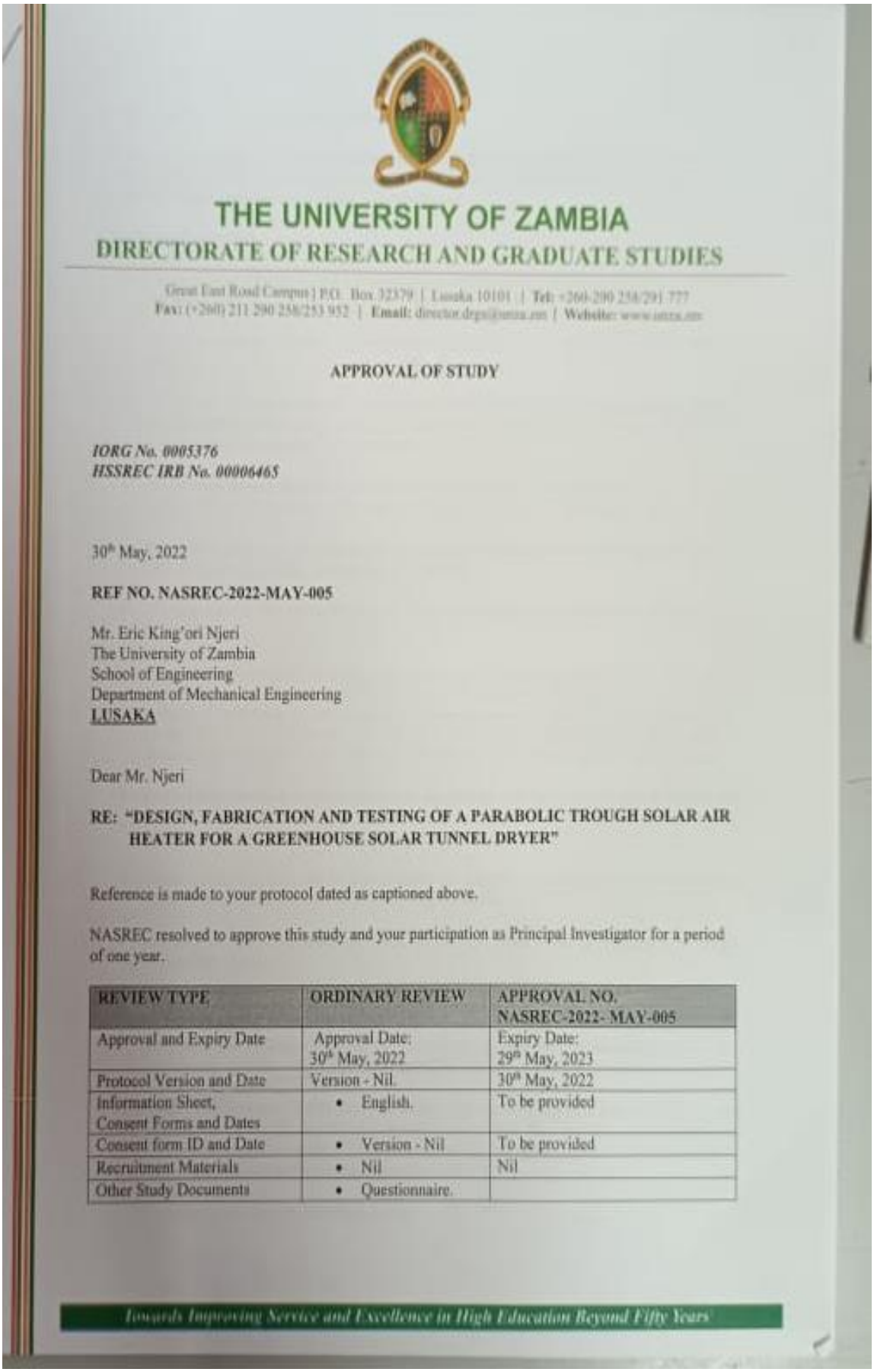

THE UNIVERSITY OF ZAMBIA

DIRECTORATE OF RESEARCH AND GRADUATE STUDIES

Great East Road Campus | P.O. Box 32379 | Lusaka 10101 | Tel: +260-200 256/291 777
Fax: (+260) 211 290 258/253 952 | Email: director.drgs@unza.zm | Website: www.unza.zm

APPROVAL OF STUDY

IORG No. 0005376
HSSREC IRB No. 00006465

30th May, 2022

REF NO. NASREC-2022-MAY-005

Mr. Eric King'ori Njeri
The University of Zambia
School of Engineering
Department of Mechanical Engineering
LUSAKA

Dear Mr. Njeri

RE: "DESIGN, FABRICATION AND TESTING OF A PARABOLIC TROUGH SOLAR AIR HEATER FOR A GREENHOUSE SOLAR TUNNEL DRYER"

Reference is made to your protocol dated as captioned above.

NASREC resolved to approve this study and your participation as Principal Investigator for a period of one year.

REVIEW TYPE	ORDINARY REVIEW	APPROVAL NO. NASREC-2022- MAY-005
Approval and Expiry Date	Approval Date: 30th May, 2022	Expiry Date: 29th May, 2023
Protocol Version and Date	Version - Nil.	30th May, 2022
Information Sheet, Consent Forms and Dates	• English.	To be provided
Consent form ID and Date	• Version - Nil	To be provided
Recruitment Materials	• Nil	Nil
Other Study Documents	• Questionnaire.	

Specific conditions will apply to this approval;

As Principal Investigator it is your responsibility to ensure that the contents of this letter are adhered to. If these are not adhered to, the approval may be suspended. Should the study be suspended, study sponsors and other regulatory authorities will be informed.

Conditions of Approval

- No participant may be involved in any study procedure prior to the study approval or after the expiration date.
- All unanticipated or Serious Adverse Events (SAEs) must be reported to NASREC within 5 days.
- All protocol modifications must be approved by NASREC prior to implementation unless they are intended to reduce risk (but must still be reported for approval). Modifications will include any change of investigator/s or site address.
- All protocol deviations must be reported to NASREC within 5 working days.
- All recruitment materials must be approved by NASREC prior to being used.
- Principal investigators are responsible for initiating Continuing Review proceedings. NASREC will only approve a study for a period of 12 months.
- It is the responsibility of the PI to renew his/her ethics approval through a renewal application to NASREC.
- Where the PI desires to extend the study after expiry of the study period, documents for study extension must be received by NASREC at least 30 days before the expiry date. This is for the purpose of facilitating the review process. Documents received within 30 days after expiry will be labelled "late submissions" and will incur a penalty fee of K500.00. No study shall be renewed whose documents are submitted for renewal 30 days after expiry of the certificate.
- Every 6 (six) months a progress report form supplied by The University of Zambia Natural and Applied Sciences Research Ethics Committee as an IRB must be filled in and submitted to us. There is a penalty of K500.00 for failure to submit the report.
- When closing a project, the PI is responsible for notifying, in writing or using the Research Ethics and Management Online (REMO),both NASREC
- and the National Health Research Authority (NHRA) when ethics certification is no longer required for a project.
- In order to close an approved study, a Closing Report must be submitted in writing or through the REMO system. A Closing Report should be filed when data collection has ended and the study team will no longer be using human participants or animals or secondary data or have any direct or indirect contact with the research participants or animals for the study.
- Filing a closing report (rather than just letting your approval lapse) is important as it assists NASREC in efficiently tracking and reporting on projects. Note that some funding agencies and sponsors require a notice of closure from the IRB which had approved the study and can only be generated after the Closing Report has been filed.
- A reprint of this letter shall be done at a fee.

- All protocol modifications must be approved by NASREC by way of an application for an amendment prior to implementation unless they are intended to reduce risk (but must still be reported for approval). Modifications will include any change of investigator/s or site address or methodology and methods. Many modifications entail minimal risk adjustments to a protocol and/or consent form and can be made on an Expedited basis (via the IRB Chair). Some examples are: format changes, correcting spelling errors, adding key personnel, minor changes to questionnaires, recruiting and changes, and so forth. Other, more substantive changes, especially those that may alter the risk-benefit ratio, may require Full Board review. In all cases, except where noted above regarding subject safety, any changes to any protocol document or procedure must first be approved by NASREC before they can be implemented.

Should you have any questions regarding anything indicated in this letter, please do not hesitate to get in touch with us at the above indicated address.

On behalf of NASREC, we would like to wish you all the success as you carry out your study.

Yours faithfully,

Dr. M. Kaonda

VICECHAIRPERSON
THE UNIVERSITY OF ZAMBIA NATURAL AND APPLIED SCIENCES RESEARCH ETHICS COMMITTEE - IRB

cc: Director, Directorate of Research and Graduate Studies
Assistant Director (Research), Directorate of Research and Graduate Studies
Assistant Registrar (Research), Directorate of Research and Graduate Studies
Acting Senior Administrative Officer (Research), Directorate of Research and Graduate Studies